universität
wien

DISSERTATION

Titel der Dissertation

"Petrology and geochemistry of the Late Miocene-Pleistocene volcanic rocks from Burgenland and SE Styria, Austria"

Verfasser

M.Sc. Shehata Ali Shehata Ali

angestrebter akademischer Grad

Doktor der Naturwissenschaften (Dr. rer. nat.)

Wien, im March 2011

CONTENTS

Ali, Sh., Ntaflos, Th., 2011a. Alkali basalts from Burgenland, Austria: Petrological constraints on the origin of the westernmost magmatism in the Carpathian–Pannonian Region. Lithos 121, 176–188.

Ali, Sh., Ntaflos, Th., Upton, B.G.J., Cornelius, T., 2011b. Petrogenesis and mantle source characteristics of Quaternary alkaline mafic lavas in the western Carpathian–Pannonian Region, Styria, Austria (in submission stage).

Supplementary Tables (A & B)

ABSTRACT

The present PhD thesis deals with petrology, mineralogy and geochemistry of alkaline mafic lavas from the western part of the Carpathian-Pannonian Region (CPR). They crop out in small volcanic centres at Burgenland (Pauliberg, Oberpullendorf) and southeastern Styrian Basin (Klöch, Steinberg, Stradnerkogel, Waltrafelsen). The oldest alkaline mafic volcanism (Burgenland basalts) in the CPR occurred in Late Miocene (~11 Ma) during the late stages of extension whereas the peak of the alkaline mafic volcanism took place during the Pliocene to Quaternary post-dating the extension and coeval to the compression phase (.e.g. Styrian Basin). This type of magmatism subsequently occurred throughout the region following the post-collision calc-alkaline subduction-related volcanics in the western Carpathians. The sampled volcanic rocks comprise alkali basalts, basanites/nepheline-basanites and nephelinites. Among them the most primitive mafic magmatic rocks have geochemical characteristics that can provide important constraints on the nature of their mantle source(s) and the melting conditions (depths and degrees of partial melting). They exhibit ocean island basalts (OIB)-like geochemical signatures, despite their locally different geographic distribution and relatively wide range of variation in chemical compositions. Their geochemical characteristics resemble those of typical intra-plate *anorogenic* basalts which were not modified by contamination with crustal material and/or subduction-related fluids/melts. The Mg# [Mg-number=$100MgO/(MgO+FeO_{total})$] of the alkaline basalts varies from 53 to 68 but it is mostly >62 and they lack a negative Eu anomaly suggesting that most of these rocks have experienced insignificant crystal fractionation and approach primary magma compositions. The trace element ratios like Zr/Nb, La/Nb and Ba/Th and the isotopic compositions akin to HIMU-OIB suggest an origin of the primary magmas in the asthenospheric mantle with negligible interaction between magma and lithosphere *en route* to the surface. The concentrations of highly incompatible elements are variable and high whereas the heavy rare earth element (HREE) concentrations are low suggesting variable small degrees of partial melting in the garnet peridotite field with garnet remaining in the residue. Chemical variation within Pauliberg locality (alkali basalts and basanites) suggest variable small degrees of melting from the same asthenospheric mantle source whereas Oberpullendorf basalts have chemical and isotopic characteristics similar to Saghegy basalts of the Little Hungarian Plain. The general similarity of the trace element distribution patterns and the narrow range of the Sr-Nd isotopic ratios of the Styrian Basin lavas (basanites/nepheline-basanites and nephelinites) might suggest a similar asthenospheric mantle source.

The calculated mantle potential temperature (Tp) for the Pauliberg basalts is 1386 ^{o}C and a melt fraction of ~2%. Analogous calculations for the Klöch and Oberpullendorf mafic rocks indicate minor clinopyroxene fractionation which leads to an overestimate of the mantle Tp (1466 ^{o}C and 1530 ^{o}C respectively), making it unfeasible to calculate the degree of partial melting involved in the genesis of the primary magma. These Tp calculations imply that these magmas arose from mantle at ambient temperatures without any indication of thermal anomaly. In addition, they represent small degrees of melting and hence small volumes of the basaltic lavas erupted and low eruption rates suggesting that the asthenospheric mantle Tp was low as well as consistent with ambient mantle temperatures. Accordingly, the mantle plume activity can be excluded from their origin.

ZUSAMMENFASSUNG

Die vorliegende Doktorarbeit beschäftigt sich mit der Petrologie, Mineralogie und Geochemie alkaliner, mafischer Laven der westlichen Karpaten-Pannonischen Region (*Carpathian-Pannonian Region;* CPR). Diese Laven sind in kleineren Vulkanprovinzen im Burgenland (Pauliberg, Oberpullendorf) sowie im südöstlichen steirischen Becken (Klöch, Steinberg, Stradnerkogel, Waltrafelsen) aufgeschlossen. Die ältesten alkalinen, mafischen Vulkanite (Basalte des Burgenlandes) entstanden im Obermiozän (~ 11 Ma) während später Extensionsphasen. Die Hauptphase des Vulkanismus verbunden mit der Förderung alkaliner, mafischer Gesteine fand im Pliozän bis zum Quartär nach der Extension und zeitgleich mit der Kompression statt (z. B. steirisches Becken). Dieser in der gesamten Region auftretende Magmatismus folgte dem post-kollisionalen, kalkalkalinen, subduktionsbezogenen Vulkanismus der westlichen Karpaten. Bei den entnommenen Proben handelt es sich um Alkalibasalte, Basanite/Nephelin-Basanite und Nephelinite. Dabei können die geochemischen Charakteristiken der primitivsten mafischen Magmatite wichtige Hinweise zur Beschaffenheit der Mantelquelle(n) und den Schmelzbedingungen (Schmelztiefe, Aufschmelzgrad) liefern. Sie zeigen geochemische Signaturen der Ozeaninselbasalte (OIB) unabhängig von der geografischen Verbreitung sowie der relativ breiten Variation der chemischen Zusammensetzung. Ihre geochemischen Charakteristiken ähneln jenen der typischen *anorogenen* Intraplattenbasalte, die nicht durch Krustenkontamination und/oder subduktionsbezogene fluide Phasen/Schmelzen verändert worden. Die Mg# [Magnesiumzahl=$100MgO/(MgO+FeO_{total})$] der Alkalibasalte variiert zwischen 53 und 68, hauptsächlich jedoch > 62. Zudem ist keine negative Eu-Anomalie zu verzeichnen, was den Schluss zulässt, dass die meisten Magmen nur insignifikante Kristallfraktionierungen erfuhren und so die Zusammensetzung der Primärschmelzen wiederspiegeln. Spurenelementverhältnisse wie Zr/Nb, La/Nb und Ba/Th sowie isotopengeochemische Signaturen ähnlich denen der HIMU-OIB weisen auf die Entstehung der Primärschmelzen im asthenosphärischen Mantel hin, wobei die Interaktion mit der Lithosphäre während des Aufstieges der Schmelzen zur Erdoberfläche (*en route)* vernachlässigbar ist. Die Konzentration stark inkompatibler Elemente variiert und ist hoch. Hingegen zeigen die schweren seltenen Erdelemente (*heavy rare earth elements* HREE) nur geringe Gehalte. Es ist somit anzunehmen, dass die Schmelzen durch geringe Aufschmelzgrade im Stabilitätsfeld des Granat-Peridotits entstanden, wobei Granat als Residuum im Mantel verweilte. Die chemischen Variationen der Proben vom Pauliberg (Alkalibasalte und Basanite) deuten auf verschieden kleine Aufschmelzgrade derselben Mantelquelle hin. Die Basalte von Oberpullendorf ähneln hinsichtlich ihrer chemischen und isotopenchemischen Zusammensetzung den Saghey Basalten der „Kleinen ungarischen Ebene". Die generell analogen Verteilungsbilder der Spurenelemente sowie die geringe Variation der Sr-Nd Isotopenverhältnisse der Laven des steirischen Beckens (Basanite/Nephelin-Basanite und Nephelinite) lassen auf eine ähnliche asthenosphärische Mantelquelle schließen.

Die berechnete potentielle Manteltemperatur (Tp) der Pauliberg-Basalte beträgt 1386 °C, der Aufschmelzgrad liegt bei ~ 2 %. Analoge Berechnungen für die mafischen Gesteine von Klöch und Oberpullendorf weisen auf geringe Klinopyroxenfraktionierungen hin was zu einer Überschätzung der Temperaturen Tp (1466 °C bzw. 1530 °C) führt und die Berechnung des Aufschmelzgrades des Mantels bei der Entstehung dieser Primärschmelzen unmöglich macht. Die potentiellen Manteltemperaturen implizieren, dass es keine thermische Anomalien während der Bildungen und dem Aufstieg der Magmen gegeben hat. Überdies repräsentieren die geringen Volumina der eruptierten basaltischen Laven ebenfalls kleine Aufschmelzgrade, was bedeutet, dass die Temperatur des asthenosphärischen Mantels klein und konsistent mit der mittleren, normalen Manteltemperatur war. Demzufolge wird die Aktivität eines Manteldiapirs während der Entstehung der Schmelzen ausgeschlosse.

ACKNOWLEDGEMENTS

CHAPTER I

INTRODUCTION

CHAPTER I: INTRODUCTION

General introduction

The oceanic and continental volcanoes occurred far away from either diverging or converging plate boundaries are generally classified as intra-plate volcanoes. Those arose in the interior of the continents are predominantly basaltic in composition.

Continental intra-plate mafic rocks globally include a suite of alkaline basalts characterized by a variety of compositions, ranging from highly silica-undersaturated (strongly alkaline) to less silica-undersaturated (weakly alkaline) compositions (e.g. Fitton et al., 1991; Smith et al., 1999; Zeng et al., 2010). These basalts usually have geochemical signatures akin to ocean island basalt (OIB), though their different geographic distribution and relatively broad range of chemical variation (e.g. Lustrino and Wilson, 2007).

Widespread volcanism developed in the Alpine-Mediterranean region during the Neogene to Quaternary (Wilson and Patterson, 2001; Harangi et al., 2006; Wilson and Downes, 2006). The volcanic activity produced a wide range of magmatic rocks that can be roughly classified based on tectonic settings to *orogenic* (calc-alkaline, potassic-ultrapotassic) and *anorogenic* (Na-alkaline) types (Fig. 1) (Wilson and Bianchini, 1999; Harangi and Lenkey, 2007; Lustrino and Wilson, 2007). Predominant calc-alkaline and potassic-ultrapotassic rocks along with scattered tholeiitic and Na-alkaline rocks occurred within the Alpine-Mediterranean region whereas mainly alkaline mafic rocks developed at the periphery of the region (Harangi and Lenkey, 2007).

The CPR (Fig. 2) represents a typical Mediterranean region and is distinguished by arcuate orogenic belt, retreating subduction, back-arc extensional basin and a broad spectrum of magmas (Embey-Isztin et al., 1993; Royden 1993; Embey-Isztin and Dobosi, 1995; Downes et al., 1995a, b; Fodor et al., 1999; Seghedi et al., 2004a, b; Pecskay et al., 1995, 2006; Horvath et al., 2006; Harangi and Lenkey, 2007; Seghedi et al., 2010).

The volcanism developed in the western part of the CPR (Fig. 2) (e.g. Burgenland and SE Styrian Basin) represents a typical example of *anorogenic* intra-plate volcanism as shown by its alkaline affinity (basaltic composition) and its occurrence in the interior of a continental plate (within-plate) and far away from plate boundaries.

The origin and source of continental intra-plate alkaline basaltic mamas are highly controversial. The magma generation has been attributed either to decompression melting caused by lithospheric extension or to addition of heat supplied by a hot rising mantle plume. These magmas could have been produced from lithospheric or asthenospheric mantle source and also could represent mixing between both sources. The lithospheric mantle is too cold in order to be considered as the source of intra-plate alkaline basaltic magmas and only under special circumstances (steep geothermal gradient) can generate basaltic magmas. In order to contribute towards solving these problems we provide additional evidence from alkaline basalts of Burgenland and SE Styrian Basin at the western margin of the CPR.
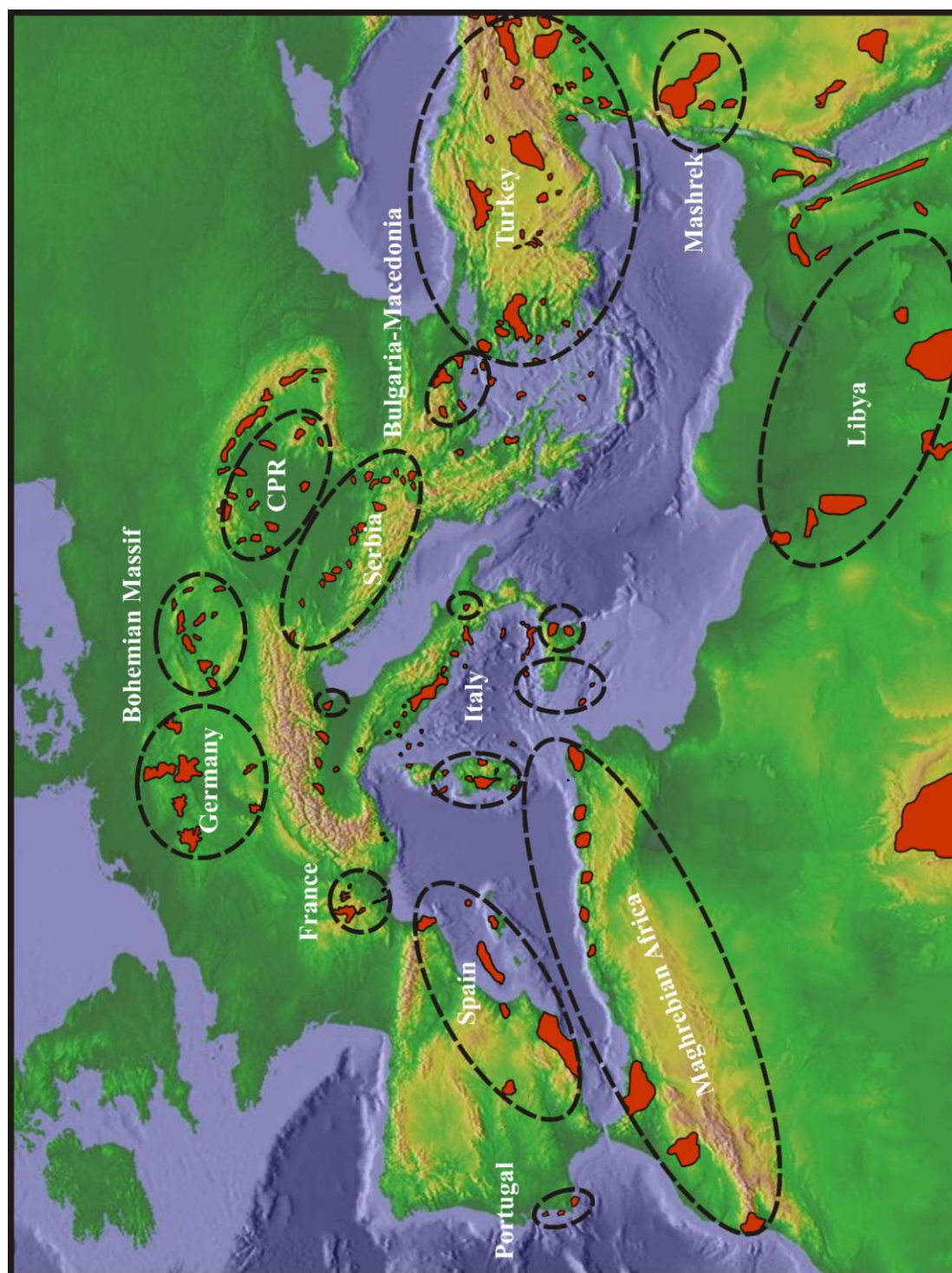
Fig. 1. Digital topography of Mediterranean and surrounding region from NOAA (http://www.ngdc.noaa.gov/mgg/image/2minrelief.html) displaying the locations of Cenozoic igneous provinces in red (*anorogenic* and *orogenic* types) (Lustrino and Wilson, 2007). *Anorogenic* provinces are outlined.
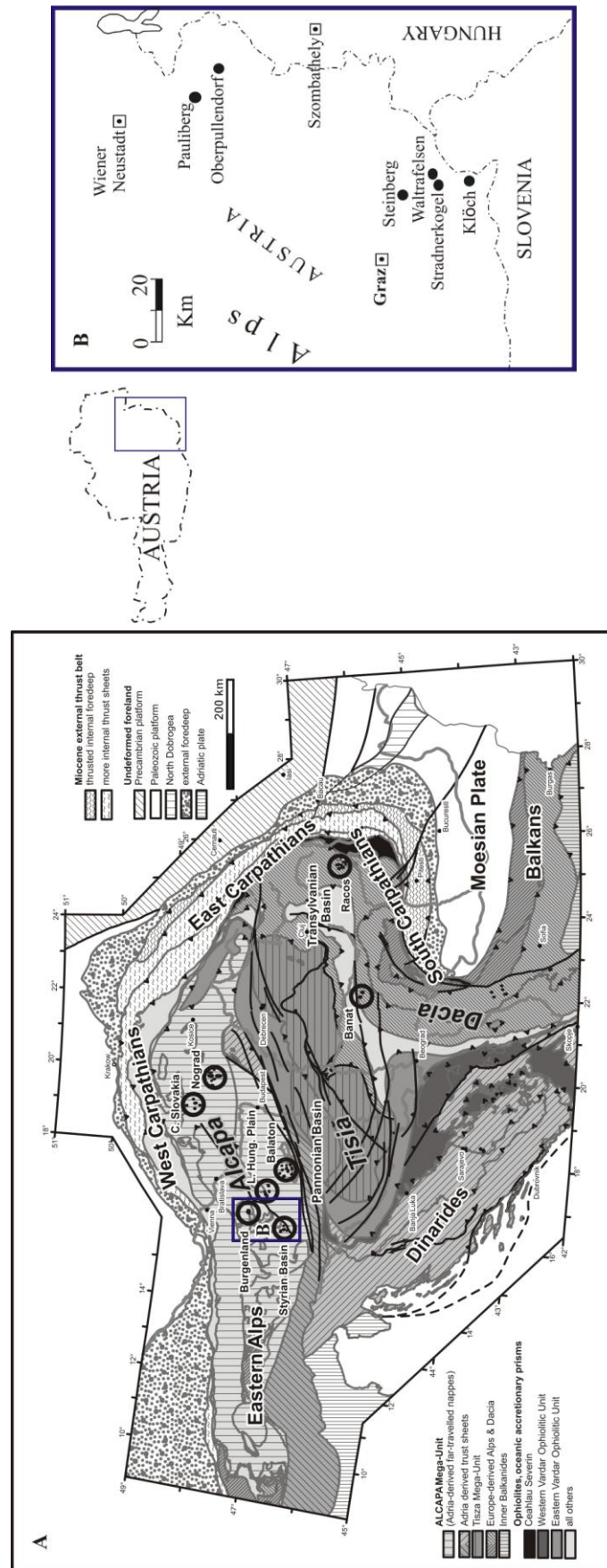
Fig. 2. (A) Geologic and tectonic map showing the distribution of Late Miocene-Pleistocene alkaline basalts within the CPR (modified after Schmid et al., 2008). Inset map (B): Location of the investigated alkali basalt occurrences.

Literature reviews

The Tertiary-Quaternary volcanism of the CPR has been the focus of many previous and recent studies as the region offers a good possibility to understand the relationship between tectonics and volcanism (Embey-Isztin et al., 1993; Embey-Isztin and Dobosi, 1995; Downes et al., 1995; Harangi, 2001; Seghedi et al., 2004a, b; Harangi et al., 2006; Pecskay et al., 1995, 2006; Harangi and Lenkey, 2007; Ali and Ntaflos, 2011). The occurrences of *orogenic* calc-alkaline volcanism in the Alpine chain and the Carpathians have been interpreted in terms of contemporaneous subduction (Harangi et al., 2006) and are beyond the scope of this dissertation. Late Miocene and Plio-Pleistocene *anorogenic* intra-plate alkaline basalts occurred in the CPR mainly postdated the main phase of *orogenic* calc-alkaline volcanism (with the exception of the SE Carpathians where it was contemporaneous; Seghedi et al., 2010) and display no evidence (or very little) for subduction-enrichment. They represent the youngest products of volcanic activity and show geochemical characteristics similar to that of an OIB-like asthenospheric source (Embey-Isztin et al., 1993; Seghedi et al., 2004b, Harangi and Lenkey, 2007; Ali and Ntaflos, 2011).

Embey-Isztin et al. (1993) suggested that the chemical and isotopic differences within Pannonian Basin basalts can not be attributed only to variable degrees of partial melting but also due to mixing between asthenospheric and lithospheric mantle-derived melts. The participation of the lithospheric mantle can be clearly seen in the Balaton and Little Hungarian Plain (LHP) of central Pannonian Basin as they are in enriched LILE (e.g. K, Rb, Sr, Pb, Ba) and have high $^{87}Sr/^{86}Sr$ and low $^{143}Nd/^{144}Nd$ ratios. This involvement has been attributed to extensive heating of the lithosphere due to asthenospheric upwelling. Conversely, the Styrian Basin mafic magmas are highly silica-undersaturated generated from melting of an asthenospheric source at great depths in the garnet stability field.

Balogh et al. (1994) determined the K/Ar dates of 10.5-11.5 Ma for Burgenland (Pauliberg and Oberpullendorf) and 1.7-3.7 Ma for the Styrian Basin alkaline mafic rocks. According to this K/Ar dating Pauliberg and Oberpullendorf were simultaneous at ~11 Ma. However, the Oberpullendorf lavas have geochemical signatures more comparable to the Sághegy lavas of the LHP that are 5.87 Ma older than the Pauliberg basalts. Considering the extensive alteration of the Oberpullendorf lavas, the age of 11Ma should be re-examined.

Pécskay et al. (1995) provide a comprehensive review of the timing of the volcanic activity. They distinguished three different types of magmatism in the CPR: i) huge volume acidic ignimbrites and tuffs with calc-alkaline character took-place during Miocene, ii) intermediate calc-alkaline Miocene to Pliocene subduction-related volcanics (mainly andesitic) and iii) alkaline volcanism represented mainly by alkali basalts occurred during Late Miocene and Pliocene-Quaternary sporadically distributed throughout the CPR.

Downes et al. (1995) concluded that despite the alkaline basalts of eastern CPR (Romania) show asthenospheric OIB-like mantle source they have been modified by subduction component.

Embey-Isztin and Dobosi (1995) suggested the basalts of western CPR (e.g. Burgenland and Styrian Basin) have geochemical characteristics similar to Western and Central Europe and were produced from the asthenospheric mantle without any subduction-related chemical signature whereas those of Balaton and LHP display subduction-enrichment which is more pronounced in the Persani Mts. basalts (SE Carpathians). Based on the HIMU affinities of the basalts they attributed the magma generation to a plume structure beneath CPR.

Harangi (2001) showed that the Neogene alkaline mafic magmas were derived from small degrees of melting at different depths due to decompression of hot asthenospheric mantle.

Seghedi et al. (2004) reviewed the alkaline magmatism in the CPR and proposed that the melt generation could be attributed to finger-like mantle plumes of an asthenospheric origin.

On the other hand, Harangi and Lenkey (2007) provide arguments (e.g. missing of regional uplift, sporadic occurrence of the alkaline volcanism and the high-velocity body beneath CPR) against the mantle plume activity beneath the Pannonian Basin and concluded that the melt generation was related to flow of heterogeneous asthenospheric mantle, close to its solidus, in association with Miocene lithospheric extension.

Ali and Ntaflos (2011) concluded that the alkaline magma generated beneath the westernmost CPR (Burgenland) during late stages of extension through passive upwelling and decompression melting of an asthenospheric OIB-type source at ambient mantle temperature, precluding mantle plume activity underneath this region.

Geological background

The CPR is located in eastern Central Europe and is bounded by the eastern Alps, the Carpathian arcuate orogenic belt and the Dinarides (Fig. 2). In the CPR, a number of basins were formed include the Styrian Basin, Vienna Basin, Little Hungarian Plain (LHP), Great Hungarian Plain and the Transylvanian Basin. These basins were created during the Neogene time by stretching of the continental lithosphere. During Palaeocene-Eocene the European plate subducted (southward) beneath the northern margin of the Pannonian Basin that is indicated by calc-alkaline volcanics. Extension, subsidence and sedimentation took place in the Pannonian basin and sub-basins during Miocene time (Fig. 3). The subsidence in the entire CPR and the concurrent under-thrusting in the Carpathians were rapidly accompanied by voluminous calc-alkaline volcanism composed mainly of andesitic and dacitic lavas along the northern (western Carpathian arc) and eastern Pannonian Basin (eastern Carpathians) (Downes et al., 1995a; Seghedi et al., 2004a; Harangi et al., 2006) (Fig. 3). They were erupted during Miocene to Quaternary with the last volcanism erupted at 10–40 ka in SE Carpathians (Pécskay et al., 1995). While in the western Carpathian arc calc-alkaline magmas were closely linked to the main phase of extension in the Pannonian Basin (e.g. Harangi 2001), in the eastern Carpathian arc the calc-alkaline volcanism were directly associated with subduction (e.g. Seghedi et al., 2004a). In the CPR, high-velocity anomaly has been documented at the bottom of the upper mantle that is explained as accumulated subduction materials (Wortel and Spakman, 2000). During Late Miocene the active extension in the Pannonian Basin ceased and the alkaline basaltic magmatism mainly post-dating the extension being similar to the Basin and Range Province of the western United States (Fig. 3) (Bradshaw et al., 1993).

Alkaline basaltic magmas (Fig. 3) erupted in the CPR form mainly monogenetic volcanic fields (Embey-Isztin et al., 1993; Embey-Isztin and Dobosi, 1995). According to Embey-Isztin et al. (1993) the oldest alkaline volcanism occurred in the western part of the Pannonian Basin and the youngest in the center of this region. In the eastern part of the CPR (Persani Mountains; Transylvanian Basin) late Tertiary-Quaternary volcanism (alkaline and calc-alkaline) accompanied both extension and subduction concurrently occurred (Downes et al., 1995b). In the western part of the CPR the alkaline basalts formed small volcanic centres presented in Burgenland, Little Hungarian Plain, Balaton and Styrian basin (Fig. 2). K/Ar dating indicate that the Burgenland basalts are the earliest alkaline mafic volcanism in the area (11.7–10.8 Ma) (Embey-Isztin et al., 1993; Balogh et al., 1994; Harangi, 2001; Seghedi et al., 2004b; Pécskay et al., 1995, 2006). These basalts erupted in Late Miocene during the late stages of extension in the CPR and could have been directly related to lithospheric thinning (Harangi and Lenkey, 2007). Ali and Ntaflos (2011) concluded that the extension of the Pannonian Basin was accountable for the alkaline magma generation beneath Burgenland through passive upwelling and adiabatic decompression melting of an asthenospheric mantle source. There are two Late Miocene alkaline mafic volcanic centres (Pauliberg and Oberpullendorf) in Burgenland overlying metamorphic rocks (Fig. 2B) (Embey-Isztin et al., 1993; Harangi et al, 1995).

These lava flows cropping out in Burgenland have a maximum thickness of 40 to 45 m and range in compositions from basanites to alkaline basalts and trachybasalts (Embey-Isztin et al., 1993; Harangi et al., 1995; Seghedi et al., 2004b; Ali and Ntaflos, 2011). The Pauliberg basanites intruded the alkali basalts forming dike-like bodies (Ali and Ntaflos, 2011).

The Neogene Styrian Basin (Fig. 2) located at the SE margin of the Alps forming an elongated shape with around 100 km long and 50 km wide. It is filled up by up to 4 km of Neogene clastic sediments and is underline by Austroalpine nappes. Its crustal structure confirms its position in a transition zone between the eastern Alps and the Pannonian region (Ebner and Sachsenhofer, 1995). The crustal thickness ranges from 30 to 27 km (Sachsenhofer et al., 1997) and the lithospheric thickness is about 100 km (Sachsenhofer et al., 1997; Horvath et al., 2006).

During Neogene to Quaternary the Styrian Basin, analogous to the Pannonian Basin, experienced a syn-rift phase of extension occurred during early to middle Miocene and a subsequent post-rift phase took place mainly during Pliocene to Quaternary (Ebner and Sachsenhofer, 1995). These tectonic evolutions accompanied by two types of volcanic activity which formed different volcanic rocks. The earliest magmatism produced K-rich acidic to intermediate volcanic rocks (Harangi, 2001) possibly of subduction-related origin (e.g. Ebner and Sachsenhofer, 1995) whereas during the second phase of volcanism basaltic lava flows were erupted in the SE Styrian Basin. The K/Ar dates of the basaltic volcanism range from 1.7 to 3.8 Ma (Balogh et al., 1994; Pecskay et al., 1995, 2006). The lava flows consist of mafic rock types ranging from highly silica-undersaturated nephelinites (Stradnerkogel, Waltrafelsen) to dominant basanites/nepheline-basanites (Klöch, Steinberg) (Fig. 2B).

Fig. 3. Temporal evolution of the Neogene-Quaternary tectonic and its related volcanism in the CPR (after Harangi and Lenkey, 2007). CA= cal-alkaline; alk.= alkaline; HK= high-K.
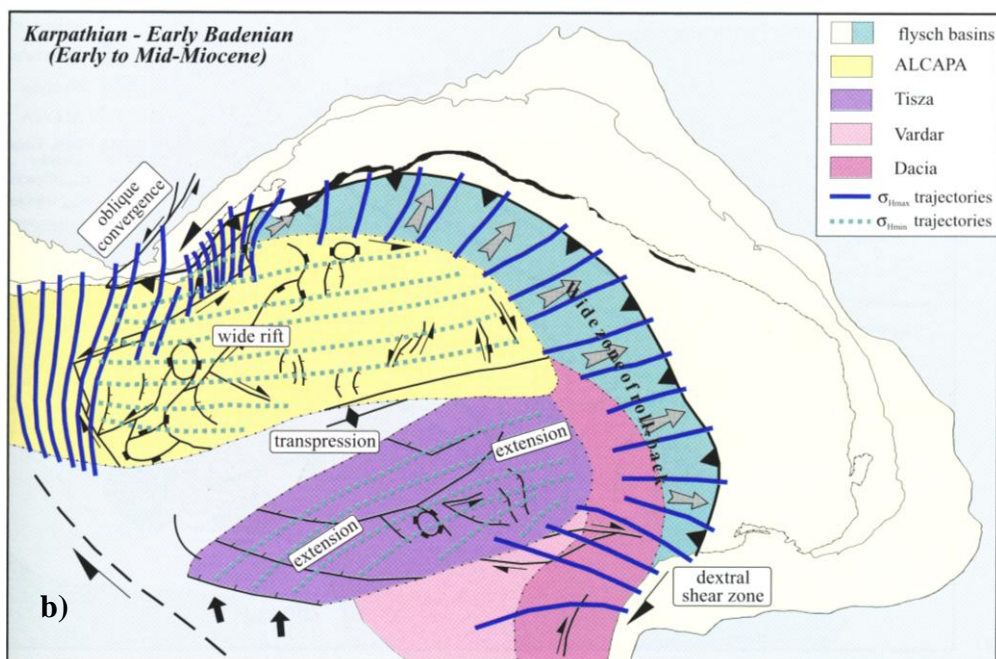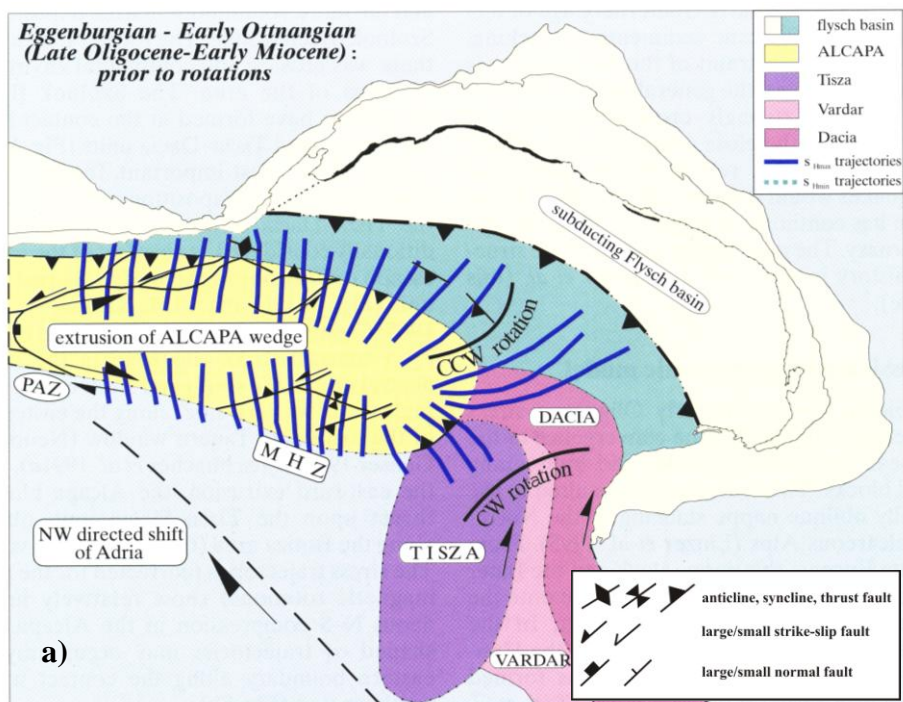
Tectonic evolution

The Intra-Carpathians of the CPR is consisted of two main tectonic terrains, the Alcapa to the northeast and Tisza-Dacia terrains to the southeast. The development of the Pannonian Basin and sub-basins was related to the northward movement of the Adriatic plate and its collision with the European content started in Late Oligocene. The Neogene to Quaternary tectonic evolution of the CPR and its related magmatism are summarized in Figures 3&4.

During Late Oligocene to Early Miocene the major tectonic event characterize the Pannonian Basin was widespread compression phase (N-S to NW-SE) due to Adria push (Fig. 4a). The convergence between European and Adriatic plates caused gravitational collapse of the eastern Alps and stimulated lateral extrusion (E-NE) of the tectonic terrains during this time (Fig. 4a) (Horvath et al., 2006). The Alcapa underwent counter-clockwise rotation whereas Tisza-Dacia rotated in a clockwise direction (Fig. 4a). Both terrains assembled at this stage forming the Pannonian unit and the boundary between the two terrains represented by the Mid-Hungarian tectonic shear zone (Fodor et al., 1999).

In the east Carpathian arc westward subduction produced eastward migration of the Pannonian lithosphere causing the first extension phase during Early to Middle Miocene (Fig. 4b). During this time pull-apart basins (e.g. Styrian basin, Vienna basin, East Slovak basin) were formed at the margins of the Pannonian Basin in transtensional regime. The Pannonian Basin and sub-basins have experienced an overall E-W extension that affected the entire region. The crust and lithosphere of the Pannonian Basin were thinned with a significant crustal thinning took-place in the central part of the basin. Passive rifting occurred due to subduction roll-back of the lithospheric slab along the Carpathian arc. This stage was characterized by lithospheric thinning, subsidence and sediment accumulation (Royden, 1993; Huismans et al., 2002) associated with widespread voluminous calc-alkaline to potassic volcanism (Fig. 3) (Seghedi et al., 2004a; 2010).

The second extension phase during Late Miocene to Early Pliocene associated with asthenospheric upwelling due to lithospheric stretching in the first stage of rifting (Huismans et al., 2002) and was characterized by eruption of alkaline basalts (Fig. 3) (partly mantle xenolith-bearing) (Embey-Isztin and Dobosi, 1995; Seghedi et al., 2004b; Harangi and Lenkey, 2007).

During the late stages of tectonic evolution of the Pannonian Basin which are also related to the continuing northward push of the Adriatic plate, entire consumption of the subducted lithospheric slab occurred and, thus, ending both the subduction along the eastern Carpathians and the extension phase. The Pannonian Basin at this stage became completely landlocked area surrounded and controlled by rigid plate boundary leading to a compression phase occurred mainly in Late Miocene to Quaternary (Fodor et al., 1999; Horvath et al., 2006; Dombradi et al., 2010). During this time basin inversion and tectonic reactivation occurred in the Pannoinan Basin (Csontos, 1995; Fodor et al., 1999; Horvath et al., 2006) (Figs. 3, 4c, d). A compressional stress field with N-S to NW-SE direction has characterized the Pannonian Basin during this stage (Fig. 4d). The compression caused a large-scale folding of the Pannonian lithosphere and subsidence of the basin interior.
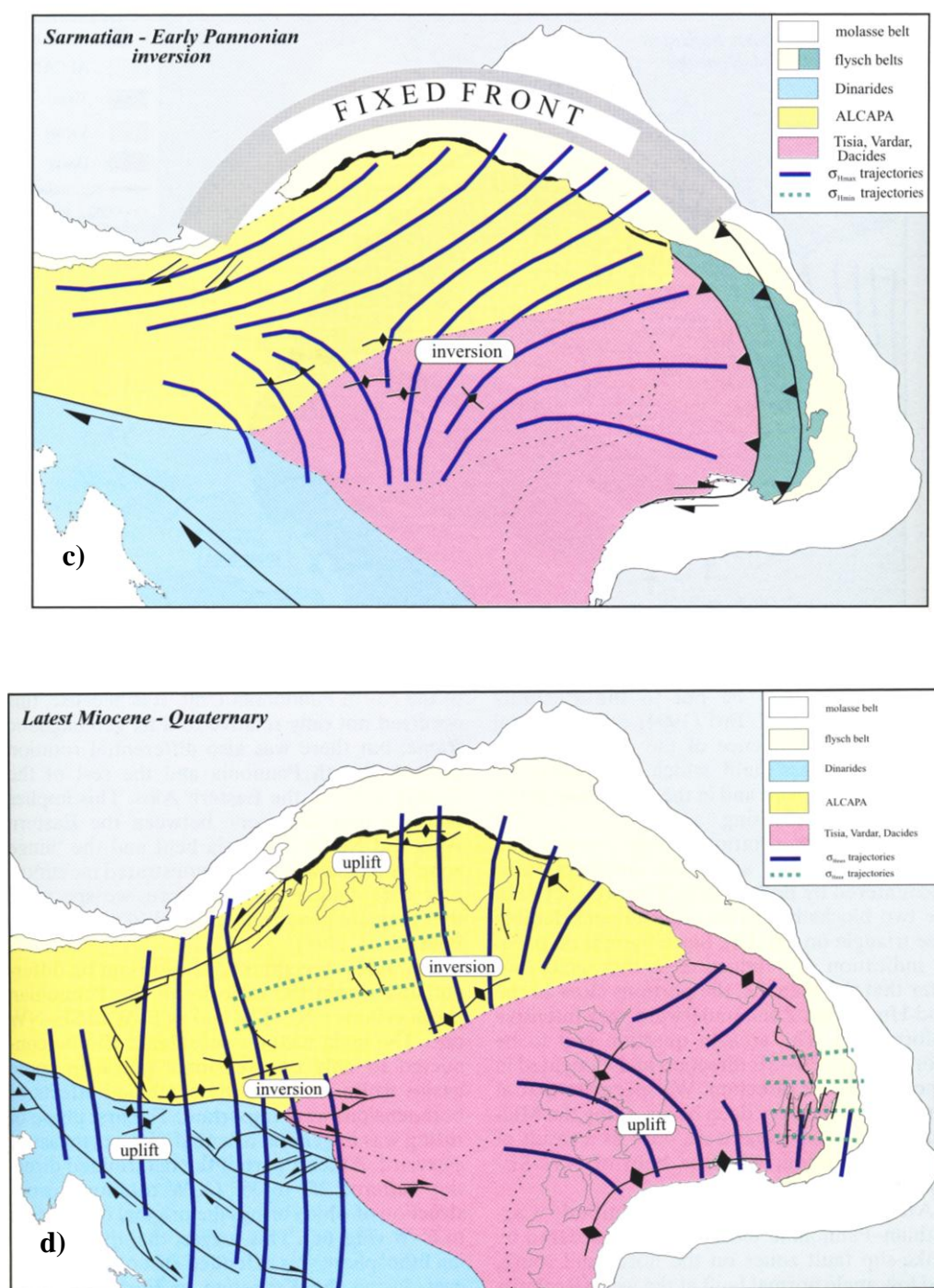
Fig. 4. Tectonic evolution of the Pannonian Basin and kinematic reconstruction of the Alcapa and Tisza-Dacia terrains (after Fodor et al., 1999). PAZ= Periadriatic zone; MHZ= Mid-Hungarian shear zone.

Objectives of this study

Continental *anorogenic* intra-plate volcanism of the CPR occurred during Neogene to Quaternary in a complicated tectonic setting is of fundamental interests for many recent geodynamic hypotheses. The importance of studying these rocks is because their chemical and isotopic data provide an excellent proxy record available to earth scientists for the geodynamics of the continental lithosphere and for geochemical evolution of the asthenospheric mantle, which otherwise inaccessible to direct study.

One of the main goals of this Dissertation was the petrological, mineralogical and geochemical characterization of the continental intra-plate alkaline basaltic magmas that occur as small eruptive centres at Burgenland and SE Styrian Basin. These volcanic rocks comprise alkali basalts, basanites/nepheline-basanites and nephelinites. The other objectives were to determine the mantle source of their primary magmas and to estimate temperature and depth of magma generation. Moreover the origin of these basaltic rocks were addressed, particularly the mechanisms of melt generation, the evolution of the magmas, crustal contamination and possible lithospheric interaction and the role of lithospheric extension and also mantle plume activity.

Methods

Several state of the art analytical methods have been used during this study to ascertain the textural, microstructural and mineralogical characteristics of the alkaline basaltic rocks and to perform mineral chemistry analyses, major and trace element and Nd- and Sr-radiogenic isotope analyses. The main objectives of the present study have been achieved by carrying out the following investigations:

- Optical polarizing microscope to acquire preliminary information on textures and mineralogical compositions of these lavas.

- Electron probe microanalysis (EPMA) for detailed study of micro-textures and mineral-phase reactions as well as mineral and matrix chemistry.

- X-ray fluorescence analysis (XRF) to determine bulk rock geochemical compositions of the lavas (major and trace elements).

- Inductively coupled plasma mass-spectrometry technique (ICP-MS) to measure bulk rock minor, trace and rare earth element compositions of the lavas.

- Thermal ionization mass spectrometry (TIMS) to measure Sr-Nd isotopic compositions which is important to identify the mantle sources of the alkaline basaltic magma.

SYNTHESIS

Chapters II and III represent the main contributions of my PhD thesis and are already in diverse stages of publication. They comprise two scientific contributions, one has been already published and one in submission stage, of the studied alkaline mafic lavas.

Chapter II deals with primitive alkali basalts from Burgenland (Pauliberg and Oberpullendorf) which located at the western CPR to provide petrological constraints on the origin of these magmatic rocks as well as in this paper the depths and degrees of partial melting and mantle Tp were discussed.

Burgenland lavas represent the earliest alkaline mafic volcanism in the CPR and were erupted in Late Miocene during the late stages of extension. These lavas composed of alkali basalts and basanites. The geochemical compositions of the Pauliberg lavas (alkali basalts and basanites) suggest derivation by variable low degrees of melting from the same mantle source. Compared to other Neogene-Quaternary alkaline basalts from the CPR, these basalts are characterized by notably higher TiO_2 and lower Al_2O_3 contents. The high Ti could be related to low degrees of melting (beneath thick lithosphere) of a peridotite mantle source that had been affected by Ti-rich recycled ancient oceanic crust, while the low Al and high La/Yb_N suggest residual garnet in the source region. The depletion in LILE and the high Nb/La and Ce/Pb ratios (OIB-like) in the Pauliberg basalts exclude any crustal contamination and/or interaction with subduction-related melts/fluids.

The Sr and Nd isotopic compositions of Burgenland basalts lie within the range of OIB values and are comparable to Tertiary–Quaternary alkaline basalts from Western and Central Europe (Wilson and Downes, 1991). The $^{206}Pb/^{204}Pb$ isotopic ratios in Burgenland basalts are relatively high (19.6–19.7) suggesting HIMU/OIB-like characteristics (Embey-Isztin et al., 1993).

The mantle Tp calculations indicate that the Burgenland basalt produced from mantle at ambient temperature without any thermal anomaly, providing an additional argument against plume activity beneath the Pannonian Basin. Therefore we propose that late Miocene lithospheric extension of the Pannonian Basin led to alkaline melt generation beneath the studied area through passive upwelling and adiabatic decompression melting of an asthenospheric mantle source.

Chapter III discusses the petrogenesis and mantle source characteristics of strongly alkaline primitive mafic volcanic rocks from the Styrian Basin. These lavas were erupted during Pliocene to Quaternary and post-date the extension phase in the CPR. They consist of highly silica-undersaturated nephelinites (Stradnerkogel and Waltrafelsen) and dominant basanites/nepheline-basanites (Klöch and Steinberg). Their geochemical compositions suggest negligible crustal contamination and/or interaction with lithospheric mantle. The high Mg# (>63) and high compatible element contents (Ni, 128–156 ppm; Cr, 124–144 ppm) of the Klöch basanites/nepheline-basanites indicate that they are close to primary magma criteria.

The increasing of silica-undersaturation, alkalis, CaO/Al_2O_3, LREE and La/Yb from basanite/nepheline-basanite to nephelinite are consistent with decreasing degrees of partial melting at increasing depths in the mantle. The estimated depths of magma generation from basanites/nepheline-basanites are mostly >100 km whereas, the nephelinitc magma could be originated at ~135 km or greater depths in the garnet stability field.

The calculated depths of magma generation verify that the magma must have been generated in the asthenosphere. The basanites/nepheline-basanites yield temperatures of melting that range from ~1400 ^{o}C to ~1500 ^{o}C.

The most primitive Styrian sample, a basanite KL-2, suggests significant olivine fractionation and slight clinopyroxene fractionation of its primary magma, consequently even if considered cautiously the calculated mantle potential temperature (1466 ^{o}C) suggests that the Styrian magmas originated from asthenospheric mantle at ambient temperature and proving that there is no plume activity beneath the study area.

Geochemical signatures of nephelinites include high Zr/Hf (51-67) and La/Yb$_{N}$ (29-31) ratios and negative K and Ti anomalies resemble those of carbonatites. These geochemical characteristics may suggest that their astheospheric mantle source underwent enrichment with carbonatitic liquids which is further indicated by presence of about 5% CO_2 in their petrogenesis. Compared to nephelinites, the basanites/nepheline-basanites have higher SiO_2 and lower CaO contents suggesting insignificant role of CO_2 at increasing degrees of melting.

The general similarity of the trace element distribution patterns and the very narrow range of the Sr-Nd isotopic ratios indicate that the Styrian lavas were derived from similar asthenospheric mantle source, volatile-enriched, close to EAR-type.

REFERENCES

Ali, Sh., Ntaflos, Th., 2011. Alkali basalts from Burgenland, Austria: Petrological constraints on the origin of the westernmost magmatism in the Carpathian–Pannonian Region. Lithos 121, 176–188.

Balogh, K., Ebner, F., Ravasz, Cs., 1994. K/Ar alter tertiärer Vulcanite de südöstlischen Steiermark und des südlischen Burgenlands, in: Császár, G., Daurer, A. (Eds.), Jubiläumsschrift 20 Jahre Geologischen Zusammenarbeit Österreich-Ungarn Lobitzer, 55– 72.

Bradshaw, T.K., Hawkesworth, C.J., Gallagher, K., 1993. Basaltic volcanism in the Southern Basin and Range: no role for a mantle plume. Earth and Planetary Science Letters 116, 45–62.

Csontos, L., 1995. Tertiary tectonic evolution of the Intra-Carpathian area: A review, in: Downes, H., Vaselli, O. (Eds.), Neogene and Related Magmatism in the Carpatho-Pannonian Region. Acta Vulcanologica 7, 1–13.

Dombrádi, E., Sokoutis, D., Bada, G., Cloetingh, S., Horváth, F., 2010. Modelling recent deformation of the Pannonian lithosphere: Lithospheric folding and tectonic topography. Tectonophysics 484, 103–118.

Downes, H., Pantó, GY., Póka, T., Mattey, D.P., Greenwood, P.B., 1995a. Calc-alkaline volcanics of the Inner Carpathian arc, Northern Hungary; new geochemical and oxygen isotopic results. Acta Vulcanologica 7, 29–41.

Downes, H., Seghedi, I., Szakacs, A., Dobosi, G., Vaselli, O., James, D.E., Rigby, I.J., Thirlwall, M.F., Rex, D., Pécskay, Z., 1995b. Petrology and geochemistry of late Tertiary/Quaternary mafic alkaline volcanism in Romania. Lithos 35, 65–81.

Ebner, F., Sachsenhofer, R.F., 1995. Palaeogeography, subsidence and thermal history of the Neogene Styrian Basin (Pannonian basin system, Austria). Tectonophysics 242, 133–150.

Embey-Isztin, A. Dobosi, G., 1995. Mantle source characteristics for Miocene–Pleistocene alkali basalts, Carpathian–Pannonian Region: a review of trace elements and isotopic composition, in: Downes, H., Vaselli, O. (Eds.), Neogene and related magmatism in the Carpatho-Pannonian Region. Acta Vulcanologica 7(2), 155–166.

Embey-Isztin, A., Downes, H., James, D.E., Upton, B.G.J., Dobosi, G., Ingram, G.A., Harmon, R.S., Scharbert, H.G., 1993. The petrogenesis of Pliocene alkaline volcanic rocks from the Pannonian Basin, Eastern Central Europe. Journal of Petrology 34, 317–343.

Fitton, J.G., James, D., Leeman, W.P., 1991. Basic magmatism associated with Late Cenozoic extension in the Western United States: compositional variations in space and time. Journal of Geophysical Research 96, 13693–13711

Fodor, L., Csontos, L., Bada, G., Györfi, I., Benkovics, L., 1999. Tertiary tectonic evolution of the Pannonian Basin system and neighboring orogens: A new synthesis of palaeostress data, in: Durand, B., Jolivet, L.F.H., Séranne, M., (Eds.), The Mediterranean Basins: Tertiary Extension within the Alpine Orogen: Geological Society of London Special Publication 156, 295–334.

Harangi, S., 2001. Neogene magmatism in the Alpine–Pannonian Transition Zone– a model for melt generation in a complex geodynamic setting. Acta Vulcanologica 13, 25–39.

Harangi, S., Downes, H., Seghedi, I., 2006. Tertiary-Quaternary subduction processes and related magmatism in the Alpine-Mediterranean region, in: Gee, D.G., Stephenson, R.A. (Eds.), European Lithosphere Dynamics. Geological Society of London Memoir 32, 167–190.

Harangi, S., Lenkey, L., 2007. Genesis of the Neogene to Quaternary volcanism in the Carpathian–Pannonian region: Role of subduction, extension, and mantle plume, in: Beccaluva, L., Bianchini, G., Wilson, M. (Eds.), Cenozoic Volcanism in the Mediterranean Area. Geological Society of America Special Paper 418, 67–92.

Harangi, S., VaseIli, O., Tonarini, S., Szabó, Cs., Harangi, R., Coradossi, N., 1995. Petrogenesis of Neogene extension-related alkaline volcanic rocks of the Little Hungarian Plain volcanic field (Western Hungary), in: Downes, H., VaseIli, O. (Eds.), Neogene and related magmatism in the Carpatho-Pannonian Region. Acta Vulcanologica 7(2), 173–187.

Horváth, F., Bada, G., Szafián, P., Tari, G., Ádám, A., Cloetingh, S.A.P.L., 2006. Formation and deformation of the Pannonian basin: Constraints from observational data, in: Gee, D.G., Stephenson, R.A. (Eds.), European Lithosphere Dynamics. Geological Society, London, Memoirs 32, 191–206.

Lustrino, M., Wilson, M., 2007. The circum-Mediterranean anorogenic Cenozoic igneous province. Earth Science Reviews 81, 1–65.

Pécskay, Z., Lexa, J., Szakacs, A., Balogh, K., Shegedi, I., Konecy, V., Kovacs, M., Marton, E., Kaliciak, M., Szeki-Fux, V., Poka, T., Gyarmati, P., Edelstein, O., Rosu, E., Zec, B., 1995. Space and time distribution of Neogene–Quaternary volcanism in the Carpatho-Pannonian region, in: Downes, H., Vaselli, O. (Eds.), Neogene and related volcanism in the Carpatho-Pannonian Region. Acta Volcanologica Special Issue 7, 15–28.

Pécskay, Z., Lexa, J., Szakács, A., Seghedi, I., Balogh, K., Konečný, V., Zelenka, T., Kovacs, M., Póka, T., Fülöp, A., Márton, E., Panaiotu, C., Cvetković, V., 2006. Geochronology of Neogene magmatism in the Carpathian arc and Intra-Carpathian area: a review. Geologica Carpathica 57, 511–530.

Royden, L.H., 1993. Evolution of retreating subduction boundaries formed during continental collision. Tectonics 12, 629–638.

Sachsenhofer, R.F., Lankreijer, A., Cloetingh, S.A.P.L., Ebner, F., 1997. Subsidence analysis and quantitative basin modeling in the Styrian Basin (Pannonian Basin system, Austria). Tectonophysics 272, 175–196.

Schmid, S.M., Bernoulli, D., Fügenschuh, B., Matenco, L., Schefer, S., Schuster, R., Tischler, M., Ustaszewski, K., 2008. The Alpine–Carpathian–Dinaridic orogenic system: correlation and evolution of tectonic units. Swiss Journal of Geosciences 101 (1), 139–183.

Seghedi, I., Downes, H., Szakacs, A., Mason, P.R.D., Thirlwall, M.F., Rosu, E., Pecskay, Z., Marton, E., Panaiotu, C., 2004a. Neogene–Quaternary magmatism and geodynamics in the Carpathian–Pannonian region: A synthesis. Lithos 72, 117–146.

Seghedi, I., Downes, H., Vaselli, O., Szakács, A., Balogh, K. and Pécskay, Z., 2004b. Post-collisional Tertiary–Quaternary mafic alkalic magmatism in the Carpathian–Pannonian region: a review. Tectonophysics 393, 43–62.

Seghedi, I., Maţenco, L., Downes, H., Mason, P.R.D., Szakács, A., Pécskay, Z., 2010. Tectonic significance of changes in post-subduction Pliocene–Quaternary magmatism in the south east part of the Carpathian–Pannonian Region. Tectonophysics. doi:10.1016/j.tecto.2009.12.003.

Smith, E.I., Sánchez, A., Walker, J.D., Wang, K., 1999. Geochemistry of mafic magmas in the Hurricane Volcanic Field, Utah: implications for small- and large scale chemical variability of the lithospheric mantle. Journal of Geology 107, 433–48.

Wilson, M., Bianchini, G., 1999. Tertiary-Quaternary magmatism within the Mediterranean and surrounding regions, in: Durand, B., Jolivet, L., Horvath, F., Seranne, M. (Eds.), The Mediterranean Basins: Tertiary Extension within the Alpine Orogen. Geological Society of London Special Publication 156, 141–168.

Wilson, M., Downes, H., 1991. Tertiary-Quaternary extension-related alkaline magmatism in Western and Central Europe. Journal of Petrology 32, 811–849.

Wilson, M., Downes, H., 2006. Tertiary-Quaternary intra-plate magmatism in Europe and its relation to mantle dynamics, in: Gee, D.G., Stephenson, R.A. (Eds.), European Lithosphere Dynamics. Geological Society of London, Memoirs 32, 147–166.

Wilson, M., Patterson, R., 2001. Intra–plate magmatism related to short wavelength convective instabilities in the upper mantle: Evidence from the Tertiary–Quaternary volcanic province of western and central Europe, in: Ernst, R.E., Buchan, K.L. (Eds.), Mantle Plumes: Their Identification through Time. Geological Society of America Special Paper 352, 37–58.

Wortel, M.J.R., Spakman, W., 2000. Subduction and slab detachment in the Mediterranean-Carpathian region: Science 290, 1910–1917.

Zeng, G., Chen, L.-H., Xu, X.-S., Jiang, S.-Y., Hofmann, A.W., 2010. Carbonated mantle sources for Cenozoic intra-plate alkaline basalts in Shandong, North China. Chemical Geology 273, 35–45.
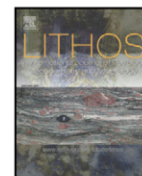
CHAPTER II

Ali, Sh., Ntaflos, Th., 2011a. Alkali basalts from Burgenland, Austria: Petrological constraints on the origin of the westernmost magmatism in the Carpathian–Pannonian Region. Lithos 121, 176–188.

Contents lists available at ScienceDirect

Lithos

journal homepage: www.elsevier.com/locate/lithos

Alkali basalts from Burgenland, Austria: Petrological constraints on the origin of the westernmost magmatism in the Carpathian–Pannonian Region

Shehata Ali [a,b,*], Theodoros Ntaflos [a]

[a] Department of Lithospheric Research, University of Vienna, Althanstrasse 14, A-1090 Vienna, Austria
[b] Geology Department, Faculty of Science, Minia University, El-Minia, Egypt

ARTICLE INFO

ABSTRACT

At the end of the syn-extensional phase in the Carpathian–Pannonian Region (CPR), alkaline mafic magmas were erupted during the Late Miocene in Burgenland.

The majority of these lavas (Pauliberg and Oberpullendorf) are basalts and tephrite basanites. They have been slightly affected by high-pressure (>1.3 GPa) clinopyroxene fractionation. In the Burgenland basalts, olivine and clinopyroxene phenocrysts, as well as groundmass olivine, clinopyroxene and plagioclase grew at lower pressures. The geochemistry of the Pauliberg lavas (alkali basalts and basanites) indicates that they originated by low, but variable, degrees of melting from the same source mantle. The Pauliberg basaltic rocks have significantly higher TiO_2 and lower Al_2O_3 contents, compared to those of Late Miocene to Recent alkaline basalts from the Pannonian Basin. The Ti enrichment could be attributed to low degrees of melting (beneath thick lithosphere) of a peridotite source that had been affected by Ti-rich recycled ancient oceanic crust, whereas the low Al and high $(La/Yb)_N$ suggest that there was residual garnet after partial melting. The depletion in K, Rb and Ba relative to Nb and the high Nb/La and Ce/Pb ratios (OIB-like) in the Pauliberg basalts, rule out any interaction with subduction-related melts/fluids and/or contamination with crustal material.

Sr and Nd radiogenic isotopes range from 0.703687 to 0.704279 and from 0.512736 to 0.512774 respectively, with the basanites being the most depleted. The Oberpullendorf sample has Sr and Nd isotopic ratios ($^{87}Sr/^{86}Sr = 0.704279$; $^{143}Nd/^{144}Nd = 0.512736$) similar to those of other Pannonian basalts, e.g. Saghegy. The Burgenland basalts have relatively high $^{206}Pb/^{204}Pb$ isotopic ratios (19.6–19.7) suggesting a HIMU/OIB-like character (Embey-Isztin et al., 1993).

The calculated mantle potential temperature for the Pauliberg basalts is 1386 °C and a melt fraction of ~2%. Similar calculations for the Oberpullendorf basalt indicate clinopyroxene fractionation. This leads to an overestimate of the mantle potential temperature (1530 °C), making it impossible to calculate the degree of partial melting involved in the genesis of the primary magma. These calculations indicate that the Burgenland basalt melted from mantle at ambient temperature. i.e. no thermal anomaly is indicated, providing an additional argument against plume activity beneath the Pannonian Basin. Consequently we propose that late Miocene lithospheric extension of the Pannonian Basin gave rise to alkaline melt generation beneath the studied area through passive upwelling and adiabatic decompressional melting of an asthenospheric mantle source.

© 2010 Elsevier B.V. All rights reserved.

1. Introduction

In the Carpathian–Pannonian Region (CPR), Neogene volcanism occurred in a complex geodynamic setting. The syn-extensional phase comprised Middle Miocene potassic intermediate to acidic volcanic rocks in the Styrian Basin and Late Miocene alkali basalts in Burgenland and Little Hungarian Plain (Harangi, 2001). The post-extensional phase was characterized by eruption of alkali basalts during the Pliocene to Quaternary in the Styrian Basin. The potassic volcanism has been attributed to decompression melting of attenuated lithospheric mantle, which had been previously affected by hydrous K-rich metasomatic agents (Harangi, 2001). In contrast, the alkaline basaltic magma generation was attributed to passive upwelling and decompression melting (Harangi, 2001) or to the rise of finger-like plumes of an asthenospheric source (Seghedi et al., 2004b). In the western Pannonian area the alkaline mafic volcanism was preceded by calc-alkaline magmatism related to post-collision subduction.

The Neogene alkaline volcanism of the Carpathian–Pannonian Region has been extensively studied (e.g. Embey-Isztin et al., 1993; Embey-Isztin and Dobosi, 1995; Harangi, 2001; Seghedi et al., 2004b). Pécskay et al. (1995a) present a comprehensive review of the timing of magmatic activity. Embey-Isztin et al. (1993b) suggested that the Pannonian Basin magmas were mainly generated from melting of an asthenospheric source. Harangi (2001) proposed that the Neogene

* Corresponding author.
E-mail addresses: Shehata_aly@yahoo.com, Shehata.ali@univie.ac.at (Sh. Ali).

alkaline mafic magmas were derived from low degrees of melting at different depths due to decompression of hot asthenospheric mantle. Embey-Isztin and Dobosi (1995) and Seghedi et al. (2004b) proposed that mantle plumes were involved in the petrogenesis of the alkali basalts.

Harangi and Lenkey (2007) argued against the existence of mantle plume underneath the studied area and concluded that the melt generation was related to flow of heterogeneous asthenospheric mantle, close to its solidus, in association with Miocene lithospheric extension.

The composition and origin of continental intra-plate alkaline basalts have been the subject of debate for several decades. The magma genesis has been attributed either to decompression melting triggered by lithospheric extension or to temperature increase resulting from an upwelling mantle plume. To what extent the lithospheric mantle participates in such magma generation remains contentious. In order to contribute towards answering this question we provide additional evidence from Burgenland at the western margin of the Pannonian Basin. Apart from a few analyses from the Burgenland volcanoes (a total of five analyses over the last 25 years) reported in review papers (Embey-Isztin et al., 1993; Harangi et al., 1995; Seghedi et al., 2004b), there are no detailed or comprehensive studies of the lavas. The present paper deals with the petrology, mineralogy and geochemistry of the alkaline basalts that occur in small volcanic centres at Pauliberg and Oberpullendorf, in Burgenland.

This study presents data on these primitive mafic rocks in order to provide constraints relating to the composition and mineralogy of their mantle sources and the depth and degree of partial melting that were involved.

2. Geodynamic background

The Pannonian Basin is surrounded by the Alpine, Carpathian and Dinaride orogenic belts (Fig. 1) and is characterized by thin mantle lithosphere (50–80 km thick) of which the crust composes the upper 22–30 km (Horváth et al., 2006). The intra-Carpathian region consists mainly of two terrains: i) the Eastern Alpine–Western Carpathian–Northern Pannonian ("ALCAPA") and ii) the Southern Pannonian–Eastern Carpathian ("Tisza–Dacia") terrain. The formation of the Pannonian Basin and sub-basins, such as the Styrian and the Vienna Basins, is attributed to the northward motion of the Adriatic plate and its collision with the Southern Alps starting in the late Oligocene. As a consequence of compressional forces, the ALCAPA terrain was separated from the Southern Alps, migrating eastward with a counter-clockwise rotation and the Tisza–Dacia terrain simultaneously moving north-eastwards with a clockwise rotation. These tectonics led to the amalgamation of the two terrains and the creation of the Pannonian unit which, in the Early Miocene experienced extension as the result of the retreat and roll-back of the subducting lithospheric slab along the Carpathian arc. Two stages of extension have been recognized in the Pannonian basin. The first stage (17.5–14 Ma) produced a passive rift characterized by lithosphere thinning, subsidence and sediment accumulation (Huismans et al., 2002; Royden, 1993) with widespread voluminous calc-alkaline- to potassic volcanism (Seghedi et al., 2004a). The second stage (Late Miocene to Recent) has been attributed to the strong asthenospheric upwelling related to the lithospheric extension that occurred in the first stage of rifting (Huismans et al., 2002). The second stage was characterized by small volume alkali magma generation (partly mantle xenolith-bearing) (Embey-Isztin and Dobosi, 1995; Harangi and Lenkey, 2007).

Alkali basaltic magmas erupted in the western Carpathian–Pannonian Region formed small volcanic centres in Burgenland, the Little Hungarian Plain, Balaton and the Styrian basin. According to K/Ar dating, the Burgenland basalts are the oldest alkaline mafic volcanic rocks in the area (11.7–10.8 Ma) (Balogh et al., 1994; Embey-Isztin et al., 1993; Harangi, 2001; Pécskay et al., 1995, 2006; Seghedi et al., 2004b). Burgenland contains two Late Miocene alkaline
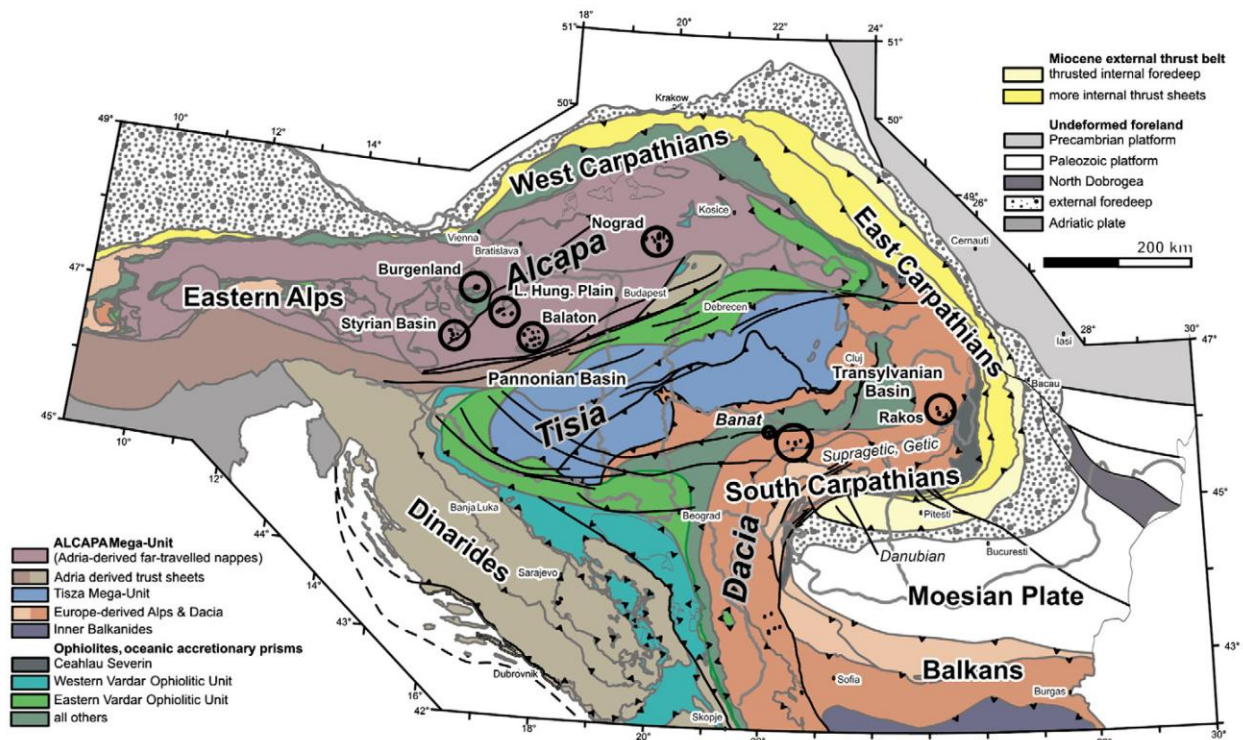

Fig. 1. Geologic/tectonic map of the Carpathian–Pannonian and Eastern Alpine region. Late Miocene–Pleistocene alkaline basalt occurrences in the region are outlined (after Embey-Isztin et al., 1993; Tschegg et al., 2010).

mafic volcanic centres (Pauliberg and Oberpullendorf), overlying metamorphic rocks (Embey-Isztin et al., 1993; Harangi et al., 1995). The lava flows have a maximum thickness of 40–45 m (Harangi et al., 1995) and range from basanites to alkaline basalts and trachybasalts (Embey-Isztin et al., 1993; Harangi et al., 1995; Seghedi et al., 2004b). The Pauliberg basanites form dike-like bodies intruding the alkaline basalts. The sampled volcanic rocks are alkali basalts and basanites.

3. Analytical methods

The petrography of representative thin-sections of the samples was investigated using an optical polarizing microscope. Microtextures, mineral- and matrix-chemistry as well as mineral-phase reactions were investigated using polished carbon-coated thin-sections and a CAMECA SX-100 electron microprobe (University of Vienna, Department of Lithospheric Research). All analyses were made against natural and synthetic mineral standards, using four wavelength-dispersive spectrometers; acceleration voltage and beam current were 15 kV and 20 nA respectively, and standard correction procedures were applied. Pyroxenes and oxides were analyzed with a focused 1 μm beam, whereas all feldspar analyses were carried out with an expanded 5 μm beam diameter, minimizing the loss of Na and K.

Whole rock major and the trace elements Ba, Co, Cr, Ga, Ni, Rb, Sc, Sr, V, Zn and Zr were analyzed with the sequential X-ray spectrometer Phillips PW 2400, equipped with a Rh-excitation source (University of Vienna, Department of Lithospheric Research). Fused beads were produced at 950 °C from a mixture of specimen and $Li_2B_4O_7$ flux, diluted 1:5 to gain accurate and precise results. The Oberpullendorf samples are heavily altered and only one sample (OB-1), with Ba/Rb = 14 satisfied the criteria for freshness of Halliday et al. (1995) i.e. that Ba/Rb should be between 5 and 20. Compared to the other samples, this sample, under the microscope, shows only moderate alteration. Replicate analyses of geo-standard GSR-3 gave an overall procedural error better than 2% for major elements and 5%, (Cu = 8.5%) for trace elements (The relative procedural error and accuracy are given in Supplementary Table A).

Rare earth elements (REE), Y, Nb, Ta, Hf, U and Th were analyzed by ICP-MS techniques (ELAN 6100) at the University of Vienna, Dept. of Lithospheric Research. Replicate analyses of geo-standard BHVO-1 gave an overall procedural error better than 2% and for Th 7.5% (The relative procedural error and accuracy are given in Supplementary Table A). Sm–Nd and Rb–Sr analysis was performed at the Laboratory of Geochronology, Dept. of Lithospheric Research, University of Vienna, with a ThermoFinnigan® Triton TI TIMS. During the period of measurement, standard values were: $^{87}Sr/^{86}Sr = 0.710270 \pm 0.000004$ (n = 6) for NBS987 and Nd = 0.511842 ± 0.000002 (n = 7) for La Jolla international standards. Sample preparation and analytical procedures are described by Thöni et al. (2008).

4. Results

4.1. Petrography

The Burgenland basalts are porphyritic with a fine-grained holocrystalline groundmass (Fig. 2a,b). The samples studied comprise olivine and minor clinopyroxene phenocrysts in a groundmass of olivine, clinopyroxene and plagioclase. Whereas alkali feldspar and titanomagnetite occur as minor components in all the alkali basalts, nepheline, leucite and phlogopite are found only in the Pauliberg samples.

The olivines phenocrysts are clear, rounded, tabular and prismatic euhedral to subhedral crystals, 200 to 1000 μm across. In some samples, rare, anhedral, olivine xenocrysts (2 mm) have been found. Clinopyroxenes form euhedral to subhedral phenocrysts (150–1000 μm) and needle to lath-shaped crystals in the groundmass (~30 μm). Usually, they exhibit oscillatory and sector zoning (Fig. 2b).
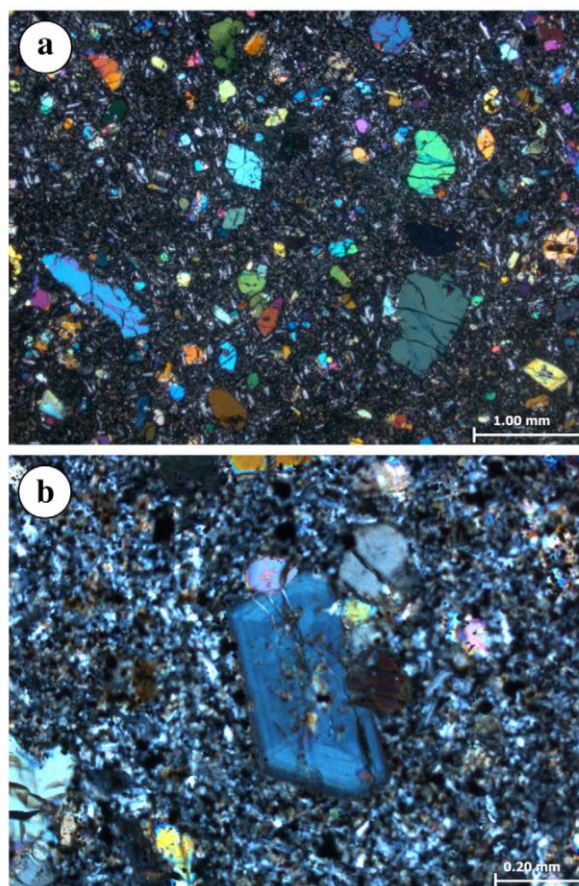
Fig. 2. Photomicrographs showing the petrography features of the investigated basalts taken in crossed polarized light. a) Porphyritic texture shows olivine phenocrysts set in fine-grained matrix. b) Euhedral clinopyroxene phenocryst displaying oscillatory and sector zoning.

Plagioclase is restricted to the groundmass and, in a few cases, is overgrown by anorthoclase. Small, late-stage crystals of alkali feldspar can occur within the groundmass as can phlogopite.

The accessory minerals include titanomagnetite, ilmenite, spinel and apatite. An insignificant amount of secondary minerals such as calcite, dolomite and zeolite, growing in free spaces were also found. Summary of the petrographic description of the samples is listed in Table 1.

4.2. Mineral chemistry

4.2.1. Olivines

Representative compositions of the olivines are presented in Supplementary Table B1. The phenocryst cores range from $Fo_{87–79}$ whereas xenocrysts from Pauliberg have compositions typical of depleted mantle peridotites ($Fo_{92–91}$). Olivine phenocrysts from both, Pauliberg and Oberpullendorf, are typically normally zoned with rim compositions of $Fo_{80–66}$, comparable to the groundmass olivines. The NiO contents decrease with the Mg-number, whereas CaO and MnO contents increase (Fig. 3). The most fayalitic olivines contain generally 0.40–0.59 wt.% MnO and 0.23–0.51 wt.% CaO.

4.2.2. Clinopyroxenes

Representative clinopyroxene compositions are given in Supplementary Table B2. The phenocrysts are usually zoned, either showing concentric or sector zoning (Fig. 2b). Some cores show hour-glass

Table 1
Summary of the petrographic description of the samples.

Sample	Rock type	Phenocrysts	Microphenocrysts and groundmass	Textures/structure
PLB-1	Basanite	Ol, Cpx	Cpx, Ol, Pl, Afs, Ne, Lc, Phl, Ti-mag, Ap	Fine grained, porphyritic, seriate, massive
PLB-3	Basalt	Ol	Pl, Cpx, Ol, Ti-mag, Ilm	Porphyritic, intergranular, skeletal olivine
PLB-4	Basalt	Ol, Cpx	Ol, Cpx, Pl, Phl, Ti-mag	Glomero-porphyritic, intergranular, massive
PLB-5	Basalt	Ol	Cpx, Ol, Pl, Phl, Ti-mag, Ilm	Seriate, Glomero-porphyritic, skeletal olivine
PLB-6	Basalt	Ol, Cpx	Cpx, Ol, Pl, Phl, Ti-mag, Ap	Fine grained, porphyritic, seriate, massive
PLB-7	Basalt	Ol	Cpx, Ol, Pl, Afs, Phl, Lc, Ti-mag, Ilm, Ap, Spl, Cal	Glomero-porphyritic, intergranular, seriate
PLB-8	Basalt	Ol	Cpx, Ol, Pl, Ne, Lc, Phl, Ti-mag	Glomero-porphyritic, seriate, massive
PLB-9	Basalt	Ol, Cpx	Cpx, Ol, Pl, Phl, Ti-mag, Ilm, Cal	Fine grained, porphyritic, skeletal olivine
PLB-10	Basanite	Ol	Ol, Cpx, Pl, Phl, Afs, Ne, Ti-mag, Ilm, Ap	Porphyritic, amygdaloidal, fine grained
PLB-11	Basalt	Ol, Cpx	Ol, cpx, pl, phl, Ti-mag, Ilm	Intergranular, glomero-porphyritic, massive
PLB-12	Basalt	Ol, Cpx	Ol, Cpx, Pl, Phl, Ti-mag	Porphyritic, seriate, massive, fine grained
PLB-13	Basalt	Ol, Cpx	Cpx, Ol, Pl, Phl, Ti-mag, Ilm, Ap	Intergranular, porphyritic, massive
PLB-14	Basalt	Ol, Cpx	Ol, cpx, pl, phl, Ti-mag, Ilm	Porphyritic, seriate, intergranular
PLB-15	Basalt	Ol, Cpx	Ol, Cpx, Pl, Afs, Ilm, Ti-mag, Spl	Vesicular, porphyritic, fine grained
OB-1	Basalt	Ol, Cpx	Ol, Cpx, Pl, Ti-mag, Ilm, Afs, Ap	Porphyritic, seriate, amygdaloidal

Abbreviations: Afs = alkali feldspar; Ap = apatite; Cal = calcite; Cpx = clinopyroxene; Ilm = ilmenite; Lc = leucite; Ne = nepheline; Ol = olivine, Phl = phlogopite; Pl = plagioclase; Spl = spinel; Ti-mag = titanomagnetite.

sector zoning. The variation between core and rim compositions follows the normal fractionation trend, the cores have higher Mg, Si and Cr and lower Fe, Mn, Ti and Al than the rims.

The compositions (based on the IMA nomenclature, after Morimoto et al., 1988) are displayed in Fig. 4. Whilst the majority of Pauliberg pyroxenes plot in the diopside field, some plot in the augite field. Conversely, the Oberpullendorf clinopyroxenes plot mainly in the augite field. The cores are generally poorer than the rims in Ca and Fe (Fig. 4). The phenocryst rims and groundmass grains in the Pauliberg basalts have more Ca than comparable late-stage pyroxenes from Oberpullendorf (Fig. 4). Ti and Al contents vary widely: TiO_2 ranges from 0.6 to 4.56 wt.% whereas Al_2O_3 contents range between 2.01 and 7.08 wt.%.

4.2.3. Phlogopites

Phlogopite occurs as a minor constituent in the interstices between the groundmass minerals of the Pauliberg basalts (but is absent in the Oberpullendorf rocks). TiO_2 and MgO contents vary from 4.97 to 9.88 wt.% and from 15.1 to 18.5 wt.% respectively and K_2O varies from 8.48 to 9.47 wt.%. CaO and Na_2O contents are low (<1 wt.%), as well as, MnO (<0.1 wt.%). Fluorine (0.99–1.27 wt.%) and BaO (0.18–0.33 wt.%) contents are notably low (Supplementary Table B3).

4.2.4. Plagioclases

Representative compositions of the plagioclases are presented in Supplementary Table B4, together with their structural formulae and compositional ratios. Those from Oberpullendorf have the highest An-contents ($An_{60.2–26}$) whereas plagioclases in the Pauliberg basalts range from $An_{54.1–17}$. The compositions are plotted (Fig. 5) in the Ab–Or–An ternary plot. All the points lie close to the An–Ab join: orthoclase shows systematic increase with decreasing anorthite content.

The plagioclases are strongly zoned: CaO decrease whilst Na_2O and K_2O increase from core to rim (Table B4). A systematic decrease in CaO
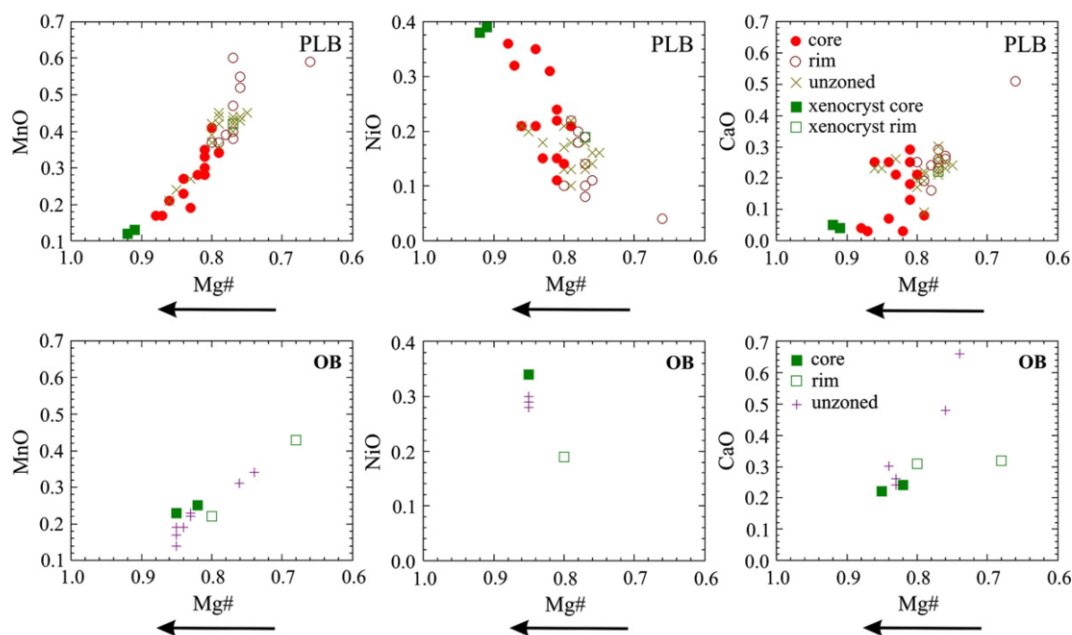
Fig. 3. Variation of MnO, CaO and NiO vs. Mg-number (Mg#) in olivines of Burgenland alkali basalts. Note, PLB = Pauliberg, OB = Oberpullendorf.
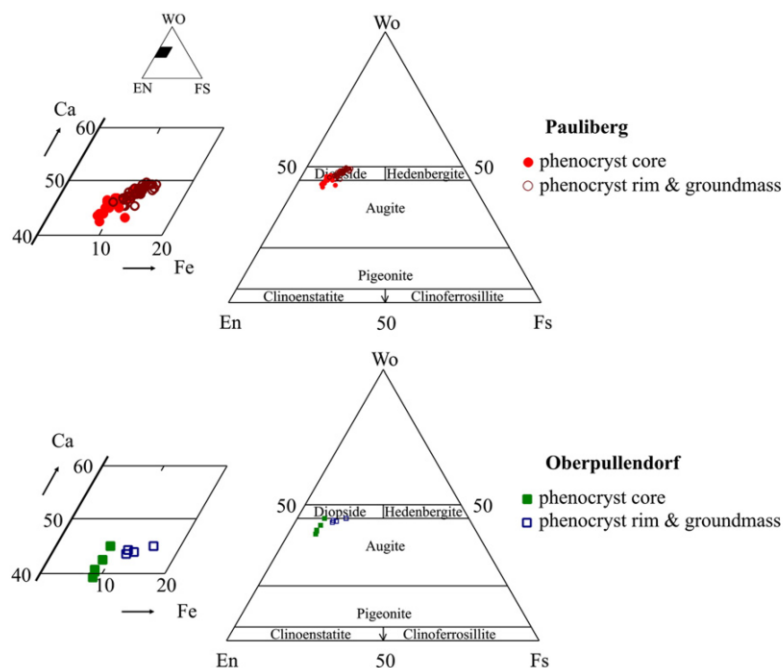
Fig. 4. En–Wo–Fs classification diagram (after Morimoto et al., 1988) showing the composition ranges of the clinopyroxenes of Burgenland alkali basalts.

from core to rim (normal zoning) is complemented by an increase in Na_2O and K_2O. The plagioclase feldspars have core compositions varying from $(Ab_{44.1}An_{54.0}Or_{1.9})$ to $(Ab_{56}An_{40}Or_4)$ and rim compositions ranging from $(Ab_{47.7}An_{50.5}Or_{1.9})$ to $(Ab_{67.6}An_{26.1}Or_{6.2})$. In one sample, plagioclase $(Ab_{43.8}An_{54.2}Or_2)$ is overgrown by anorthoclase $(Ab_{66.7}An_{19.2}Or_{14.1})$.

4.2.5. Alkali feldspars

Alkali feldspar analyses, with their calculated structural formulae are presented in Supplementary Table B5. In both the Pauliberg and Oberpullendorf samples, anorthoclases and sanidines occur within the basaltic groundmass (Fig. 5). The compositions range from $Ab_{27.4}Or_{68.1}An_{4.4}$ to $Ab_{74.7}Or_{13.4}An_{11.9}$ (Pauliberg) and from $Ab_{48.1}$-$Or_{42.5}An_{9.4}$ to $Ab_{60.4}Or_{31}An_{8.6}$ (Oberpullendorf).

4.2.6. Feldspathoids

Accessory feldspathoids (nepheline and leucite) are confined to the groundmasses and are found only in the Pauliberg basalts. Nephelines have Na_2O, 14.1–17 wt.%; K_2O, 2.09–3.42 wt.% and Al_2O_3,

29.8–32.3 wt.%, whilst leucites have Na_2O, 0.11–0.14 wt.%; K_2O, 20.5–20.8 wt.% and Al_2O_3, 23.1–23.7 wt.%, (Supplementary Table B6).

4.2.7. Opaque oxides

The Fe–Ti oxides (Supplementary Tables B7 and B8) are mostly titanomagnetites with TiO_2 between 6.3 and 30 wt.%. Cr_2O_3 can be up to 4 wt.% with Al_2O_3, 0.3–3.4 wt.% and MgO, 0.03–4.5 wt.%. Ilmenite and Al–Cr spinel also occur. The ilmenites have TiO_2, 45–53.3; FeO, 32.2–44.7; MnO, 0.12–1.34, and MgO, 1.98–7.57 in weight percents. The spinels always occur as inclusions in the olivine and clinopyroxene phenocrysts. They contain Al_2O_3, 4.33–6.4 wt.%; Cr_2O_3, 8.96–24.13 wt.% and MgO, 4.42–6.23 wt.%.

4.3. Major element geochemistry

Major element analyses of fifteen samples from Burgenland together with their Mg-numbers and saturation indices are given in Table 2. Compositions vary from 44.7 to 49.0 wt.% SiO_2 and from 8.52 to 13.2 wt.% MgO. The highest SiO_2 content (49.0 wt.%) is recorded from an

Fig. 5. Composition of the groundmass feldspars in the An–Ab–Or ternary diagram.

Table 2
Major, trace and rare earth elements compositions and Sr–Nd isotopic ratios of Burgenland basalts.

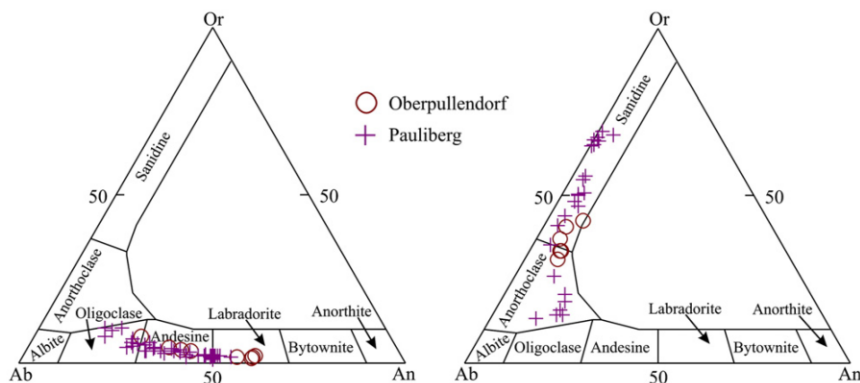| Sample no.	PLB-1	PLB-3	PLB-4	PLB-5	PLB-6	PLB-7	PLB-8	PLB-9	PLB-10	PLB-11	PLB-12	PLB-13	PLB-14	PLB-15	OB-1
Major elements (wt.%)															
SiO_2	44.9	46.0	47.7	46.7	46.8	46.6	46.7	46.4	44.7	46.6	46.9	46.6	46.6	47.1	49.0
TiO_2	4.03	4.07	3.82	3.84	3.80	3.81	3.83	3.74	3.95	3.85	3.80	3.82	3.81	4.18	2.77
Al_2O_3	10.8	11.0	11.3	10.9	10.9	10.8	10.8	10.7	10.8	10.8	10.8	10.7	10.8	11.5	12.8
FeOtotal	12.3	12.1	11.5	11.4	11.4	11.5	11.5	11.3	12.2	11.5	11.4	11.5	11.4	12.5	10.5
MnO	0.19	0.17	0.15	0.16	0.16	0.16	0.16	0.16	0.20	0.16	0.16	0.16	0.16	0.18	0.21
MgO	10.8	10.6	10.7	12.3	12.8	13.1	12.5	13.2	10.5	12.6	12.7	12.9	12.9	8.52	9.05
CaO	11.1	10.8	10.1	10.1	10.1	10.3	10.1	10.2	11.1	10.2	10.1	10.2	10.1	11.2	10.2
Na_2O	3.52	2.86	2.82	2.94	2.93	2.79	2.98	2.77	3.64	2.89	2.87	2.89	2.83	2.82	2.69
K_2O	1.56	1.49	1.50	1.40	1.31	1.17	1.22	1.33	1.72	1.22	1.39	1.29	1.36	1.36	1.34
P_2O_5	1.00	0.74	0.63	0.63	0.63	0.63	0.63	0.61	1.16	0.63	0.62	0.63	0.62	0.76	0.44
Total	100.26	99.86	100.27	100.43	100.79	100.83	100.44	100.44	99.91	100.58	100.69	100.68	100.64	100.08	99.10
LOI	-0.05	0.26	0.11	-0.26	-0.29	-0.01	-0.27	-0.04	0.05	-0.11	-0.27	-0.23	-0.23	0.92	2.12
Mg#	61.1	61.0	62.5	65.8	66.8	67.1	66.1	67.5	60.4	66.2	66.4	66.7	66.8	54.9	60.5
SI	-16.8	-7.90	-3.39	-7.23	-6.81	-6.23	-6.75	-6.99	-18.5	-6.54	-6.59	-7.05	-6.73	-3.85	1.42
Trace elements (ppm)															
Sc	14.0	18.4	16.4	18.0	21.3	17.9	20.8	18.1	15.4	18.8	18.9	18.9	18.2	20.1	20.9
Zn	133	122	117	101	112	106	110	109	134	104	110	111	104	120	94.4
Ga	19.5	18.0	16.8	15.0	16.5	16.3	16.8	16.4	22.5	15.5	15.9	16.5	16.1	18.0	14.4
Rb	39.9	34.5	39.8	30.8	35.9	26.0	47.6	31.8	32.4	31.7	31.6	37.0	31.7	25.4	21.2
Sr	1284	987	881	882	1083	921	903	897	1429	918	898	914	902	927	577
Y	40.5	34.1	31.4	31.8	31.3	31.0	31.6	30.7	44.1	31.4	31.0	31.3	30.8	35.4	27.3
Zr	594	495	498	610	502	498	546	441	652	463	439	479	441	496	364
Nb	120	89.0	72.4	81.6	98.8	82.2	82.1	79.2	138	82.4	81.4	81.7	81.5	86.3	49.8
Cs	0.839	0.501	0.677	0.509	0.658	0.506	0.620	0.509	0.721	0.740	0.518	0.638	0.520	0.638	0.342
Ba	601	529	479	458	469	464	465	445	445	423	435	456	440	493	305
Cu	65.0	72.7	78.8	54.9	81.6	89.3	70.0	82.1	60.7	87.2	89.1	84.2	90.0	53.1	41.9
Ni	200	255	274	327	308	316	316	329	192	303	308	317	322	299	324
Co	54.9	58.8	51.5	60.8	72.8	63.3	58.3	59.4	56.5	62.0	59.5	58.0	56.3	59.7	45.6
Cr	313	375	332	408	448	388	389	377	313	375	371	376	375	416	287
V	190	189	172	188	215	187	188	179	201	185	184	186	183	205	200
Hf	10.9	9.33	9.32	11.1	9.18	9.10	9.94	7.99	10.9	8.33	7.90	8.47	7.90	8.77	6.16
Ta	5.97	2.85	3.43	2.76	3.55	7.47	3.54	2.69	4.06	4.14	2.56	3.73	2.60	2.78	2.69
Th	9.71	6.30	5.26	5.14	5.30	5.16	5.22	5.03	11.6	5.24	5.11	5.14	5.10	6.29	3.64
U	2.69	1.82	1.57	1.55	1.56	1.47	1.54	1.44	3.35	1.52	1.44	1.49	1.46	1.80	0.917
Rare earth elements (ppm)															
La	79.5	53.8	43.4	42.4	44.5	43.0	43.8	42.9	92.3	43.2	42.5	42.8	42.4	52.8	25.9
Ce	174	116	94.8	93.4	96.8	94.0	95.7	93.3	187	105	92.4	93.3	91.7	112	64.2
Pr	19.9	14.5	12.1	12.0	12.3	11.9	12.1	11.8	22.1	11.9	11.8	11.9	11.7	14.0	6.9
Nd	83.3	59.5	49.7	49.4	50.6	49.4	49.9	48.8	90.2	51.7	48.4	48.9	48.2	57.6	30.7
Sm	15.1	12.1	10.5	10.4	10.5	10.2	10.3	10.1	15.5	10.1	10.1	10.1	9.95	11.6	6.16
Eu	4.46	3.54	3.07	3.09	3.11	3.02	3.05	2.97	4.43	2.96	2.96	2.98	2.93	3.41	1.92
Gd	13.4	10.5	9.20	9.07	9.23	9.00	9.10	8.95	13.7	8.99	8.84	8.85	8.75	10.1	5.82
Tb	1.68	1.38	1.23	1.20	1.21	1.19	1.19	1.16	1.69	1.16	1.16	1.17	1.15	1.31	0.806
Dy	7.98	6.56	5.89	5.80	5.80	5.70	5.83	5.68	8.13	5.64	5.60	5.67	5.62	6.32	4.11
Ho	1.36	1.12	1.04	1.00	1.01	0.974	0.999	0.979	1.38	0.969	0.961	0.979	0.964	1.09	0.755
Er	3.35	2.74	2.53	2.47	2.47	2.41	2.44	2.35	3.34	2.37	2.37	2.35	2.29	2.68	1.87
Tm	0.414	0.338	0.312	0.309	0.300	0.300	0.293	0.293	0.407	0.297	0.285	0.289	0.285	0.329	0.249
Yb	2.53	2.05	1.91	1.89	1.83	1.82	1.82	1.76	2.49	1.79	1.75	1.77	1.73	1.97	1.53
Lu	0.326	0.267	0.246	0.245	0.244	0.240	0.242	0.233	0.332	0.235	0.228	0.232	0.227	0.253	0.210
$\sum$ REE	407	284	236	233	240	233	237	231	443	246	229	231	228	276	151
Sr-Nd isotopic ratios															
87Sr/86Sr	0.703687			0.703766		0.703827			0.703804	0.703707			0.703802		0.704279
+/-2sm	0			0		0			0	0			0		0
143Nd/144Nd	0.512774			0.512758		0.512760			0.512759	0.512772			0.512758		0.512736
+/-2sm	0.000003			0		0			0	0.000003			0		0
εNd	2.8			2.4		2.5			2.5	2.7			2.4		2.0
The standards	NBS987		La Jolla												
	(n=6)		(n=7)												
87Sr/86Sr	0.710270														
+/-2sm	0.000004														
143Nd/144Nd			0.511842												
+/-2sm			0.000002												

Mg# = 100(Mg/Mg + Fetotal).

Oberpullendorf alkali basalt and the lowest (44.7–44.9 wt.%) from a Pauliberg basanite. The Mg# [Mg-number = 100(Mg/Mg + Fe$_{total}$)] of Burgenland mafic lavas varies from ~55 to 67.5. The Pauliberg alkali basalts are the most primitive, having low silica (46.0–47.7 wt.%) and high Mg# (mostly>62).

Selected major element oxides are plotted against MgO in Fig. 6. The SiO$_2$ contents in Burgenland basalts are similar to those of the Pannonian Basin (e.g. Dobosi et al., 1995; Downes et al., 1995; Embey-Isztin et al., 1993; Harangi et al., 1995). However, the Pauliberg basalts have higher TiO$_2$ and CaO and lower Al$_2$O$_3$ contents compared to
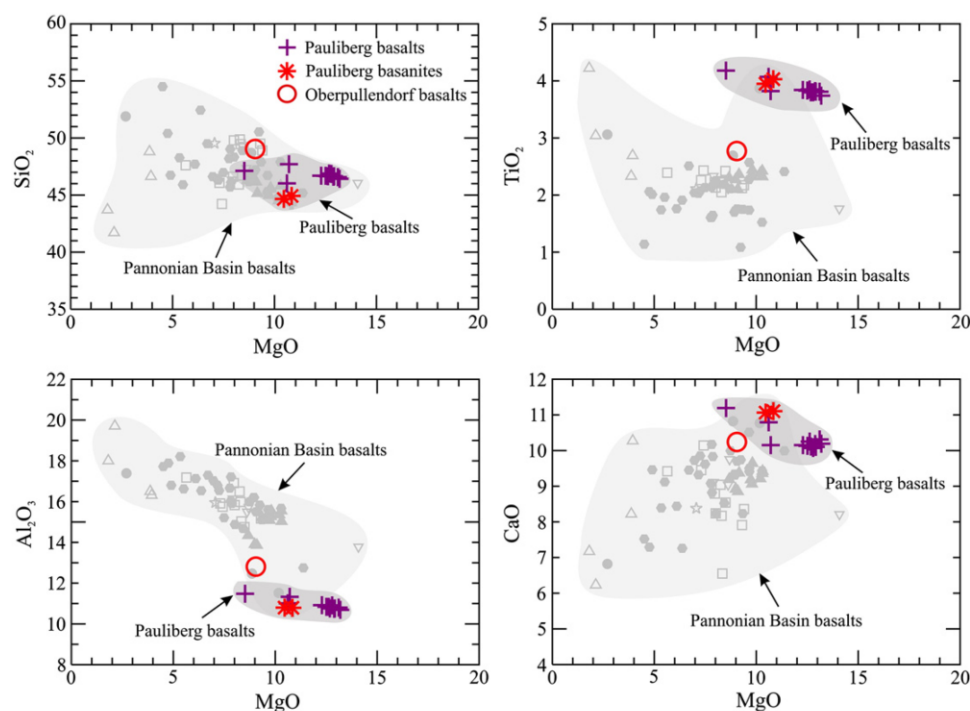
Fig. 6. Fenner variation diagrams for selected major element oxides (wt.%) against MgO (wt.%) from Burgenland alkali basalts compared with previous published data from the Pannonian Basin alkali basalts (data after Embey-Isztin et al., 1993; Dobosi et al., 1995; Downes et al., 1995; Harangi et al., 1995).

those of the Pannonian Basin. The major oxides (SiO_2, TiO_2, Al_2O_3, CaO and MgO) in Oberpullendorf basalt are identical to those of the Pannonian Basin basalts. The Pauliberg basalts have higher contents of TiO_2 and CaO and lower contents of SiO_2 and Al_2O_3 than those of Oberpullendorf. The Burgenland basalts are relatively sodic, with K_2O/Na_2O ratios of 0.41–0.53 similar to values from the peripheral areas of the Pannonian Basin (Nógrád and Rácos) (Embey-Isztin et al., 1993). The K_2O/Na_2O ratios overlap the range (0.32–0.79) for the alkaline basalts of the Pannonian Basin (Embey-Isztin et al., 1993).

4.4. Trace element geochemistry

Trace elements, including rare earth element (REE), concentrations of the Burgenland lavas are presented in Table 2. The Burgenland basaltic rocks have high concentrations of Ni and Cr, ranging from 192 to 329 ppm and 287 to 448 ppm respectively. Ni is lowest in the Pauliberg basanites (192–200 ppm) and highest in the Pauliberg alkali basalts (255–329 ppm).

As with other intra-plate alkaline lavas globally (e.g. Fitton et al., 1991) the Burgenland lavas (Fig. 7a) are enriched in LREE with La/Yb$_N$ values ranging from 11 to 25. The degree of LREE enrichment tends to correlate positively with the degree of silica-undersaturation. Oberpullendorf basalts have the lowest LREE enrichment [(La/Yb)$_N$ = 11] whereas the Pauliberg basanites have the highest [(La/Yb)$_N$ = 21–25].

The lavas are enriched in high field-strength elements (HFSE): Zr, 364–652 ppm; Nb, 50–138 ppm and Y, 27–44 ppm. Incompatible element ratios, e.g. La/Nb = 0.67, Zr/Nb = 4.3, and Ba/Th = 65 are similar to the average HIMU–OIB values (Weaver, 1991). Primitive mantle-normalized incompatible element patterns from Pauliberg and Oberpullendorf are shown in Fig. 7. In contrast to Oberpullendorf, the Pauliberg basalts display a negative K anomaly relative to Nb and La (e.g. Embey-Isztin and Dobosi, 1995; Embey-Isztin et al., 1993; Harangi, 2001). Moreover, the OIB-normalized incompatible trace

element patterns of the Oberpullendorf lavas are similar to that of St. Helena lavas (Embey-Isztin et al., 1993). The low values of large ion lithophile elements (LILE) in the Burgenland lavas are notable (Fig. 7b). Furthermore, the high Ce/Pb ratios are similar to ocean island basalt (OIB) values (Embey-Isztin et al., 1993).

4.5. Isotope geochemistry

Radiogenic isotope analyses for seven lavas are reported in Table 2. The $^{87}Sr/^{86}Sr$ ratios in Burgenland basalts are low (0.703687–0.704279) and the $^{143}Nd/^{144}Nd$ ratios are high (0.512736–0.512774); i.e., they are depleted relative to Bulk Earth. The Pauliberg basanites have the most depleted character ($^{87}Sr/^{86}Sr$ = 0.703687; $^{143}Nd/^{144}Nd$ = 0.512774), close to values from the Pauliberg alkaline basalts (Fig. 8, Table 2) whereas the Oberpullendorf basalts are the most enriched ($^{87}Sr/^{86}Sr$ = 0.704279; $^{143}Nd/^{144}Nd$ = 0.512736) of the samples studied (Fig. 8). The Sr and Nd isotopic compositions of Burgenland basalts all fall within the range of OIB values.

The Sr vs. Nd isotopic ratios plot between EAR (European Asthenospheric Reservoir)-HIMU (high μ refers to high $^{238}U/^{204}Pb$), PREMA (PREvalent MAntle) and BSE (Bulk Silicate Earth) (Fig. 8) and are similar to Tertiary–Quaternary alkaline basalts from Western and Central Europe (Eifel, Massif Central) (Wilson and Downes, 1991) and Late Tertiary alkaline basalts from the Pannonian Basin (Embey-Isztin et al., 1993; Salters et al., 1988) (Fig. 8). Pauliberg and Oberpullendorf basalts differ in their Sr and Nd isotopic ratios. Whilst the Oberpullendorf basalts have high $^{87}Sr/^{86}Sr$ and low $^{143}Nd/^{144}Nd$, the Pauliberg basalts and basanites have low $^{87}Sr/^{86}Sr$ and high $^{143}Nd/^{144}Nd$ (Table 2). The Sr and Nd isotopic compositions of the Pauliberg alkaline basalts and basanites are identical to those of the Little Hungarian Plain whereas the Oberpullendorf values are close to those of the Saghegy basalts (Harangi et al., 1995) (Fig. 8). The Burgenland basalts have the highest $^{206}Pb/^{204}Pb$ isotopic ratios (19.6–19.7) in the Pannonian Basin (Embey-Isztin et al., 1993).
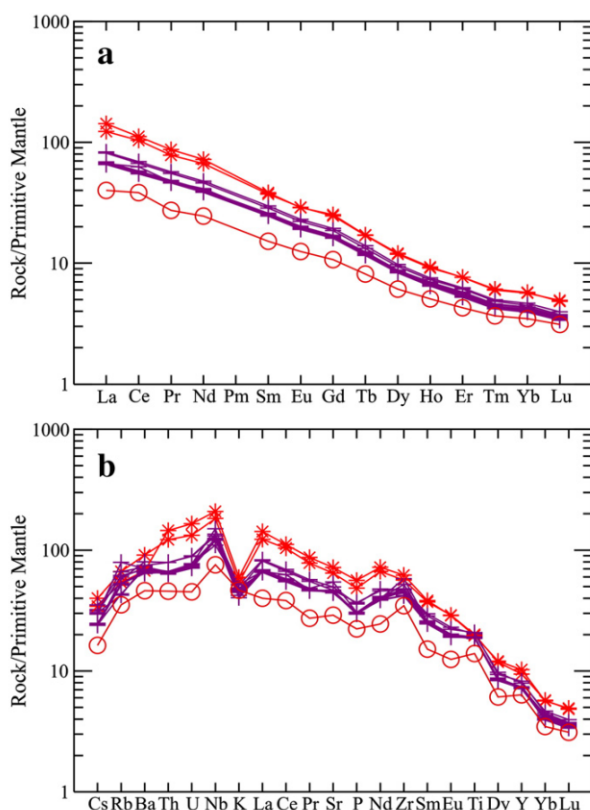
Fig. 7. Primitive mantle-normalized (a) REE patterns and (b) incompatible trace element abundances. Normalization values are from McDonough and Sun (1995). Symbols as in Fig. 6.

There are significant differences between our Pauliberg Sr–Nd isotopic ratios and those of Harangi et al. (1995a). In Table 2 we present the Sr and Nd isotope analyses and the ± 2 sigma errors of our samples, which were analyzed under the same conditions as were used for the NBS987 and La Jolla standards, whereas Harangi et al. (1995a) do not give the analytical errors. Consequently it is not possible to provide an explanation for the discrepancies between the two data sets.
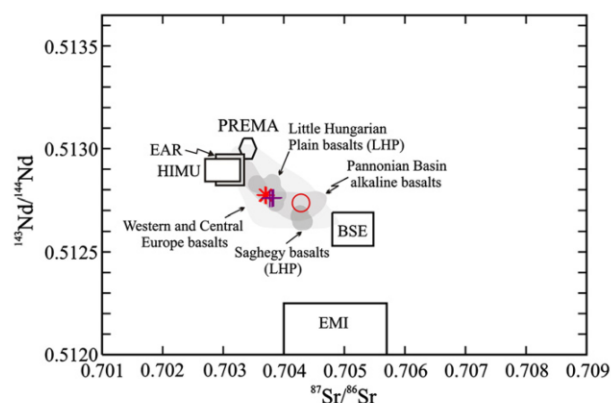
Fig. 8. Sr and Nd isotope variations of Burgenland alkali basalts compared with fields of alkaline basalts from the Pannonian Basin (data after Embey-Isztin et al., 1993; Salters et al., 1988), the Little Hungarian Plain (data after Harangi et al., 1995) and from Western and Central Europe (Wilson and Downes, 1991). EAR isotope compositions are from Lustrino and Wilson (2007). Symbols as in Fig. 6.

5. Discussion

The Burgenland localities lie at the western margin of the Pannonian Basin, SW of the Vienna Basin and north of the Styrian Basin (Fig. 1). These intra-plate lavas provide important data concerning the evolution of the Carpathian–Pannonian Region as well as providing evidence relating to the genesis of the intra-plate alkaline basalts.

5.1. Whole rock compositional variations and the source origin of the Burgenland lavas

The compositional variation within the relatively small volume of lavas in Burgenland is explicable in terms of variable degrees of mantle melting. The silica saturation index (SI; Fitton et al., 1991) ranges from −18 in the Pauliberg basanites to +1.42 in the Oberpullendorf alkali basalts suggesting variable low degrees of partial melting with the Oberpullendorf alkali basalts representing higher degrees of melting.

The compatible trace elements (Ni and Cr), together with the major element oxides, shows that the Pauliberg lavas are the more primitive and have undergone only minimal crystal fractionation. As can be seen (Figs. 6 and 7), there is a variation in the whole rock chemistry from Pauliberg. In general, the decrease in total alkalis with increase in the SiO_2 contents from basanites to alkali basalts cannot be explained by fractional crystallization. Their SI and the REE ratios (La/Yb)$_N$ suggest that they were generated by low but variable degrees of melting at depths in excess of 70–80 km. The similarity of the Sr and Nd isotopic ratios suggests that the basalts and basanites originated from the same source. Consequently variation in degree of melting of essentially the same mantle source provides an adequate explanation for the compositional range exhibited by the Pauliberg lavas.

However, the Oberpullendorf sample has Sr and Nd isotopic ratios significantly different from those at Pauliberg. (N.B., our Sr and Nd isotopic data for this sample are similar to those given by Embey-Isztin et al., 1993). According to K–Ar dating (Balogh et al., 1994) Pauliberg and Oberpullendorf were contemporaneous at ~11 Ma. However, the Oberpullendorf lavas are geochemically more similar to the Sághegy lavas of the Little Hungarian Plane (Fig. 8) that are 5.87 Ma older than the Pauliberg basalts. In view of the extensive alteration of the Oberpullendorf lavas, the age of 11 Ma should be re-examined.

One of the most striking features of the Pauliberg basalts is their high TiO_2 content, the highest of all the Late Miocene/Recent alkaline basalts in the Pannonian Basin (Fig. 6) (Dobosi et al., 1995; Downes et al., 1995; Embey-Isztin et al., 1993; Harangi et al., 1995; Seghedi et al., 2004b). In general OIBs have TiO_2 contents too high to be considered as products of primitive mantle. Even a very small degree of primitive mantle partial melting is incapable of producing the TiO_2 contents observed in the OIBs, and metasomatic agents need to be involved in order to explain the high TiO_2 contents (Prytulak and Elliott, 2007). The lithospheric mantle, according to Prytulak and Elliott (2007) and references therein, can be excluded as a possible metasomatic agent because it is depleted in Ti when compared to the primitive mantle. Contamination by Ti-rich sediments is improbable for the Burgenland lavas: it would significantly affect the Sr–Nd isotopic ratios, which is not the case (e.g. the εNd range 2–2.8, Table 2). Elevated TiO_2 contents could be attributed to accumulation of titanomagnetites if the lavas were cumulates. However, petrographical evidence and the high Mg# (assuming 1/3 of the total Fe is present as Fe^{3+} the Mg# range from 65 to75) do not support a cumulate origin of the Burgenland for the elevated TiO_2 contents. The degree of partial melting and the lithospheric thickness control the Ti abundances in the primary melts. High Ti contents are expected in melts generated after low degrees of partial melting beneath thick lithosphere and in case that the peridotitic mantle (the source) has been affected by Ti-rich recycled oceanic crust (Prytulak and Elliott, 2007), the generated lavas like the Pauliberg basalts will be enriched

in Ti. OIB lavas with primary liquids >3 wt.% TiO_2 (similar to the Pauliberg basalts) have been reported from Sao Miguel, Azores, Canary Islands and Cape Verde (Prytulak and Elliott, 2007). In each of these cases, they are, like Pauliberg, also depleted in Al, possibly related to garnet being residual after partial melting or to the source composition (Hirose and Kushiro, 1993). The high Ti-contents of the Pauliberg lavas could be attributed to local inhomogeneities.

The HFSE/LREE ratio can also be used as an indication of the origin of the lavas (Smith et al., 1999). Ratios less than unity would suggest a lithospheric origin whereas high ratios are indicative for an asthenospheric origin. The Burgenland lavas have high Nb/La ratios (average of 1.8) consistent with an (OIB-like) asthenospheric origin. The relatively high $^{206}Pb/^{204}Pb$ isotopic ratios (19.6-19.7) for the Burgenland basalts (Embey-Isztin et al., 1993) indicate HIMU–OIB-like signatures. Additionally the Ba/Ce ratio of ~4 is similar to that of OIB basalts globaly (Halliday et al., 1995). The absence of LILE enrichments in the Burgenland lavas (Fig. 7b) and the (OIB-like) high Nb/La and Ce/Pb ratios (Embey-Isztin et al., 1993), preclude interaction with subduction-related melts/fluids and/or crustal contamination.

Blundy et al. (1998) proposed that partial melts generated from a spinel-lherzolite source will have nearly flat chondreit-normalised HREE patterns, i.e. $(Dy/Yb)_N$ ratios ≤ 1.06, whereas those from garnet-lherzolite source have $(Dy/Yb)_N$ ratios>1.06. Thus, the steep HREE patterns (Fig. 7a) and the high La/Yb_N (11-25) and Dy/Yb_N (1.75-2.12) of the Burgenland basalts strongly suggests that garnet was a residual phase during the partial melting. Accordingly, the Pauliberg basalts are likely to represent the products of variable but low degrees of partial melting ($La/Yb_N = 15-25$ and $Dy/Yb_N = 2.0-2.12$) whereas the Oberpullendorf lavas were probably formed as a result of slightly higher degrees of partial melting ($La/Yb_N = 11$ and $Dy/Yb_N = 1.75$).

5.2. Depths of magma segregation

Primitive mafic alkaline lavas are of importance in the study the melt generation because their geochemical features are relatively unaffected by crystal fractionation. Almost all of the Burgenland basalts can be considered to represent primitive magma compositions (Mg#>62, MgO >9 wt.%, Ni>192 ppm and Cr>287 ppm). Consequently, these magmas underwent little olivine and/or clinopyroxene fractionation. An artificial data-set has been generated by normalizing all major oxide compositions to 15 wt.% MgO by fractional addition of olivine to approximate a primary composition. This data-set is comparable to the partial melt compositions of anhydrous lherzolite (Hirose and Kushiro, 1993).

Variations in the SiO_2 contents of mantle-derived melts are strongly pressure-dependant, whereas FeO, CaO and Al_2O_3 contents are controlled mainly by the degree of partial melting and source composition (Hirose and Kushiro, 1993). The SiO_2 content of the recalculated Burgenland data set varies from 44.2 wt.% to 47.6 wt.%, implying that the Burgenland mafic magmas segregated at different pressures, i.e. at different depths. We used the formula P(kbar) = 213.6 - 4.05 SiO_2 (Scarrow and Cox, 1995) to calculate the apparent pressure of magma segregation. This leads to estimates of approximate pressure for magma segregation of ~2.1 - ~3.5 GPa, corresponding to a depth range of about 70-110 km. The magmas of Pauliberg alkali basalt could have segregated at 2.4- 3.0 GPa, i.e. at 76-95 km depth. The *hy*-normative Oberpullendorf basaltic magmas could have segregated at lower pressures and shallower levels, (~2.1 GPa corresponding to 70 km) whereas the Pauliberg basanitic magmas could have segregated at higher pressures 3.4-3.5 GPa, corresponding to 106-110 km. These estimates for the Pauliberg basaltic magmas imply that melt generation took-place in the garnet stability field which is consistent with the trace element data (Fig. 7a). Our calculations concerning the depth of magma generation are similar to those obtained by Harangi (2001) who also pointed to the asthenospheric origin of the mafic magmas in the region. However, our data for the Burgenland magmas shows no evidence

for involvement of a lithospheric component, as was proposed by Harangi (2001).

5.3. High-pressure liquidus clinopyroxene

Burgenland lavas are mostly olivine-phyric mafic rocks (Fig. 2a) suggesting liquidus olivine, however, they also display minor depletions in Ca (Fig. 9). Fractional crystallization of clinopyroxene at depth could explain this Ca deficiency and the relative low Sc contents (Table 2), although no petrographic evidence remains. High-pressure clinopyroxene fractionation in small-volume alkaline basalts, such as the Burgenland lavas, has been recognized in the volumetrically small volcanic deposits in the Crater Hill, Auckland, New Zealand (Smith et al., 2008). Considering that small magma volumes should have narrow conduits, the process that allows crystallization of clinopyroxene in the depth before olivine is related to the under cooling of an ascending magma in the dyke margins. The geochemical parameter controlling this processes is the whole rock CaO/(CaO + MgO) ratio, which increases as the pressure decreases (Smith et al., 2008). The CaO/(CaO + MgO) ratios of Burgenland basalts vary from 0.44 to 0.53 with Mg# decreasing from 67.5 to 60.5. Applying the mathematical formulation P(GPa) = 5.4405 – 7.9364CaO/(CaO + MgO), Smith et al. (2008), we infer a pressure range from 2.0-1.3 GPa (corresponding to depths of 40-65 km) in which the clinopyroxene fractionation occurred. However, it is not possible to estimate how much high-pressure clinopyroxene fractionation may have occurred. Using the Herzberg and Asimow (2008) PRIMELT2, almost all of the Burgenland samples plot very close to the thin dashed-line dividing the peridotite and pyroxenite partial melt fields (Fig. 9), suggesting that any high-pressure clinopyroxene fractionation was minimal.

5.4. Evidence for low pressure crystallization

En route low pressure crystallization appears to be the most obvious process in Burgenland basalts. Plagioclase compositions (Fig. 5) vary from oligoclase to labradorite, suggesting variable degrees of fractional crystallization. In zoned plagioclase, the decrease in CaO from core to rim is complemented by increase in Na_2O and K_2O which might reflect crystal–liquid interaction during the late stage of crystallization.

Zoned clinopyroxenes display a sharp transition between cores and rims. Clinopyroxenes in the Pauliberg basalts, as well as, the phenocryst rims and groundmass clinopyroxenes in the Oberpullendorf basalts

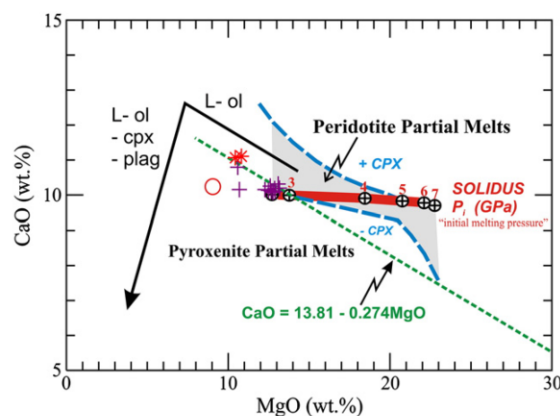**Fig. 9.** CaO and MgO contents of the investigated lavas compared with partial melts of pyroxenite and peridotite after Herzberg and Asimow (2008). Lavas with CaO contents lower than those defined by the thin dot line are potential pyroxenite partial melts and/or peridotite partial melts that had cpx removed. Black arrow: liquid line of descent for primary magmas that crystallize gabbro in the crust.

approach the 0.5 Ti/Al ratio (Fig. 10), suggesting crystallization under low pressures (Dobosi et al., 1991; Wilkinson, 1974). The Ti/Al ratios of the cores in both localities are lower than those of the rims. The distinction between the cores and rims is clear in the Oberpullendorf basalts (Fig. 10) and, in general, the cores appear to have crystallized at slightly higher pressures than the rims. Moreover, clinopyroxene phenocryst cores at Oberpullendorf seem to have crystallized at slightly higher pressures than those at Pauliberg. Additional evidence for low pressure clinopyroxene crystallization comes from their low Al^{VI}/Al^{IV} ratios (0–0.48). Since the Al^{VI}/Al^{IV} ratio in clinopyroxenes correlates positively with pressure (Wass, 1979), the low Al^{VI}/Al^{IV} values in the Burgenland clinopyroxenes suggest low crystallization pressures. Using the crude empirical geobarometer (Wass, 1979), a crystallization pressure for <1 GPa can be inferred for the Burgenland pyroxenes.

Fig. 11 shows that the Ti contents of the clinopyroxenes increase as the Mg-number decreases. The accommodation of Ti (as a $CaTiAl_2O_6$ component) in pyroxene is favored by low pressure and temperature (Sack and Carmichael, 1984). Therefore clinopyroxene fractionation during ascent could account for the gradual increase in Ti. The early clinopyroxenes are significantly enriched in Cr but the Cr content decreases with falling Mg-number (Fig. 11). The cores of the clinopyroxenes have Cr_2O_3 contents of 1.39 wt.% whereas the Cr_2O_3 content of the rims and groundmass grains approaches the detection limit.

5.5. Modeling primary magma and mantle potential temperature calculations

The PRIMELT2.XLS software (Herzberg and Asimow, 2008) was used to calculate primary magma compositions from the lava compositions and to infer the mantle potential temperature (T_P). Clinopyroxene can accumulate in the mantle (Albarède et al., 1997; Keshav et al., 2007), from primary or derivative liquids having high MgO (>10 wt.%). However, shallow augite fractionation could have the same effect on the CaO contents of high MgO primary magmas as deep crystallization of high-CaO augite and, accordingly, calculated mantle potential temperatures become overestimated.

There are three Burgenland lava samples out of fifteen that plot above the thin dashed-line in Fig. 9 that qualify as olivine-fractionated derivatives of primary magmas from peridotitic sources. It is obvious that, apart from sample PLB-7 (Fig. 9) most of these lavas have been affected by clinopyroxene fractionation. The composition of PLB-7 fulfills all the requirements to be considered as representing primary magma. However, as mentioned earlier, because almost all of the samples plot close to the dividing line between peridotite and pyroxenite partial melts (Fig. 9), other samples with compositions similar to PLB-7, even if they do not accord with the Herzberg and Asimow (2008), model calculations, could be also considered as

primary magmas. The $Fe_2O_3/TiO_2 = 1.0$ ratio was used to estimate the Fe_2O_3 in order to calculate the most appropriate primary magma composition for the Pauliberg lavas (Herzberg and Asimow, 2008). The calculated primary melt composition contained 46.1 SiO_2, 3.82 TiO_2, 10.8 Al_2O_3, 3.82 Fe_2O_3, 7.94 FeO, 12.4 MgO, and 10.3 CaO (all in wt.%).

The calculated mantle potential temperature from Pauliberg lava is 1386 °C and the calculated melt fractions are low, (~2%). Despite uncertainties due to pyroxene fractionation, an approximate mantle potential temperature for the Oberpullendorf lava is 1530 °C. Because clinopyroxene fractionation was likely, this temperature is likely to be an overestimate but should provide an upper temperature limit. The calculated potential temperatures are consistent with ambient mantle temperatures that produce MORB, namely ~1300–1454 °C (Herzberg et al., 2007; Putirka et al., 2007), suggesting that the Burgenland magmas arose from ambient mantle i.e. no thermal anomaly is indicated.

5.6. A plume beneath the Carpathian–Panonnian region?

The proposal of a mantle plume beneath the Carpathian–Pannonian region, based on the HIMU-like isotopic signature of the Pannonian basalts (Embey-Isztin and Dobosi, 1995) is highly contentious. Finger-like small-scale convective upwellings from the base of the upper mantle could explain the origin of the widespread Tertiary–Quaternary volcanic provinces of western and central Europe, (Wilson and Patterson, 2001; Seghedi et al., 2004b) and possibly also the Circum-Mediterranean Anorogenic Cenozoic Igneous provinces (Lustrino and Wilson, 2007). The geochemical and petrologic data of the present study are consistent with this model. The primitive mantle-normalized trace element patterns show similarities to those of the Massif Central basanites as well as to typical HIMU–OIB basalts (Fig. 7b). Apart from the positive Nb anomaly relative to neighbouring elements, the Pauliberg lavas are characterized by positive Zr and Ti and negative K anomalies. The negative K anomaly, among other characteristics of HIMU lavas, has been attributed either to i) low degree partial melting leaving residual amphibole and/or phlogopite (Class et al., 1998), ii) K-depletion in the source (Chauvel et al., 1992), or iii) magmatically-enriched recycled oceanic lithosphere (Hofmann, 2004). Accordingly, the elevated HFSE and the negative K anomaly, typical of the Pauliberg basalts should reflect source characteristics (Hofmann, 2004; Lustrino and Wilson, 2007). As can be inferred from the elevated HFSE, interaction of upwelling asthenosphere with lithospheric melts leaving residual amphibole or phlogopite is not a viable explanation. Additionally, interaction of asthenospheric magmas with lithospheric melts can be excluded since the Rb/Nb and Ba/Nb ratios are similar to the HIMU ratios. Although the Nd and Sr isotopic ratios of the Massif
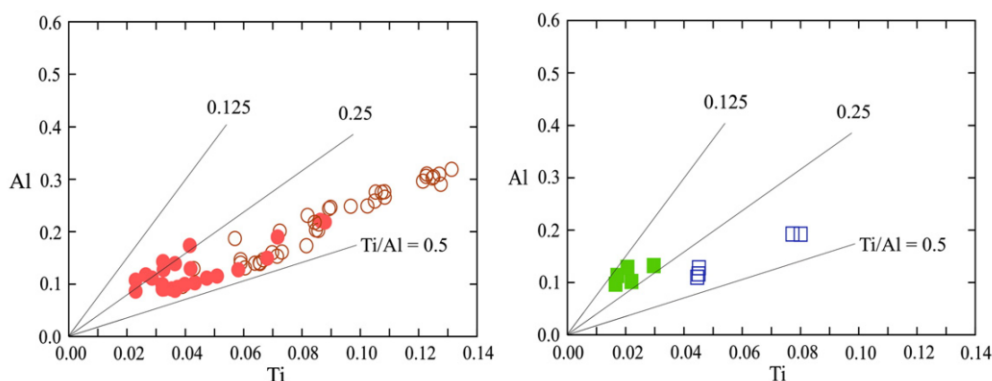
Fig. 10. Variation of Ti and Al (cations per formula unit based on 6 O) in clinopyroxenes of Burgenland alkali basalts. Symbols as in Fig. 4.
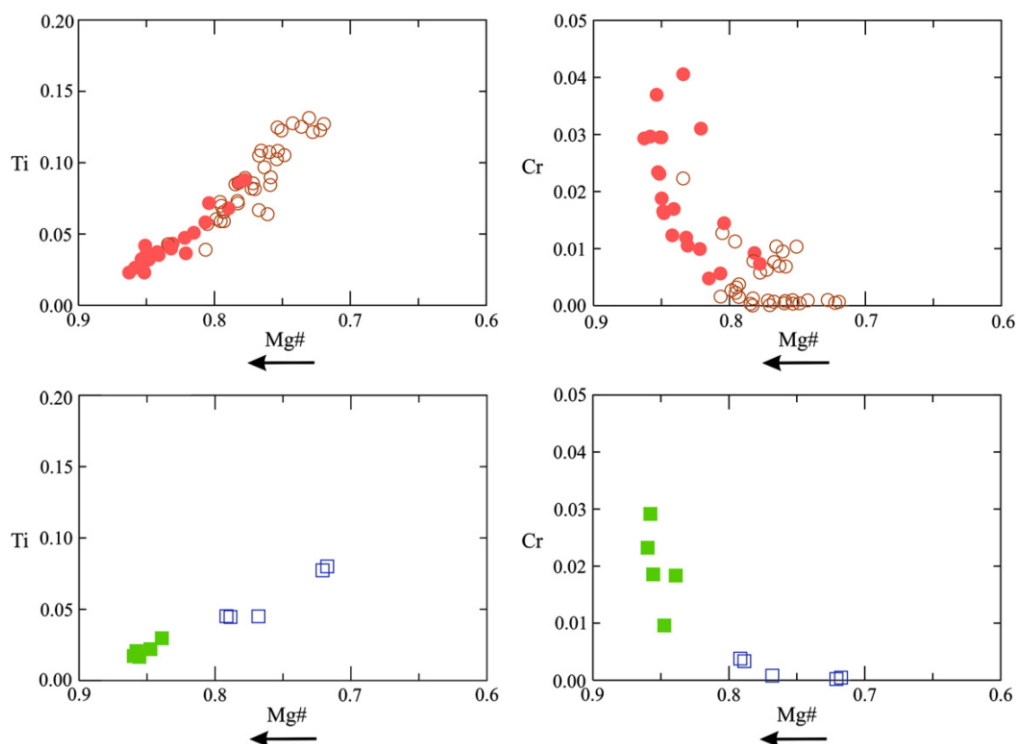
Fig. 11. Plots of Ti and Cr (cations per formula unit based on 6 O) vs. Mg-number (Mg#) in clinopyroxenes of Burgenland alkali basalts. Symbols as in Fig. 4.

Central lavas have a marked affinity to the EAR component, the Burgenland Sr and Nd isotopic ratios plot between the EAR–HIMU and BSE fields. This shifting towards BSE is consistent with the suggestion (Hofmann, 2004) that recycled oceanic lithosphere becomes metasomatically affected by low degree partial melts enriched in the HFS elements. Additional evidence supporting the plume hypothesis in the studied area comes from seismic tomography that indicates upwelling upper mantle from the eastern Atlantic to western and central Europe (Hoernle et al., 1995). Conversely, Goes et al. (1999) provide tomographic images that suggest a low-velocity structure at depths between 660 and 2000 km gave rise to a cluster of small plumes beneath central Europe and that these were responsible for the alkaline volcanism.

Noble gas studies in mantle xenoliths from the Pannonian Basin do not clarify the plume issue as they lead to ambiguous interpretations. Whilst Buikin et al. (2005) conclude that their results support the plume activity from the lower mantle, Gautheron et al. (2005) argue against deep-seated plume origin, as their Ne and Ar isotopic ratios show mantle components similar to MORB.

Harangi and Lenkey (2007) argue against the existence of plume structures in the area, suggesting that the melt generation occurred as a result of a sub-vertical mantle flow from the Alpine regime in heterogeneous asthenosphere close to its solidus as a result of Miocene lithospheric extension. However, this model fails to explain why this sub-vertical mantle flow should be from a cold margin towards the hotter asthenospheric centre of the Pannonian Basin where the lithosphere is ~60 km thick and the heat flow is >100 mW/m^2 (Lenkey et al., 2002).

The relatively low heat flow (65 mW/m^2), (Sachsenhofer et al., 1997) in the area during the late Miocene when the Burgenland basalts were erupted, suggests that a mantle plume could not account for the magma generation. Other genetic process (e.g. lithospheric extension), as proposed by Harangi and Lenkey (2007), appears more plausible. Furthermore, basalt generation and uplift of lithospheric

mantle in the second rift phase (late Miocene–Pliocene) are considered to have been syn- and/or post-rift and therefore prescribe a plume origin because alkaline volcanism and mantle lithosphere upwelling should precede rifting (Huismans et al., 2002).

5.7. Melt generation in Burgenland

The present lithospheric thickness below Pauliberg and Oberpullendorf is ~110 km (Horváth et al., 2006). Hastie and Kerr (2010) showed that the upper mantle at "normal" ambient mantle potential temperatures (~1300–1475 °C; Herzberg et al., 2007; Kinzler and Grove, 1992) and would only commence decompression melting at depths<100 km. Considering the asthenospheric nature of the erupted lavas and the fact that most basalts have olivine, and pyroxene as liquidus phases, which according to Green (1971) indicates pressures ranging from 1.2 to 3 GPa (40 to 100 km depths), imply that the lithosphere at the eruption time was less than 100 km thick. Magmatic underplating in the late Miocene (Harangi, 2001), after the volcanic activity in the area could be considered responsible for the present day lithosphere thickness.

If, as argued earlier, a mantle plume was not responsible for the volcanism other processes need to be considered. Subduction-related Middle to Late Miocene back-arc extension in the in the Carpathian–Pannonian region should be considered. The second (late Miocene) rifting was associated with small-scale asthenospheric upwelling of the mantle which accompanied the first rifting event (Huismans et al., 2002). Considering the asthenospheric origin and small volumes of the Burgenland magmas, the lithospheric thinning was probably very limited. The fact that Pauliberg lies at the margins of the Styrian, Vienna and Pannonian Basin, combined with the relaxation of the ALCAPA fragment at the time of the eruptions, could have provided the appropriate conditions for minor lithospheric attenuation and resultant (small degree) melting of the asthenospheric mantle. Therefore, extension of the lithosphere played a major role in melt

generation beneath the studied area and the partial melting of the asthenospheric mantle can be attributed to Late Miocene extension of the Pannonian Basin.

6. Conclusions

The Late Miocene Pauliberg basalts had undergone insignificant crystal fractionation and consequently have primitive compositions. Their geochemistry is primarily due to variable low degrees of partial melting from the same source area despite minor subsequent modification by crystal fractionation.

The high TiO_2 in Pauliberg rocks could be attributed to low degrees of melting, beneath thick lithosphere, of an asthenospheric peridotites that were affected by Ti-rich recycled ancient oceanic crust (Prytulak and Elliott, 2007), whereas, the low Al_2O_3 and high $(La/Yb)_N$ suggest garnet remained in the residue after partial melting (e.g. Blundy et al., 1998; Hirose and Kushiro, 1993).

The low contents of LILE and the high Nb/La and Ce/Pb ratios in the Burgenland lavas preclude any interaction with subduction-related melts/fluids and/or crustal contamination.

The Sr and Nd isotopes indicate an origin from a depleted mantle source: the relatively high $^{206}Pb/^{204}Pb$ isotopic ratios suggest that the latter was of HIMU–OIB type (Embey-Isztin et al., 1993). The most primitive Pauliberg sample (PLB-7) suggests minor clinopyroxene fractionation but significant olivine fractionation of its primary magma. The calculated mantle potential temperature from Pauliberg basalts is 1386 °C and the melt fractions are inferred to be ~2%. Similar calculations for the Oberpullendorf basalts indicate clinopyroxene fractionation leading to overestimation of the mantle potential temperature (1530 °C). This makes it impossible to calculate the degree of partial melting that generated the primary magma.

The mantle potential temperatures indicate that the Burgenland basalt originated from mantle at ambient temperature, thus not supporting the mantle plume hypothesis. The asthenospheric geochemical signature and the small volumes of the basalts indicate that lithospheric thinning was minimal and the extensional asthenospheric melting was small. The Late Miocene lithospheric extension in the Pannonian Basin was responsible for the alkaline melt generation beneath Burgenland. The alkaline mafic magmas were produced due to passive upwelling and decompressional melting of asthenospheric mantle source, which appears to be associated with the post-rifting asthenospheric upwelling in the Pannonian Basin.

Supplementary materials related to this article can be found online at doi:10.1016/j.lithos.2010.11.001.

References

Albarède, F., Luais, B., Fitton, G., Semet, M., Kaminski, E., Upton, B.G.J., Bachèlery, P., Cheminée, J.-L., 1997. The geochemical regimes of Piton de la Fournaise volcano (Réunion) during the last 530000 years. Journal of Petrology 38, 171–201.

Balogh, K., Ebner, F., Ravasz, C.S., 1994. K/Ar alter tertiärer Vulcanite de südöstlichen Steiermark und des südlichen Burgenlands. In: Császár, G., Daurer, A. (Eds.), Jubiläumsschrift 20 Jahre Geologischen Zusammenarbeit Österreich-Ungarn Lobitzer, pp. 55–72.

Blundy, J.D., Robinson, J.A.C., Wood, B.J., 1998. Heavy REE are compatible in clinopyroxene on the spinel lherzolite solidus. Earth and Planetary Science Letters 160, 493–504.

Buikin, A., Trieloff, M., Hopp, J., Althaus, T., Korochantseva, E., Schwarz, W.H., Altherr, R., 2005. Noble gas isotopes suggest deep mantle plume source of late Cenozoic mafic alkaline volcanism in Europe. Earth and Planetary Science Letters 230, 143–162.

Chauvel, C., Hofmann, A.W., Vidal, P., 1992. HIMU-EM: the French Polynesia connection. Earth and Planetary Science Letters 110, 99–119.

Class, C., Goldstein, L.S., Altherr, R., Bachelery, P., 1998. The process of plume-lithosphere interactions in the ocean basins — the case of Grande Comore. Journal of Petrology 39, 881–903.

Dobosi, G., Schultz-Güttler, R., Kurat, G., Kracher, A., 1991. Pyroxene chemistry and evolution of alkali basaltic rocks from Burgenland and Styria, Austria. Mineralogy and Petrology 43, 275–292.

Dobosi, G., Fodor, R.V., Goldberg, S.A., 1995. Late-Cenozoic alkalic basalt magmatism in northern Hungary and Slovakia: petrology, source compositions and relationship to tectonics. Acta Vulcanologica 7, 199–207.

Downes, H., Seghedi, I., Szakacs, A., Dobosi, G., Vaselli, O., James, D.E., Rigby, I.J., Thirlwall, M.F., Rex, D., Pécskay, Z., 1995. Petrology and geochemistry of late Tertiary/Quaternary mafic alkaline volcanism in Romania. Lithos 35, 65–81.

Embey-Isztin, A., Dobosi, G., 1995. Mantle source characteristics for Miocene–Pleistocene alkali basalts, Carpathian–Pannonian Region: a review of trace elements and isotopic composition. In: Downes, H., Vaselli, O. (Eds.), Neogene and related magmatism in the Carpatho-Pannonian Region: Acta Vulcanologica, vol. 7,(2), pp. 155–166.

Embey-Isztin, A., Downes, H., James, D.E., Upton, B.G.J., Dobosi, G., Ingram, G.A., Harmon, R.S., Scharbert, H.G., 1993. The petrogenesis of Pliocene alkaline volcanic rocks from the Pannonian Basin, Eastern Central Europe. Journal of Petrology 34, 317–343.

Fitton, J.G., James, D., Leeman, W.P., 1991. Basic magmatism associated with Late Cenozoic extension in the Western United States: compositional variations in space and time. Journal of Geophysical Research 96, 13693–13711.

Gautheron, C., Moreira, M., Allègre, C., 2005. He, Ne and Ar composition of the European lithospheric mantle. Chemical Geology 217, 97–112.

Goes, S., Spakman, W., Bijwaard, H., 1999. A lower mantle source for central European volcanism. Science 286, 1928–1931.

Green, D.H., 1971. Composition of basaltic magmas as indicators of conditions of origin: application to oceanic volcanism. Philosophical Transactions of the Royal Society of London, Series A 268, 707–725.

Halliday, A.N., Lee, D.-C., Tommasini, S., Davies, G.R., Paslick, C.R., Fitton, J.D., James, D.E., 1995. Incompatible trace elements in OIB and MORB and source enrichment in the sub-oceanic mantle. Earth and Planetary Science Letters 133, 379–395.

Harangi, S., 2001. Neogene magmatism in the Alpine-Pannonian Transition Zone — a model for melt generation in a complex geodynamic setting. Acta Vulcanologica 13, 25–39.

Harangi, S., Lenkey, L., 2007. Genesis of the Neogene to Quaternary volcanism in the Carpathian–Pannonian region: role of subduction, extension, and mantle plume. In: Beccaluva, L., Bianchini, G., Wilson, M. (Eds.), Cenozoic Volcanism in the Mediterranean Area: Geological Society of America Special Paper, vol. 418, pp. 67–92.

Harangi, S., Vaselli, O., Tonarini, S., Szabó, C.S., Harangi, R., Coradossi, N., 1995. Petrogenesis of Neogene extension-related alkaline volcanic rocks of the Little Hungarian Plain volcanic field (Western Hungary). In: Downes, H., Vaselli, O. (Eds.), Neogene and related magmatism in the Carpatho-Pannonian Region: Acta Vulcanologica, vol. 7,(2), pp. 173–187.

Hastie, A.R., Kerr, A.C., 2010. Mantle plume or slab window?: physical and geochemical constraints on the origin of the Caribbean oceanic plateau. Earth Science Reviews 98, 283–293.

Herzberg, C., Asimow, P.D., 2008. Petrology of some oceanic island basalts: PRIMELT2. XLS software for primary magma calculation. Geochemistry, Geophysics, Geosystems 9. doi:10.1029/2008GC002057.

Herzberg, C., Asimow, P.D., Arndt, N., Niu, Y., Lesher, C.M., Fitton, J.G., Cheadle, M.J., Saunders, A.D., 2007. Temperatures in ambient mantle and plumes: constraints from basalts, picrites, and komatiites. Geochemistry, Geophysics, Geosystems 8. doi:10.1029/2006GC001390.

Hirose, K., Kushiro, I., 1993. Partial melting of dry peridotites at high pressures: determination of composition of melts segregated from peridotite using aggregate of diamonds. Earth and Planetary Science Letters 114, 477–489.

Hoernle, K., Zhang, Y.S., Graham, D., 1995. Seismic and geochemical evidence for large-scale mantle upwelling beneath the eastern Atlantic and western and central Europe. Nature 374, 34–39.

Hofmann, A.W., 2004. Sampling mantle heterogeneity through oceanic basalts: isotopes and trace elements. In: Carlson, R.W. (Ed.), The Mantle and Core, Treatise in Geochemistry. Elsevier, Amstradem, pp. 61–103.

Horváth, F., Bada, G., Szafián, P., Tari, G., Ádám, A., Cloetingh, S.A.P.L., 2006. Formation and deformation of the Pannonian basin: constraints from observational data. In: Gee, D.G., Stephenson, R.A. (Eds.), European Lithosphere Dynamics: Geological Society, London, Memoirs, vol. 32, pp. 191–206.

Huismans, R.S., Podladchikov, Y.Y., Cloetingh, S.A.P.L., 2002. The Pannonian basin: dynamic modelling of the transition from passive to active rifting. European Geosciences Union Stephan Mueller Special Publication Series 3, 41–63.

Keshav, S., Sen, G., Presnall, D.C., 2007. Garnet-bearing xenoliths from Salt Lake Crater, Oahu, Hawaii: high-pressure fractional crystallization in the oceanic mantle. Journal of Petrology 48, 1681–1724.

Kinzler, R.J., Grove, T.L., 1992. Primary magmas of mid-ocean ridge basalts 2, applications. Journal of Geophysical Research 97, 6907–6926.

Lenkey, L., Dövényi, P., Horváth, F., Cloetingh, S.A.P.L., 2002. Geothermics of the Pannonian basin and its bearing on the neotectonics. European Geosciences Union Stephan Mueller Special Publications Series 3, 29–40.

Lustrino, M., Wilson, M., 2007. The circum-Mediterranean anorogenic Cenozoic igneous province. Earth Science Reviews 81, 1–65.

McDonough, W.F., Sun, S.S., 1995. The composition of the Earth. Chemical Geology 120, 223–253.

Morimoto, N., Fabries, J., Ferguson, A.K., Ginzburg, I.V., Ross, M., Seifert, F.A., Zussman, J., Aoki, K., Gottardi, G., 1988. Nomenclature of pyroxenes. Mineralogical Magazine 52, 535–550.

Pécskay, Z., Lexa, J., Szakacs, A., Balogh, K., Shegedi, I., Konecy, V., Kovacs, M., Marton, E., Kaliciak, M., Szeki-Fux, V., Poka, T., Gyarmati, P., Edelstein, O., Rosu, E., Zec, B., 1995. Space and time distribution of Neogene–Quaternary volcanism in the Carpatho-Pannonian region. In: Downes, H., Vaselli, O. (Eds.), Neogene and related volcanism in the Carpatho-Pannonian Region: Acta Volcanologica Special Issue, vol. 7, pp. 15–28.

Pécskay, Z., Lexa, J., Szakács, A., Seghedi, I., Balogh, K., Konečný, V., Zelenka, T., Kovacs, M., Póka, T., Fülöp, A., Márton, E., Panaiotu, C., Cvetković, V., 2006. Geochronology of Neogene magmatism in the Carpathian arc and Intra-Carpathian area: a review. Geologica Carpathica 57, 511–530.

Prytulak, J., Elliott, T., 2007. TiO$_2$ enrichment in ocean island basalts. Earth and Planetary Science Letters 263, 388–403.

Putirka, K.D., Perfit, M., Ryerson, F.J., Jackson, M.G., 2007. Ambient and excess mantle temperatures, olivine thermometry, and active vs. passive upwelling. Chemical Geology 241, 177–206.

Royden, L.H., 1993. Evolution of retreating subduction boundaries formed during continental collision. Tectonics 12, 629–638.

Sachsenhofer, R.F., Lankreijer, A., Cloetingh, S.A.P.L., Ebner, F., 1997. Subsidence analysis and quantitative basin modeling in the Styrian Basin (Pannonian Basin system, Austria). Tectonophysics 272, 175–196.

Sack, R.O., Carmichael, I.S.E., 1984. Fe^2 = Mg^2 and TiAl$_2$ = MgSi$_2$ exchange reactions between clinopyroxene and silicate melts. Contributions to Mineralogy and Petrology 85, 103–115.

Salters, V.J.M., Hart, S.R., Panto, G., 1988. Origin of late Cenozoic volcanic rocks of the Carpathian Arc, Hungary. In: Royden, L.H., Horvath, F. (Eds.), The Pannonian Basin; a Study in Basin Evolution: American Association of Petroleum Geologists Memoir, vol. 45, pp. 279–292.

Scarrow, J.H., Cox, K.G., 1995. Basalts generated by decompressive adiabatic melting of a mantle plume: a case study from the Isle of Skye, NW Scotland. Journal of Petrology 36 (1), 3–22.

Seghedi, I., Downes, H., Szakacs, A., Mason, P.R.D., Thirlwall, M.F., Rosu, E., Pecskay, Z., Marton, E., Panaiotu, C., 2004a. Neogene–Quaternary magmatism and geodynamics in the Carpathian–Pannonian region: a synthesis. Lithos 72, 117–146.

Seghedi, I., Downes, H., Vaselli, O., Szakács, A., Balogh, K., Pécskay, Z., 2004b. Post-collisional Tertiary–Quaternary mafic alkalic magmatism in the Carpathian–Pannonian region: a review. Tectonophysics 393, 43–62.

Smith, E.I., Sánchez, A., Walker, J.D., Wang, K., 1999. Geochemistry of mafic magmas in the Hurricane Volcanic Field, Utah: implications for small- and large scale chemical variability of the lithospheric mantle. Journal of Geology 107, 433–448.

Smith, I.E.M., Blake, S., Wilson, C.J.N., Houghton, B.F., 2008. Deep-seated fractionation during the rise of a small-volume basalt magma batch: Crater Hill, Auckland, New Zealand. Contributions to Mineralogy and Petrology 155, 511–527.

Thöni, M., Miller, C., Blichert-Toft, J., Whitehouse, M.J., Konzett, J., Zanetti, A., 2008. Timing of high-pressure metamorphism and exhumation of the eclogite type-locality (Kupplerbrunn–Prickler Halt, Saualpe, south-eastern Austria): constraints from correlations of the Sm–Nd, Lu–Hf, U–Pb and Rb–Sr isotopic systems. Journal of Metamorphic Geology 26, 561–581.

Tschegg, C., Ntaflos, Th., Seghedi, I., Harangi, S., Kosler, J., Coltorti, M., 2010. Paleogene alkaline magmatism in the South Carpathians (Poiana Ruscă, Romania): Asthenospheric melts with geodynamic and lithospheric information. Lithos 120, 393–406.

Wass, S.Y., 1979. Multiple origins of clinopyroxene in alkalic basaltic rock. Lithos 12, 115–132.

Weaver, B.L., 1991. Trace element evidence for the origin of ocean–island basalts. Geology 19, 123–126.

Wilkinson, J.F.G., 1974. The mineralogy and petrology of alkali basaltic rocks. In: Sørensen, H. (Ed.), The Alkaline Rocks. John Willy and Sons, London, pp. 67–95.

Wilson, M., Downes, H., 1991. Tertiary-Quaternary extension-related alkaline magmatism in Western and Central Europe. Journal of Petrology 32, 811–849.

Wilson, M., Patterson, R., 2001. Intra-plate magmatism related to short wavelength convective instabilities in the upper mantle: evidence from the Tertiary–Quaternary volcanic province of western and central Europe. In: Ernst, R.E., Buchan, K.L. (Eds.), Mantle Plumes: Their Identification through Time: Geological Society of America Special Paper, vol. 352, pp. 37–58.

CHAPTER III

Ali, Sh., Ntaflos, Th., Upton, B.G.J., Cornelius, T., 2011b. Petrogenesis and mantle source characteristics of Quaternary alkaline mafic lavas in the western Carpathian–Pannonian Region, Styria, Austria (in submission stage).

Petrogenesis and mantle source characteristics of Quaternary alkaline mafic lavas in the western Carpathian–Pannonian Region, Styria, Austria

Shehata Ali [1,2,*], Theodoros Ntaflos [1], Brian G.J. Upton [3], Cornelius Tschegg [1]

[1] *Department of Lithospheric Research, University of Vienna, Althanstrasse 14, A-1090 Vienna, Austria;, [2] Geology Department, Faculty of Science, Minia University, El–Minia, Egypt; [3] Grant Institute, The King's Buildings, West Mains Road, Edinburgh EH9 3JW, UK*

* Corresponding author: Shehata_aly@yahoo.com; Shehata.ali@univie.ac.at

Abstract

In the Styrian Basin, the westernmost part of Carpathian-Pannonian Region (CPR), the post-extensional phase occurred during the Pliocene to Quaternary and is characterized by eruption of alkaline mafic magmas that occasionally carry mantle xenoliths. The rocks range from highly undersaturated nephelinites (Stradnerkogel and Waltrafelsen) to predominant basanites/nepheline-basanites (Klöch and Steinberg). They have high Ce/Pb, Nb/U and Nb/La ratios (OIB-like) reflecting asthenospheric mantle source characteristics with negligible crustal contamination and/or interaction with lithospheric mantle. Moreover, they are silica-undersaturated (S.I. range from -26 to -59) and have high MgO content (> 6 wt.%), and weak correlation between MgO and other oxides implying minor differentiation *en route* to the surface. The Klöch basanites/nepheline-basanites have high Mg# (>63) and high compatible element contents (Ni, 128–156 ppm; Cr, 124–144 ppm) being close to primary magma criteria.

The increasing of silica-undersaturation, alkalis, CaO/Al_2O_3, LREE and La/Yb from basanite/nepheline-basanite to nephelinite principally results from decreasing degrees of partial melting at increasing depths in the mantle. The calculated depths of magma generation indicate >100 km for basanites/nepheline-basanites and an increase towards 135 km or deeper level for nephelinites, implying an origin in the garnet stability field. Their enrichment in incompatible elements is consistent with generally low degrees of melting in the asthenosphere. The temperatures of melting of the basanites/nepheline-basanites range from ~1400 ^{o}C to ~1500 ^{o}C.

The most primitive Styrian sample, a basanite, suggests considerable olivine and minor clinopyroxene fractionation of its primary magma. Considering the calculated Tp of 1466 ^{o}C, we conclude that the Styrian magmas generated from asthenospheric mantle at ambient temperature precluding plume activity beneath the study area.

The nephelinites have geochemical characteristics including elevated Zr/Hf (51-67) and La/Yb$_N$ (29-31) ratios and negative K and Ti anomalies on the PM-normalized multi-element diagrams being similar to those of carbonatites. These may suggest that their asthenospheric mantle source underwent enrichment with carbonatitic liquids which is further indicated by presence of about 5% CO_2 in their petrogenesis. Conversely, the basanites/nepheline-basanites display small participation of CO_2 and higher SiO_2 and lower CaO which indicates increasing in the degrees of melting compared to nephelinites.

According to the overall similarity of the trace element distribution patterns and their narrow range of the Sr-Nd isotopic ratios all the rocks belongs to a similar asthenospheric mantle source, volatile-enriched, close to EAR-type.

1. Introduction

The Neogene to Quaternary evolution of the CPR was accompanied by extensive volcanic activity that produced a wide spectrum of magmatic rocks (Balogh et al., 1994; Embey-Isztin et al., 1993; Embey-Isztin and Dobosi, 1995; Harangi 2001; Harangi et al., 1995; Harangi et al., 2006; Pecskay et al., 1995, 2006; Seghedi et al 2004a, b). Three main distinct types of magmatism have been recognized: i) Early to Middle Miocene large volume acidic ignimbrites and tuffs with calc-alkaline affinity, ii) Middle Miocene to Recent intermediate calc-alkaline subduction-related volcanic rocks (mainly andesitic) and iii) Late Miocene to Recent alkaline basalts that crop up sporadic throughout the CPR.

The oldest known alkaline mafic volcanism (Burgenland basalts) occurred in Late Miocene (~11 Ma) and then between 8 Ma - present in various regions of CPR (e.g. Nógrád, Styrian Basin and eastern Transylvania) (Balogh et al., 1994; Embey-Isztin et al., 1993; Pecskay et al., 2006). SE Carpathians (Persani and Harghita Mts.) is an exception due to simultaneous generation of mafic alkaline basalts, K-alkalic and calc-alkaline volcanics (Downes et al., 1995; Seghedi et al., 2004a, 2010).

Although most of alkaline mafic rocks in CPR have geochemical characteristics similar to those of typical intra-plate basalts (e.g. Nógrád, Burgenland and Styrian Basin; Ali and Ntaflos 2011; Embey-Isztin and Dobosi, 1995; Embey-Isztin et al., 1993) some others show some modification by contamination with crustal material and/or subduction-related fluids/melts (e.g. Balaton, Little Hungarian Plain and Persani Mts.) (Downes et al., 1995; Embey-Isztin et al., 1993; Harangi et al., 1995). In the situation of the western and central Europe alkaline basalts the deviation from the typical continental intra-plate magmas has been attributed to mixing of partial melts from lithospheric and asthenospheric mantle sources (e.g. Wilson and Patterson, 2001).

Several studies on petrology of continental intra-plate volcanics globally reveal that they often contain a suite of alkaline mafic basalts characterized by a variety of compositions, ranging from highly silica-undersaturated (strongly alkaline) to less silica-undersaturated (weakly alkaline) compositions (e.g. Fitton et al., 1991; Smith et al., 1999; Zeng et al., 2010). Although their various geographic distribution and relatively wide range of variation in chemical compositions, these basalts usually display ocean island basalt (OIB)-like geochemical characteristics (e.g. Lustrino and Wilson, 2007).

Primitive mafic magmatic rocks have geochemical characteristics that can provide important constraints on the nature of their mantle source and the melting conditions (depths and degrees of partial melting). The Stradnerkogel, Waltrafelsen, Klöch and Steinberg volcanics from the SE Styrian Basin are relatively less studied rocks therefore we present new mineralogical , geochemical and Sr-Nd isotopic data to provide a detailed and comprehensive petrological study of these lavas to understand their origin and source characteristics and to demonstrate their primitive character.

2. Geodynamic setting

The Pannonian Basin system (Fig. 1) is located in the eastern Central Europe and was formed during Neogene time as an extensional back-arc basin (e.g. Horvath et al., 2006). The Pannonian lithosphere is composed of two main tectonic terrains, the Alcapa (Alpine-Carpathian-Panonnian) to the northwest and Tisza-Dacia terrains to the southeast. The Pannonian Basin system including sub-basins (e.g. Styrian Basin) was formed as a result of northward push of the Adriatic plate and its collision with the European content commenced in late Oligocene. This collision caused gravitational collapse of the eastern Alps and stimulated lateral extrusion (E-NE) of the tectonic terrains during late Oligocene to early Miocene (Horvath et al., 2006).

The extrusion and extension were assisted by the contemporaneous retreating subduction in the Carpathian area. The Alcapa terrain was detached from the Southern Alps and extruded eastward with a counter-clockwise rotations whereas the Tisza–Dacia terrain at the same time moved north-eastwards with a clockwise rotations because of compression forces (Adria push). The two terrains assembled at the early Miocene and formed the Pannonian unit which underwent extension at this time as a consequence of subduction roll-back of the lithospheric slab of the Carpathian flysch basin. Extension of the Pannonian Basin occurred in two main stages: i) an Early to Middle Miocene passive rifting caused by subduction roll-back, characterized by lithosphere thinning, subsidence and sediment accumulation (Huismans et al., 2002; Royden, 1993) associated with calc-alkaline volcanics (Harangi et al., 2006; Seghedi et al., 2004a); ii) a Late Miocene to Early Pliocene accompanied by asthenospheric upwelling owing to lithospheric stretching in the first stage of rifting (Huismans et al., 2002) and was characterized by eruption of alkaline mafic lavas (partly mantle xenolith-bearing) (Embey-Isztin and Dobosi, 1995; Harangi and Lenkey, 2007).

The geodynamic evolution of the Pannonian Basin during the late stages were also closely related to the ongoing compression of the Adriatic plate and led to entire consumption of the subducted lithospheric slab and, thus, ending the extension phase. The Pannonian Basin at this stage became completely landlocked area surrounded and controlled by rigid plate boundary leading to a compression phase occurred mainly during Pliocene to Quaternary (Dombradi et al., 2010; Horvath et al., 2006). The compression caused a large-scale folding of the Pannonian lithosphere and subsidence of the basin interior.

The Neogene Styrian Basin (Fig. 1) from geodynamic point of view belongs to the Alcapa tectonic terrain of the Pannonian Basin and is situated at the SE margin of the Alps. It forms an elongated shape with around 100 km long and 50 km wide and its formation and evolution was directly related to the Pannonian Basin geodynamics.

The basin is filled up by Neogene clastic sediments (up to 4 km) and is underlined by Austroalpine nappe system. The crustal structure beneath the Styrian Basin indicates that it is located in a transition zone between the eastern Alps and the Pannonian area (Ebner and Sachsenhofer, 1995). Presently, the Styrian Basin has a lithospheric thickness of about 100 km (Sachsenhofer et al., 1997; Horvath et al., 2006) whereas the crustal thickness ranges from 30 to 27 km (Sachsenhofer et al., 1997 and ref. therein).

The geodynamic evolution of the Styrian Basin, similarly to the Pannonian Basin, comprised a syn-rift phase of extension occurred during early to middle Miocene followed by a post-rift phase took place mainly during Pliocene to Quaternary. Two kinds of magmatism associated with these geodynamics have been recognized producing diverse volcanic rocks. The first volcanic phase took place during Middle Miocene and formed K-alkalic to intermediate volcanic rocks (Harangi, 2001) showing subduction-related components (e.g. Ebner and Sachsenhofer, 1995). The second volcanic phase occurred during Pliocene-Pleistocene and produced alkaline mafic lava flows and various pyroclastic rocks in the SE Styrian Basin that are following the Late Miocene mafic volcanism in Burgenland (Ali and Ntaflos, 2011). This volcanic activity suggests that the magmas were formed at greater depths during this time (Sachsenhofer et al., 1997). The K/Ar ages of the second volcanism range from 1.7 to 3.8 Ma (Balogh et al., 1994; Pecskay et al., 1995, 2006). Since the present work deals with alkaline mafic lavas erupted in the SE Styrian Basin that include small volcanic centres in Stradnerkogel, Waltrafelsen, Klöch and Steinberg we consider the former K/Ar ages that according to Embey-Isztin et al. (1993) and ref. therein are of 1.9 Ma for Stradnerkogel, 2.2 Ma for Steinberg and 2.4 Ma for Klöch.
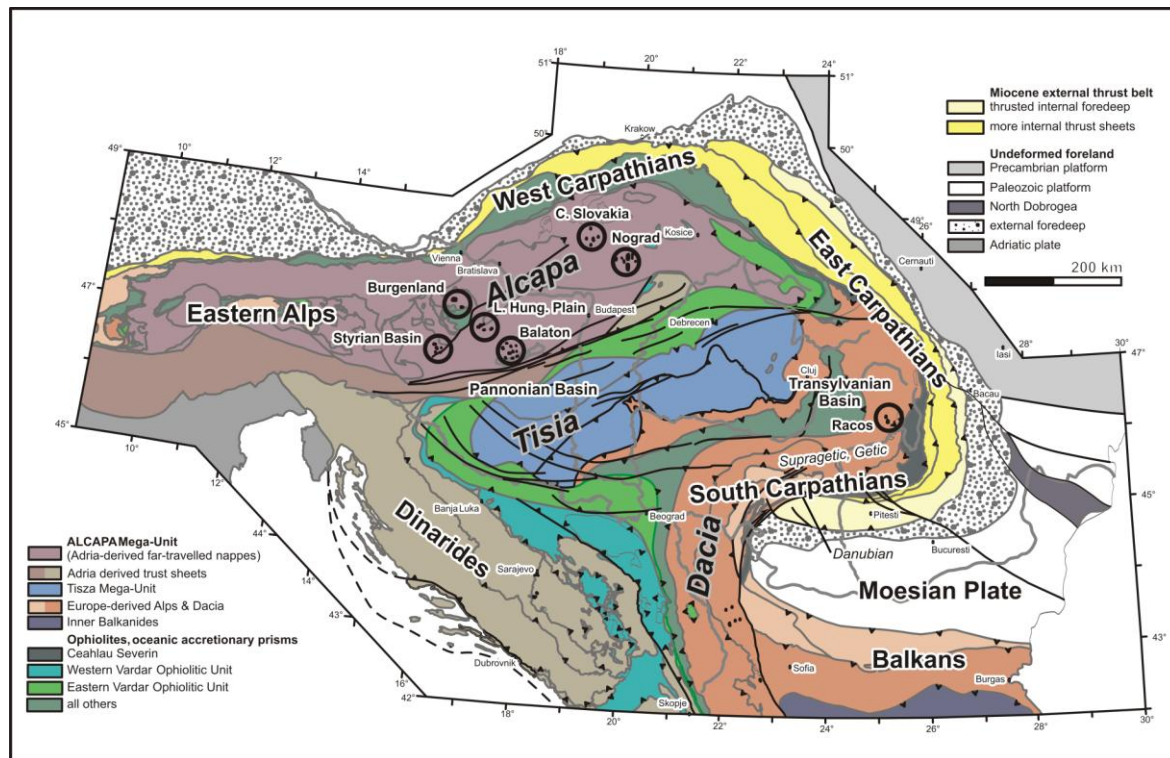
Fig. 1. Geologic and tectonic map showing the distribution of Late Miocene-Pleistocene alkaline basalts within the Carpathian-Pannonian and Eastern Alps region (modified after Schmid et al., 2008). Samples studied are from the Styrian Basin.

3. Analytical Methodology

Petrography description of representative thin-sections of the samples was done with an optical polarizing microscope. Microtextures, mineral and matrix chemistry as well as mineral-phase reactions were investigated by CAMECA SX-100 electron-microprobe (University of Vienna, Department of Lithospheric Research) using polished carbon-coated thin-sections. All analyses were made against natural and synthetic mineral standards, using four wavelength-dispersive spectrometers; acceleration voltage and beam current were 15 kV and 20 nA respectively, and standard correction procedures were applied. Pyroxenes and oxides were analyzed with a focused 1 μm beam, whereas all feldspar analyses were carried out with an expanded 5 μm beam diameter to minimize the loss of Na and K.

Whole rock major and the trace elements Ba, Co, Cr, Ga, Ni, Rb, Sc, Sr, V, Zn and Zr were analyzed with the sequential X-ray spectrometer Phillips PW 2400, equipped with a Rh-excitation source (University of Vienna, Department of Lithospheric Research). Fused beads were produced at 950° C from a mixture of specimen and $Li_2B_4O_7$ flux, diluted 1:5 to gain accurate and precise results. Replicate analyses of geo-standard GSR-3 gave an overall procedural error better than 2% for major elements and 5%, (Cu=8.5%) for trace elements. Rare earth elements (REE), Y, Nb, Ta, Hf, U and Th were analyzed by ICP-MS techniques (ELAN 6100) at the University of Vienna, Department of Lithospheric Research. Replicate analyses of geo-standard BHVO-1 gave an overall procedural error better than 2% and for Th 7.5%. For the relative procedural error and accuracy of the analyses see Ali and Ntaflos (2011).

Sm–Nd and Rb–Sr analysis was done using a ThermoFinnigan® Triton TI TIMS at the Laboratory of Geochronology, Department of Lithospheric Research, University of Vienna. During the period of measurement, standard values were: $^{87}Sr/^{86}Sr = 0.710270 \pm 0.000004$ (n=6) for NBS987 and $^{143}Nd/^{144}Nd = 0.511842 \pm 0.000002$ (n=7) for La Jolla international standards. Sample preparation and detailed analytical procedures are described by Thöni et al. (2008).

4. Results

4.1. Petrography

The Styrian lavas are generally fine-grained massive with porphyritic appearance. They show olivine phenocrysts sometimes accompanied by clinopyroxene. The groundmass is usually made of clinopyroxene, olivine, plagioclase and Fe-Ti oxides assemblages with nepheline, leucite, phlogopite and alkali feldspar filling the intergranular spaces. The Stradnerkogel and Waltrafelsen nephelintes are distinctly different from the other rocks as they composed mainly of nepheline and clinopyroxene and containing a significant amount of titanomagnetite in the groundmass with minor amounts of olivine, apatite, leucite and Ba-feldspar. Generally, the rock samples are characterized by porphyritic (Fig. 2), glommero-porphyritic, overgrowth, seriate, intergranular, and poikilitic textures.

Clinopyroxenes display pale greenish to reddish color and occur as subhedral to euhedral prismatic and tabular phenocryst (2000 to 150 μm), as needle-shaped crystal and small grain in the groundmass (~50 μm). They exhibit concentric and hourglass sector zoning (Fig. 2a). Olivine is colorless and varies within the same range in size as the clinopyroxenes. The phenocrysts are suhedral to euhedral zoned crystals (Fig. 2b). Occasionally, olivines rim are altered to iddingsite. They usually enclosed by clinopyroxenes. Zoned plagioclase crystals are present as euhedral to subhedral lath-shaped crystals confined to the groundmass. Alkali feldspar crystals are rarely observed and occur as small grains filling the intergranular groundmass. Ba-feldspars are uncommon groundmass mineral recognized in the Stradnerkogel and Waltrafelsen nephelinites. Phlogopites present in minor amount as small flakes and shreds in the groundmass. Nepheline crystals are smaller, transparent and are confined to the groundmass. Minor amounts of leucite present as subhedral crystals. Rare subhedral crystals of rhönite can be identified in the groundmass of Klöch basanites/nepheline-basanites.
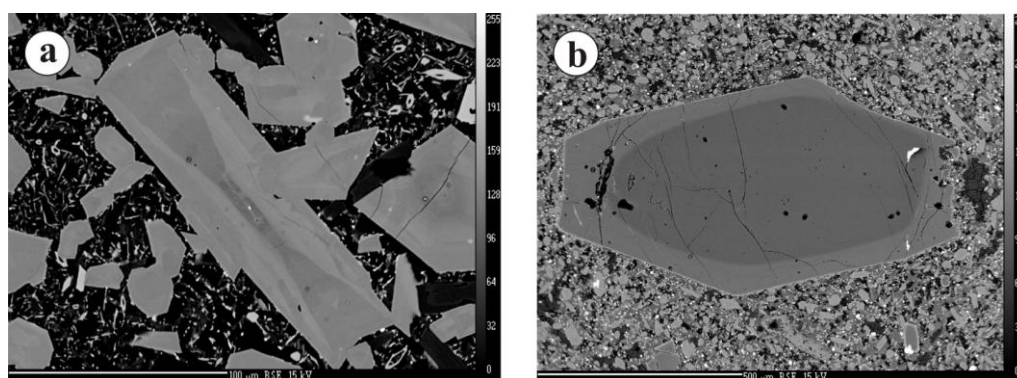
Fig. 2. Back-scattered electron image (BSE) showing the petrography features of the Styrian lavas. a) Clinopyroxene phenocryst displays hourglass sector zoning in the Klöch basanite/nepheline-basanite (KL-9). Scale bar 100μm. b) Euhedral olivine phenocryst exhibits compositional zoning in the Steinberg basanite/nepheline-basanite (ST-10). Note the porphyritic texture. Scale bar 500μm.

The main accessory constituents are titanomagnetite, ilmenite, leucite, pyrite, spinel and apatite. Ilmenite occurs mainly as small grain in the groundmass and as exsolution lamella in titanomagnetite. The uncommon secondary minerals (calcite and zeolite) were found as cavity filling.

4.2. Mineral chemistry

4.2.1. Olivines

Olivine phenocrysts cores are usually Mg-rich (Fo_{84-88}) (Table 1). The forsterite contents decrease from Fo_{88-84} in the core of the phenocrysts to Fo_{84-74} at the rim and in the groundmass. Generally, the evolution of olivine composition shows an increase in FeO, CaO and MnO and a decrease in MgO and NiO contents (Table 1). The most fayalitic olivines usually contain 0.52–1.54 wt.% MnO and 0.35–0.67 wt.% CaO. Fayalitic olivines from the Stradnerkogel nephelinites have considerably higher contents of MnO and CaO than those from the Klöch and Steinberg basanites/nepheline-basanites (Table 1). Occasionally, large anhedral (up to 2.5 mm in size) olivine xenocrysts are present in the Klöch basanites/nepheline-basanites and have typical depleted mantle composition with Fo_{89-90}.

4.2.2. Clinopyroxenes

The clinopyroxene phenocrysts are usually zoned and their compositions vary from $Wo_{45.5-49.3}$ $En_{45.7-39.9}$ $Fs_{8.8-10.7}$ in cores to $Wo_{47.5-52.6}$ $En_{42.1-33.6}$ $Fs_{10.4-13.8}$ in rims which are similar to groundmass clinopyroxenes (Table 2). The Mg# (Mg-number = Mg/Mg+Fe$_{total}$) of the clinopyroxenes varies from 0.70–0.87 in nephelinites and from 0.72–0.84 in basanites/nepheline-basanites. The composition evolution includes an increasing in TiO_2, FeO$_{total}$, and CaO and a decreasing in SiO_2, Cr_2O_3 and MgO contents (Table 2). According to nomenclature of Morimoto et al. (1988), the clinopyroxenes can be classified as diopside. There is significant variation in TiO_2 (0.98–5.1 wt.%) and Al_2O_3 (2.18–10.6 wt.%) contents.

4.2.3. Plagioclases

Plagioclase feldspar is one of the main mineral constituents of both Klöch and Steinberg basanites/nepheline-basanites and occurs as elongated lath-shaped crystals in the groundmass. Its composition varies from $An_{79.4}$ to An_{22} (Table 3). Plagioclase compositions in Klöch basanites/nepheline-basanites range from $An_{79.4}$ to An_{22} whereas those of Steinberg basalts vary between $An_{66.7}$ and $An_{48.8}$. The highest content ($An_{79.4}$) present in Klöch basanites/nepheline-basanites. Their compositions plot within the oligoclase, andesine, labradorite and bytownite fields in the An-Ab-Or ternary diagram (not shown).

4.2.4. Alkali feldspars

Alkali feldspars occur as minor constituents in the groundmass of both Klöch and Steinberg basanites/nepheline-basanites. Their compositions vary between $Ab_{66.2}Or_{17}An_{16.8}$ and $Ab_{26.2}Or_{73.2}An_{0.7}$ (Table 3).

4.2.5. Barium feldspars

The accessory barium feldspars found only in the intergranular groundmass of the nephelinites. They are represented by unzoned crystals with compositional range varying from ($Or_{49.4}$ $Cn_{34.6}$ $Ab_{15.6}$ $An_{0.395}$) to ($Or_{53.6}$ $Cn_{22.1}$ Ab_{24} $An_{0.321}$) (Table 3).

4.2.6. Feldspathoids

Feldspathoids comprise both nepheline and leucite (Table 4). They occur as groundmass minerals in minor amounts except in Stradnerkogel and Waltrafelsen nephelinites where nepheline is one of the main mineral constituents. In nephelines Na_2O ranges from 15.3–16.6 wt.%, K_2O from 4.0–6.9 wt.% and Al_2O_3 from 32.8 to 34.4 wt.% whereas leucites have Na_2O (up to 0.22 wt.%), K_2O (20.3–21.3 wt.%) and Al_2O_3 varying from 22.8 to 23.5 wt.%.

4.2.7. Phlogopites

Phlogopites shreds and flakes occur as minor constituents in the groundmass of both Klöch and Steinberg basanites/nepheline-basanites. Their compositions (wt.%) correspond to titanian phlogopite: TiO_2, 4.3–10; FeO_{total}, 10.1–11.6; MgO, 14.2–18.9; K_2O, 8.9–9.2 (Table 5).

4.2.8. Rhönites

Rhönite was found as accessory mineral in the groundmass of the Klöch basanites/nepheline-basanites. They have uniform compositions (wt.%): SiO_2, 24.1–24.6; TiO_2, 9.5–10.2; Al_2O_3, 16.2–17.1 and FeO, 21.6–23.1 (Table 5). Their compositions, however, are identical to some rhönite found in undersaturated volcanic rocks of Hocheifel, Germany (Kunzmann, 1989).

4.2.9. Opaque minerals

The opaques consist of titanomanetite, ilmenite and spinel (Table 6). Titanomagnetite is the commonest Fe-Ti oxides. It contains TiO_2 (8.5–33.1), Al_2O_3 (0.16–9.8), MgO (0.61–5.2) and MnO (0.64–1.70) (all in wt.%). Ilmenite presents mainly as exsolution laths in the titanomagnetites. It contains (wt.%) TiO_2 (49.8–59.3), FeO (31.8–40.2), MnO (0.98–2.7), and MgO (1.21–5.6). Spinel occurs as small grains mainly in the rim of the olivine phenocrysts. Their compositions (wt.%) correspond to Cr-Al spinel (13.8–16.7 Cr_2O_3, 15.5–18.3 Al_2O_3; Table 6).

Table 1: Representative microprobe analyses and chemical formulae of olivines in the Styrian Basin lavas.

Sample No.	SK1-11	SK6-172	SK16-60c	SK16-61r	WA1-33c	WA1-34r	KL5-38c	KL5-39r	KL6-21c	KL6-22r	ST9-17c	ST9-18r	ST13-181c	ST13-182r
SiO_2	40.1	37.8	40.6	40.2	40.4	39.5	39.7	38.2	40.6	38.5	40.2	38.0	40.2	39.5
TiO_2	0.02	0.04	0.04	0.03	<0.02	0.02	0.02	0.04	0.02	<0.02	0.04	0.06	0.03	0.04
Al_2O_3	0.04	<0.02	0.04	0.02	0.05	0.03	0.03	0.03	0.02	<0.02	0.04	0.02	0.04	0.04
FeO_{total}	11.8	21.7	12.8	15.4	13.6	16.5	15.0	23.4	11.4	22.7	13.6	23.1	12.0	15.1
MnO	0.20	1.54	0.22	0.49	0.40	0.73	0.27	0.67	0.19	0.62	0.22	0.52	0.18	0.31
NiO	0.15	0.06	0.19	0.17	0.21	0.18	0.22	0.09	0.27	0.09	0.32	0.09	0.33	0.19
MgO	46.5	37.4	46.4	44.4	45.3	43.0	44.7	37.6	47.6	38.4	45.7	37.8	46.9	44.2
CaO	0.19	0.67	0.20	0.19	0.24	0.37	0.18	0.35	0.04	0.39	0.23	0.37	0.15	0.30
Total	98.91	99.21	100.52	100.91	100.23	100.32	100.10	100.46	100.17	100.65	100.44	99.92	99.79	99.65
Cations based on 4 O														
Si	1.004	0.998	1.005	1.004	1.005	0.999	0.998	0.997	1.001	1.000	1.001	0.997	0.999	0.997
Al	0.001	0.000	0.001	0.001	0.001	0.001	0.001	0.001	0.000	0.000	0.001	0.000	0.001	0.001
Ti	0.000	0.001	0.001	0.001	0.000	0.000	0.000	0.001	0.000	0.000	0.001	0.001	0.001	0.001
Fe_{total}	0.246	0.479	0.264	0.322	0.284	0.348	0.315	0.512	0.235	0.494	0.284	0.508	0.249	0.319
Mn	0.004	0.034	0.005	0.010	0.008	0.016	0.006	0.015	0.004	0.014	0.005	0.011	0.004	0.007
Mg	1.734	1.469	1.712	1.652	1.684	1.622	1.672	1.464	1.752	1.489	1.699	1.481	1.735	1.666
Ca	0.005	0.019	0.005	0.005	0.006	0.010	0.005	0.010	0.001	0.011	0.006	0.010	0.004	0.008
Ni	0.003	0.001	0.004	0.003	0.004	0.004	0.004	0.002	0.005	0.002	0.006	0.002	0.007	0.004
Fo%	88	75	87	84	86	82	84	74	88	75	86	74	87	84

Abbreviations:
c = core, r = rim, g = groundmass
SK= Stradnerkogel; WA= Waltrafelsen; KL= Klöch; ST= Steinberg

Table 2: Representative microprobe analyses and chemical formulae of clinopyroxenes in the Styrian Basin lavas.

Sample No.	SK4-11c	SK4-12r	SK16-4g	WA1-13c	WA1-14r	KL1-26c	KL1-27r	KL9-87c	KL9-88r	KL11-149g	ST13-189c	ST13-190r	ST99-9c	ST99-10r
SiO$_2$	51.2	50.5	50.4	49.6	44.3	47.0	41.3	47.6	43.7	42.0	49.1	42.9	49.8	48.2
TiO$_2$	0.98	1.41	1.57	1.30	3.3	2.6	5.1	2.31	3.7	4.6	1.25	3.8	1.17	1.55
Al$_2$O$_3$	5.3	3.1	2.18	4.1	7.5	6.1	10.6	6.2	10.2	10.5	6.7	9.5	6.8	7.5
Cr$_2$O$_3$	0.21	<0.02	0.04	0.02	<0.02	0.05	0.05	0.07	0.04	0.04	0.55	0.04	0.66	0.66
Fe$_2$O$_3$	1.89	3.7	4.2	4.2	6.5	4.8	5.5	3.7	4.1	4.9	2.40	5.2	1.80	3.2
FeO	2.7	2.7	3.5	2.6	3.0	2.5	2.9	3.1	3.4	3.3	3.4	3.4	3.4	3.0
MnO	0.09	0.22	0.31	0.12	0.24	0.13	0.08	0.12	0.11	0.09	0.13	0.12	0.10	0.12
MgO	15.7	14.2	13.4	14.2	10.8	13.5	10.6	13.5	11.1	10.7	13.9	10.8	14.9	13.5
CaO	21.6	24.0	24.2	23.5	23.2	23.2	23.2	23.2	23.0	22.9	21.2	22.6	20.6	21.2
Na$_2$O	0.81	0.55	0.67	0.49	0.82	0.42	0.52	0.45	0.61	0.55	0.93	0.58	0.90	1.01
Total	100.45	100.39	100.46	100.09	99.64	100.43	99.85	100.14	99.87	99.71	99.60	98.98	100.03	99.88
						Cations based on 6 O								
Si	1.867	1.877	1.892	1.852	1.702	1.761	1.580	1.779	1.650	1.603	1.822	1.648	1.828	1.790
Al^{IV}	0.133	0.123	0.096	0.148	0.298	0.239	0.420	0.221	0.350	0.397	0.178	0.352	0.172	0.210
Al^{VI}	0.096	0.014	0.000	0.033	0.041	0.031	0.059	0.052	0.104	0.077	0.115	0.079	0.120	0.118
Fe(iii)	0.052	0.102	0.117	0.116	0.186	0.135	0.155	0.103	0.116	0.139	0.067	0.147	0.049	0.088
Cr	0.006	0.000	0.001	0.001	0.000	0.002	0.001	0.002	0.001	0.001	0.016	0.001	0.019	0.019
Ti	0.027	0.040	0.044	0.037	0.096	0.074	0.146	0.065	0.106	0.133	0.035	0.109	0.032	0.043
Fe(ii)	0.081	0.084	0.108	0.080	0.094	0.078	0.090	0.095	0.105	0.105	0.104	0.109	0.105	0.092
Mn	0.003	0.007	0.010	0.004	0.008	0.004	0.003	0.004	0.004	0.003	0.004	0.004	0.003	0.004
Mg	0.852	0.790	0.748	0.790	0.618	0.757	0.606	0.751	0.626	0.610	0.771	0.621	0.813	0.747
Ca	0.843	0.956	0.972	0.941	0.953	0.932	0.950	0.928	0.930	0.935	0.842	0.931	0.809	0.843
Na	0.057	0.039	0.049	0.036	0.061	0.030	0.038	0.032	0.045	0.040	0.067	0.043	0.064	0.073
Wo	46.1	49.3	49.7	48.7	51.3	48.9	52.6	49.3	52.2	52.2	47.1	51.4	45.5	47.5
En	46.6	40.7	38.2	40.9	33.2	39.7	33.6	39.9	35.2	34.0	43.1	34.3	45.7	42.1
Fs	7.4	9.9	12.0	10.4	15.5	11.4	13.8	10.7	12.6	13.8	9.8	14.4	8.8	10.4
Al^{VI}/Al^{IV}	0.72	0.12	0.00	0.22	0.14	0.13	0.14	0.24	0.30	0.19	0.65	0.22	0.70	0.56
Ti/Al	0.12	0.29	0.46	0.20	0.28	0.27	0.31	0.24	0.23	0.28	0.12	0.25	0.11	0.13
Mg#	0.87	0.81	0.77	0.81	0.70	0.79	0.72	0.80	0.75	0.72	0.82	0.72	0.84	0.81

Mg#=Mg/(Mg+Fe$_{total}$)

Table 3: Representative microprobe analyses and chemical formulae of feldspars in the Styrian Basin lavas.

Mineral	Plagioclase							Alkali feldspar				Ba-feldspar		
Sample No.	KL1-12	KL1-24	KL5-19	KL9-66	ST4-79	ST9-8	ST9-9	KL11-142	KL6-32	ST13-221	ST9-12	Sample No.	SK8-8	WA1-31
SiO_2	61.2	54.3	52.4	48.0	54.8	52.8	50.5	62.1	63.4	63.3	64.6	SiO_2	50.1	55.4
TiO_2	0.18	0.12	0.14	0.09	0.07	0.12	0.11	0.19	0.21	0.12	0.08	Al_2O_3	21.6	20.1
Al_2O_3	23.6	28.4	29.4	33.3	28.2	29.6	31.0	22.5	20.7	19.7	18.9	FeO_{total}	0.71	1.32
FeO_{total}	0.39	0.51	0.56	0.58	0.65	0.38	0.56	0.37	0.35	0.70	0.49	BaO	16.9	11.4
CaO	4.6	10.3	12.6	16.0	10.1	11.6	13.4	3.4	1.38	1.65	0.13	CaO	0.07	0.06
Na_2O	7.7	5.3	3.6	2.20	5.7	4.6	3.5	7.3	5.8	5.5	2.9	Na_2O	1.55	2.5
K_2O	1.95	0.42	0.83	0.16	0.29	0.41	0.23	2.9	6.7	8.1	12.4	K_2O	7.4	8.5
Total	99.6	99.36	99.59	100.38	99.82	99.48	99.39	98.75	98.62	99.01	99.59	Total	98.41	99.42
Cations based on 32 O														
Si	10.983	9.881	9.571	8.774	9.928	9.622	9.260	11.215	11.563	11.611	11.877	Si	10.541	11.058
Al	4.988	6.088	6.327	7.175	6.008	6.356	6.704	4.790	4.451	4.249	4.094	Al	5.367	4.735
Ti	0.024	0.016	0.019	0.012	0.010	0.016	0.015	0.026	0.029	0.017	0.011	Fe_{total}	0.125	0.220
Fe_{total}	0.059	0.078	0.086	0.089	0.098	0.058	0.086	0.056	0.053	0.107	0.075	Ba	1.398	0.894
Ca	0.878	2.002	2.476	3.142	1.968	2.261	2.629	0.652	0.270	0.324	0.026	Ca	0.016	0.013
Na	2.661	1.866	1.258	0.780	1.999	1.612	1.259	2.564	2.058	1.943	1.040	Na	0.633	0.971
K	0.446	0.097	0.194	0.037	0.067	0.095	0.054	0.657	1.558	1.894	2.907	K	1.999	2.171
Ab%	66.8	47.1	32	19.7	49.6	40.6	31.9	66.2	53	46.7	26.2	Or%	49.4	53.6
An%	22	50.5	63	79.4	48.8	57	66.7	16.8	6.9	7.8	0.7	Cn%	34.6	22.1
Or%	11.2	2.4	4.9	0.9	1.7	2.4	1.4	17	40.1	45.5	73.2	Ab%	15.6	24.0
												An%	0.395	0.321

Table 4: Representative microprobe analyses and chemical formulae of feldspathoids in the Styrian Basin lavas.

Mineral	Nepheline								Leucite					
Sample No.	SK6-149	SK8-17	SK16-37	WA1-35	KL5-18	KL6-5	ST5-40	ST12-10	SK9-25	WA1-32	KL5-7	KL6-45	ST13-223	ST99-23
SiO_2	42.8	42.0	42.7	43.0	43.9	43.2	44.3	44.6	54.4	54.5	55.2	55.0	54.5	55.1
TiO_2	0.03	0.05	0.05	0.05	0.19	0.06	0.07	<0.02	0.12	0.08	0.10	0.13	0.10	0.05
Al_2O_3	33.4	33.8	32.8	33.3	33.5	34.4	33.1	34.0	23.0	23.3	23.2	23.5	22.8	23.0
FeO_{total}	1.31	1.36	1.41	1.32	0.98	0.72	0.81	0.75	1.14	0.90	0.45	0.42	0.54	0.82
MgO	0.03	0.03	0.02	0.02	0.47	<0.02	0.12	0.05	<0.02	<0.02	<0.02	<0.02	0.02	0.05
CaO	0.29	0.16	0.15	0.26	2.50	1.05	1.52	0.97	0.07	0.09	0.04	<0.02	0.04	0.37
Na_2O	16.4	16.3	15.7	16.6	15.3	16.5	15.6	16.3	<0.02	0.17	0.10	0.09	0.16	0.22
K_2O	5.9	6.5	6.9	5.3	4.0	5.0	4.6	4.1	21.2	20.8	20.9	21.3	21.0	20.3
Total	100.1	100.14	99.76	99.82	100.74	100.85	100.08	100.76	99.84	99.84	100.06	100.46	99.16	99.83
	Cations based on 32 O								Cations based on 6 O					
Si	8.262	8.141	8.303	8.296	8.324	8.220	8.452	8.426	1.987	1.987	2.003	1.989	2.000	2.001
Al	7.590	7.706	7.522	7.562	7.472	7.699	7.432	7.549	0.990	1.000	0.990	1.002	0.984	0.983
Ti	0.004	0.007	0.007	0.007	0.027	0.009	0.010	0.001	0.003	0.002	0.003	0.004	0.003	0.001
Mg	0.009	0.009	0.006	0.006	0.133	0.003	0.034	0.014	0.001	0.000	0.001	0.001	0.001	0.003
Fe_{total}	0.211	0.221	0.229	0.213	0.155	0.115	0.129	0.118	0.035	0.027	0.014	0.013	0.017	0.025
Na	6.135	6.128	5.921	6.229	5.609	6.082	5.761	5.982	0.000	0.012	0.007	0.006	0.011	0.016
Ca	0.060	0.033	0.031	0.054	0.508	0.214	0.311	0.196	0.003	0.004	0.002	0.000	0.002	0.014
K	1.443	1.608	1.712	1.305	0.958	1.214	1.127	0.980	0.987	0.966	0.968	0.985	0.983	0.942

Table 5: Representative electron microprobe analyses of phlogopites and rhönites in the Styrian Basin lavas.

	Phlogopite								Rhonite			
Sample No.	KL5-23	KL5-25	KL5-49	KL5-64	KL5-65	KL6-26	KL6-27	Sample No.	KL9-1	KL9-2	KL9-4	KL9-5
SiO_2	37.2	36.9	36.7	36.4	37.0	38.6	38.6	SiO_2	24.1	24.3	24.6	24.1
TiO_2	9.1	9.8	10.0	9.8	9.2	5.2	4.3	TiO_2	9.5	10.2	9.9	9.6
Al_2O_3	13.6	13.8	13.8	13.8	13.6	12.8	13.0	Al_2O_3	17.1	16.5	16.2	17.1
FeO_{total}	10.7	10.4	11.4	11.6	11.3	11.5	10.1	Cr_2O_3	0.09	<0.02	<0.02	0.09
MnO	0.11	0.10	0.09	0.10	0.12	0.16	0.15	FeO	22.2	23.1	22.6	21.6
MgO	15.6	15.3	14.6	14.2	15.1	17.4	18.9	MnO	0.18	0.22	0.22	0.18
CaO	0.09	0.12	0.11	0.08	0.08	0.05	0.47	MgO	12.2	11.4	11.4	12.0
Na_2O	0.54	0.56	0.52	0.51	0.57	0.79	0.81	CaO	11.9	11.6	11.3	11.8
K_2O	9.2	9.2	8.9	9.1	9.1	9.1	9.1	Na_2O	1.10	1.21	1.26	1.08
Total	96.12	96.28	96.00	95.69	96.21	95.69	95.45	K_2O	0.02	0.03	0.02	<0.02
	Cations based on 22 O							Total	98.42	98.60	97.41	97.53
Si	4.931	4.884	4.885	4.875	4.917	5.146	5.127					
Al	2.118	2.155	2.155	2.177	2.129	2.012	2.029					
Ti	0.909	0.976	0.996	0.987	0.922	0.524	0.433					
Fe_{total}	1.181	1.151	1.268	1.303	1.256	1.286	1.124					
Mn	0.012	0.011	0.010	0.011	0.014	0.018	0.017					
Mg	3.090	3.018	2.891	2.834	2.996	3.451	3.749					
Ca	0.013	0.017	0.016	0.011	0.011	0.007	0.067					
Na	0.139	0.144	0.134	0.132	0.147	0.204	0.209					
K	1.552	1.550	1.502	1.561	1.549	1.549	1.548					

Table 6: Representative microprobe analyses and chemical formulae of opaque minerals in the Styrian Basin lavas.

Mineral	Titanomagnetite								Spinel		Mineral	Ilmenite		
Sample No.	SK4-5	SK6-125	SK16B-22	WA1-37	KL11-115	KL11-123	ST4-42	ST10-39	KL11-136	ST12-24	Sample No.	SK2-3	KL5-28	ST10-18
SiO_2	0.03	0.10	0.02	0.03	0.07	0.06	0.11	0.16	0.27	0.07	SiO_2	0.03	0.08	0.03
TiO_2	17.5	33.1	13.3	14.9	13.8	23.3	8.5	25.4	3.0	6.4	TiO_2	59.3	49.8	53.3
Al_2O_3	0.16	0.20	2.22	0.58	9.8	1.62	5.4	3.4	18.3	15.5	Al_2O_3	0.02	0.11	0.14
Cr_2O_3	0.06	0.03	<0.02	0.05	0.55	0.35	0.05	0.10	13.8	16.7	FeO_{total}	31.8	40.2	39.1
Fe_2O_3	31.2	3.25	42.2	39.0	31.5	22.5	44.8	14.3	27.9	22.5	MnO	2.7	0.98	1.07
FeO	43.4	57.7	33.8	40.5	36.5	45.6	33.0	47.4	28.0	30.6	MgO	1.21	5.6	4.9
MnO	1.03	1.70	1.13	1.50	0.64	0.92	1.07	1.14	0.57	0.53	CaO	0.13	0.28	0.16
MgO	0.61	1.02	5.2	1.53	5.2	3.8	2.9	2.9	5.3	5.3	Total	95.19	97.16	98.84
CaO	0.16	0.08	0.20	0.06	0.05	0.07	0.22	0.89	0.08	0.07				
Total	94.08	97.22	98.07	98.10	98.05	98.15	95.98	95.77	97.21	97.58				
	Cations based on 32 O										Cations based on 6 O			
Si	0.010	0.030	0.006	0.008	0.020	0.019	0.032	0.047	0.073	0.019	Si	0.002	0.004	0.001
Ti	4.202	7.559	2.933	3.412	2.935	5.162	1.921	5.716	0.620	1.326	Ti	2.230	1.900	1.979
Al	0.060	0.071	0.768	0.208	3.279	0.564	1.926	1.216	5.902	5.029	Al	0.001	0.007	0.008
Cr	0.015	0.007	0.000	0.013	0.122	0.081	0.012	0.024	2.987	3.631	Fe_{total}	1.328	1.708	1.614
Fe(iii)	7.502	0.743	9.354	8.940	6.689	4.993	10.158	3.233	5.725	4.649	Mn	0.113	0.042	0.044
Fe(ii)	11.592	14.665	8.327	10.315	8.612	11.245	8.305	11.887	6.389	7.029	Mg	0.090	0.422	0.364
Mn	0.278	0.437	0.282	0.388	0.153	0.229	0.273	0.288	0.132	0.124	Ca	0.007	0.015	0.009
Mg	0.288	0.461	2.267	0.696	2.176	1.685	1.304	1.303	2.150	2.172				
Ca	0.053	0.026	0.062	0.020	0.015	0.022	0.071	0.286	0.022	0.019				

4.3. Major, trace and rare-earth element geochemistry

Major, trace and rare-earth element compositions of thirty nine representative samples of the Quaternary lavas from the Styrian Basin have been analyzed and their representative analyses, Mg-numbers, and saturation indices (Fitton et al., 1991) are presented in Table 7. The lavas range in composition from 41.0 to 46.9 wt.% SiO_2, 2.01–2.35 wt.% TiO_2, 14.1–16.2 wt.% Al_2O_3, 9.10–10.6 wt.% FeO_{total}, 6.30–10.0 wt.% MgO and 10.1–13.5 wt.% CaO (Table 7). They are strongly alkaline (Na_2O+K_2O=6.73–9.3 wt.%) and represent primitive mafic magmatic rocks having low silica (< 50 wt.%) and high MgO (> 6 wt.%) (e.g. Wilson and Downes, 2006). Their Mg# [Mg-number=$100MgO/(MgO+FeO_{total})$] varies from 53 to 65.9. According to the classification diagram of Le Bas et al. (1986), samples from the Klöch and Steinberg are basanites and those from the Stradnerkogel and Waltrafelsen are nephelinites (Fig. 3). Based on Le Maitre (2002) classification, most of the Klöch and Steinberg samples are transional between basanites and nephelinites, so we used the term nepheline-basanites (e.g. Balogh et al., 1994) for these samples whereas a few samples are basanites. Thus collectively the Klöch and Steinberg samples are basanites/nepheline-basanites (in the entire manuscript). The Klöch and Steinberg basanites/nepheline-basanites are higher in total alkalis compared to the Pauliberg basanites (Ali and Ntaflos, 2011). The Stradnerkogel and Waltrafelsen nephelinites have the highest alkalis compared to those of the Pannonian Basin basaltic rocks (Fig. 3) (Ali and Ntaflos, 2011; Dobosi et al., 1995; Downes et al., 1995; Embey-Isztin et al., 1993; Harangi et al., 1995; Seghedi et al., 2004b).
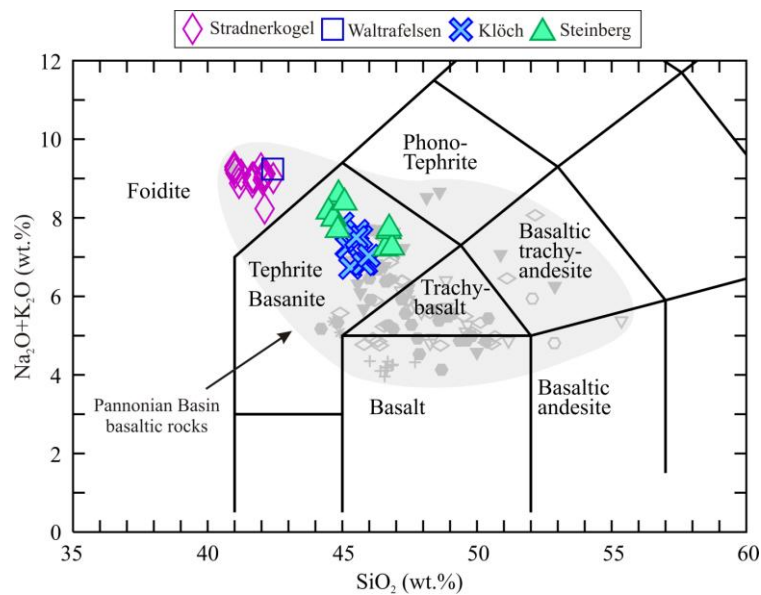
Fig. 3. Total alkalis vs. SiO_2 classification diagram (Le Bas et al., 1986) for the Styrian lavas. The field of the Pannonian Basin alkaline basalts is also shown (data after Ali and Ntaflos, 2011; Dobosi et al., 1995; Downes et al., 1995b; Embey-Isztin et al., 1993b; Harangi et al., 1995a; Seghedi et al., 2004b).

Table 7: Major, trace and rare earth elements compositions and Sr-Nd isotopic ratios of the Styrian Basin lavas.

Sample	SK-1	SK-2	SK-3	SK-4	SK-5	SK-6	SK-7	SK-8	SK-9	SK-10
Major elements (wt.%)										
SiO_2	42.1	42.4	41.2	42.0	42.1	42.1	41.0	41.6	41.0	41.7
TiO_2	2.04	2.03	2.05	2.04	2.06	2.03	2.07	2.06	2.06	2.06
Al_2O_3	14.4	14.6	14.3	14.5	14.4	14.5	14.2	14.3	14.2	14.3
FeO_{total}	10.2	10.2	10.5	10.3	10.3	10.2	10.5	10.3	10.6	10.3
MnO	0.25	0.25	0.27	0.26	0.25	0.25	0.27	0.25	0.27	0.26
MgO	6.70	6.65	6.64	6.63	6.71	6.92	6.67	6.86	6.69	6.75
CaO	12.8	12.8	13.3	12.8	12.9	13.2	13.4	13.2	13.4	13.0
Na_2O	6.31	6.49	6.12	6.42	6.26	5.91	6.47	6.27	6.50	6.44
K_2O	2.80	2.52	2.98	2.84	2.77	2.32	2.81	2.75	2.80	2.59
P_2O_5	1.38	1.38	1.47	1.41	1.38	1.38	1.46	1.42	1.47	1.36
Total	99.07	99.48	98.91	99.15	99.16	98.79	98.79	99.00	98.87	98.78
LOI	0.58	0.95	1.03	0.58	0.75	1.59	0.42	0.53	0.43	0.66
Mg#	53.9	53.6	53.0	53.5	53.6	54.7	53.0	54.2	53.0	53.9
SI	-54.4	-53.8	-56.3	-55.7	-54.0	-49.2	-58.9	-55.4	-59.3	-55.4
Trace elements (ppm)										
Sc	6.9	9.3	8.3	7.9	7.5	7.5	6.8	7.6	7.0	9.5
Zn	101	97.6	99.7	115	96.9	95.7	108	91.8	97.1	94.8
Ga	42.4	41.3	40.5	42.9	41.8	46.4	36.6	36.9	36.3	38.1
Rb	95.8	86.5	99.6	96.9	90.4	80.8	83.8	81.3	82.6	79.8
Sr	1771	1724	1781	1770	1769	1950	1825	1711	1797	1724
Y	43.4	42.4	46.5	45.1	43.9	44.1	46.4	44.4	46.3	44.9
Zr	559	480	582	658	521	480	495	490	495	495
Nb	147	151	151	152	149	152	152	139	148	153
Cs	2.03	1.87	2.22	2.14	2.03	1.99	1.92	1.98	1.91	1.87
Ba	1070	1056	1050	1152	1121	1280	969	988	958	1014
Cu	28.2	20.8	24.0	18.7	30.2	22.2	27.2	19.3	23.0	25.6
Ni	64.6	60.2	60.4	64.8	62.0	64.7	63.0	65.8	64.1	62.6
Co	30.5	31.7	30.6	31.0	29.4	30.2	31.3	28.7	28.5	30.2
Cr	53.7	57.2	54.8	49.8	53.7	56.1	51.3	56.7	53.7	54.3
V	154	149	143	156	154	152	148	149	150	148
Hf	9.08	7.70	9.49	11.0	8.52	7.78	8.07	8.13	8.03	8.12
Ta	6.27	5.66	6.79	6.75	6.20	4.32	10.9	7.17	6.30	3.61
Th	17.4	16.6	18.6	17.9	16.9	17.5	17.7	16.6	17.2	17.6
U	4.18	4.17	4.57	4.44	4.30	4.07	4.22	4.01	4.18	4.30
Rare earth elements (ppm)										
La	126	121	135	126	123	123	130	121	128	123
Ce	223	217	239	224	220	220	232	228	228	219
Pr	23.5	22.9	25.4	23.8	23.5	23.4	24.7	23.5	24.5	23.5
Nd	96.1	93.7	104	97.2	95.5	95.3	101	97.5	99.5	95.5
Sm	13.4	13.0	14.4	13.6	13.4	13.3	14.0	13.5	14.0	13.5
Eu	4.00	3.88	4.24	4.05	4.00	4.01	4.16	3.99	4.10	4.04
Gd	12.0	11.6	12.8	12.1	12.0	11.9	12.5	12.1	12.5	12.0
Tb	1.47	1.43	1.56	1.49	1.46	1.47	1.54	1.47	1.52	1.46
Dy	7.13	6.93	7.58	7.23	7.22	7.14	7.43	7.12	7.38	7.20
Ho	1.29	1.24	1.38	1.31	1.30	1.28	1.33	1.29	1.34	1.30
Er	3.39	3.32	3.60	3.45	3.36	3.34	3.51	3.37	3.49	3.42
Tm	0.44	0.43	0.47	0.45	0.43	0.44	0.45	0.45	0.45	0.44
Yb	2.79	2.68	2.93	2.88	2.79	2.76	2.86	2.78	2.82	2.83
Lu	0.39	0.38	0.41	0.40	0.39	0.38	0.39	0.39	0.39	0.38
∑REE	515	500	552	518	509	508	535	517	529	508
Sr-Nd isotopic ratios										
$^{87}Sr/^{86}Sr$						0.703529			0.703506	
$^{143}Nd/^{144}Nd$						0.512853			0.512855	

SK= Stradnerkogel; WA= Waltrafelsen; KL= Klöch; ST= Steinberg

Mg#=100*Mg/(Mg+Fe$_{total}$)

Table 7: Continued

Sample	SK-11	SK-12	SK-13	SK-14	SK-15	SK-16A	SK-16B	WA-1	KL-1	KL-2
Major elements (wt.%)										
SiO_2	41.7	41.2	42.1	42.2	42.1	41.0	41.0	42.4	45.2	45.3
TiO_2	2.06	2.06	2.06	2.03	2.04	2.06	2.06	2.01	2.35	2.33
Al_2O_3	14.2	14.1	14.4	14.5	14.5	14.1	14.1	14.6	15.7	15.7
FeO_{total}	10.3	10.5	10.3	10.2	10.3	10.4	10.4	10.1	9.38	9.34
MnO	0.25	0.26	0.26	0.25	0.25	0.26	0.26	0.25	0.18	0.17
MgO	6.84	6.76	6.64	6.69	6.66	6.74	6.82	6.55	9.51	10.0
CaO	13.1	13.5	12.9	12.8	12.9	13.3	13.4	12.6	10.9	10.9
Na_2O	6.15	6.26	6.29	6.39	6.21	6.36	6.30	6.51	5.15	4.57
K_2O	2.75	2.62	2.67	2.73	2.83	2.86	2.84	2.73	2.12	2.16
P_2O_5	1.39	1.45	1.37	1.38	1.36	1.45	1.46	1.36	0.78	0.77
Total	98.70	98.67	99.00	99.13	99.12	98.56	98.68	99.19	101.24	101.19
LOI	0.53	0.79	0.79	0.63	0.83	0.40	0.42	0.62	1.80	2.60
Mg#	54.2	53.4	53.4	53.9	53.6	53.6	53.9	53.6	64.4	65.7
SI	-54.1	-56.1	-53.7	-54.6	-53.8	-58.1	-57.8	-54.6	-34.2	-29.5
Trace elements (ppm)										
Sc	7.5	9.2	8.8	4.3	8.5	7.6	8.4	7.7	17.2	17.7
Zn	138	95.5	97.3	101	96.7	100	97.1	105	75.4	73.5
Ga	40.1	36.5	39.5	41.1	41.7	39.8	38.1	44.2	26.4	26.4
Rb	82.8	84.4	86.3	85.9	96.2	87.7	85.5	101	50.2	52.5
Sr	1766	1770	1694	1786	1710	1789	1767	1716	978	1011
Y	44.0	45.0	43.9	44.4	44.7	44.6	45.4	43.2	29.4	29.1
Zr	475	472	471	478	478	510	457	478	336	381
Nb	146	147	148	148	149	150	145	145	98.4	98.5
Cs	1.80	1.83	1.69	2.06	2.12	1.96	1.89	1.87	1.38	1.44
Ba	1079	946	1030	1056	1070	998	960	930	561	561
Cu	28.1	26.0	25.1	23.7	23.1	25.5	25.9	28.1	40.1	27.1
Ni	64.7	68.9	60.0	64.0	58.4	63.9	65.2	58.8	139	156
Co	28.8	33.8	30.4	33.1	31.0	29.6	29.2	27.4	36.9	37.9
Cr	52.6	54.8	48.6	50.6	53.7	55.8	56.4	60.3	142	134
V	148	152	151	155	152	148	152	181	224	224
Hf	7.75	7.74	7.46	7.73	7.68	8.20	7.38	7.19	5.58	6.35
Ta	4.10	4.33	4.33	6.85	8.07	6.56	7.66	4.43	5.25	5.56
Th	16.7	16.6	16.6	16.9	17.2	16.4	17.1	16.2	9.97	9.81
U	4.07	4.08	4.18	4.13	4.20	4.21	4.15	3.36	2.49	2.46
Rare earth elements (ppm)										
La	121	123	121	122	123	122	123	112	58.9	57.9
Ce	216	220	216	227	226	216	220	197	108	115
Pr	23.3	23.6	23.2	23.2	23.3	23.2	23.6	21.0	11.8	11.6
Nd	94.5	96.2	94.0	96.1	96.4	94.0	95.6	85.0	47.9	49.3
Sm	13.3	13.4	13.2	13.2	13.3	13.2	13.5	11.7	7.55	7.34
Eu	3.96	4.01	3.92	3.91	3.91	3.95	3.98	3.48	2.28	2.25
Gd	11.9	12.2	11.7	11.9	12.1	11.9	12.1	10.7	6.89	6.89
Tb	1.46	1.48	1.44	1.45	1.46	1.45	1.48	1.29	0.90	0.88
Dy	7.09	7.20	7.06	7.09	7.15	7.12	7.21	6.36	4.56	4.46
Ho	1.28	1.30	1.26	1.28	1.29	1.28	1.29	1.18	0.83	0.82
Er	3.33	3.38	3.36	3.36	3.40	3.37	3.40	3.05	2.15	2.14
Tm	0.44	0.45	0.44	0.44	0.43	0.45	0.44	0.41	0.29	0.29
Yb	2.74	2.78	2.70	2.75	2.77	2.73	2.77	2.50	1.85	1.85
Lu	0.38	0.38	0.37	0.38	0.39	0.39	0.38	0.35	0.26	0.26
$\sum$ REE	501	509	500	513	515	501	509	456	254	261
Sr-Nd isotopic ratios										
$^{87}Sr/^{86}Sr$	0.703521					0.703505		0.703525	0.703593	
$^{143}Nd/^{144}Nd$	0.512858					0.512856		0.512851	0.512849	

Table 7: Continued

Sample	KL-3	KL-4	KL-5	KL-6	KL-7	KL-8	KL-9	KL-10	KL-11	ST-5
Major elements (wt.%)										
SiO_2	45.2	45.9	45.6	45.6	45.8	45.7	45.5	45.0	46.0	44.9
TiO_2	2.33	2.30	2.29	2.30	2.31	2.28	2.30	2.32	2.32	2.09
Al_2O_3	15.6	15.9	15.9	16.0	15.8	15.9	15.9	15.5	15.9	15.8
FeO_{tot}	9.38	9.21	9.11	9.13	9.19	9.12	9.10	9.28	9.33	10.1
MnO	0.18	0.17	0.17	0.17	0.17	0.17	0.17	0.17	0.17	0.22
MgO	9.54	9.60	9.45	9.04	9.96	9.07	9.19	9.81	8.86	6.30
CaO	10.8	10.4	10.4	10.5	10.5	10.5	10.7	10.3	10.5	11.2
Na_2O	5.06	4.68	5.09	5.19	4.42	5.15	5.10	5.75	4.71	5.87
K_2O	2.19	2.15	2.33	2.47	2.40	2.36	2.40	2.10	2.32	2.72
P_2O_5	0.77	0.74	0.74	0.75	0.72	0.74	0.76	0.77	0.78	1.19
Total	101.14	101.06	101.03	101.12	101.22	101.07	101.11	101.07	100.91	100.41
LOI	3.10	0.98	0.73	0.75	0.93	0.87	0.57	1.91	1.78	0.99
Mg#	64.5	65.0	64.9	63.9	65.9	64.0	64.3	65.3	62.9	52.7
SI	-33.6	-27.8	-32.7	-34.2	-27.8	-33.1	-33.8	-38.3	-28.4	-41.5
Trace elements (ppm)										
Sc	16.3	19.4	17.6	17.8	16.8	16.9	16.3	17.0	17.4	10.5
Zn	76.9	76.8	75.5	77.8	75.7	78.4	76.6	78.3	80.7	99.2
Ga	27.5	27.8	27.6	28.5	27.7	28.5	26.9	27.6	29.6	37.4
Rb	53.9	52.8	54.4	56.5	54.1	52.0	55.4	50.8	51.8	55.2
Sr	913	1008	1003	1034	1013	1025	1044	1003	1151	1392
Y	28.6	28.5	29.1	28.9	27.7	29.6	28.6	29.5	30.5	36.2
Zr	356	368	386	439	393	424	398	368	418	462
Nb	95.7	94.2	96.1	101	96.0	96.3	95.1	96.1	98.1	130
Cs	1.19	1.25	1.30	1.33	1.27	1.47	1.16	1.27	1.69	1.84
Ba	592	581	581	611	584	596	545	582	623	785
Cu	25.5	34.3	33.3	32.0	32.9	34.7	33.5	30.8	34.1	29.2
Ni	128	138	130	137	131	132	147	134	135	54.4
Co	37.6	38.1	34.6	35.2	35.5	35.0	38.6	36.5	33.2	31.2
Cr	126	136	124	128	132	125	144	136	126	98.3
V	221	215	214	215	214	213	217	225	215	185
Hf	5.85	5.96	6.25	7.03	6.35	6.88	6.60	6.01	6.66	7.13
Ta	5.43	5.12	5.26	5.16	5.24	5.22	5.11	5.40	5.39	5.82
Th	9.50	9.90	10.2	10.3	9.53	10.4	9.60	9.74	10.7	14.5
U	2.39	2.54	2.56	2.83	2.54	2.67	2.49	2.38	2.60	3.62
Rare earth elements (ppm)										
La	57.4	56.6	56.4	58.2	54.8	58.3	53.9	57.7	59.0	85.8
Ce	106	104	103	107	101	106	110	106	107	153
Pr	11.6	11.4	11.3	11.7	11.0	11.6	10.9	11.6	11.8	16.3
Nd	46.9	46.2	45.9	47.4	44.9	47.1	46.6	47.1	47.6	66.2
Sm	7.40	7.26	7.21	7.38	7.11	7.37	7.02	7.40	7.49	9.67
Eu	2.25	2.24	2.18	2.25	2.16	2.25	2.16	2.25	2.28	2.96
Gd	6.78	6.68	6.64	6.76	6.46	6.75	6.53	6.76	6.81	8.79
Tb	0.88	0.87	0.86	0.87	0.83	0.88	0.85	0.87	0.87	1.12
Dy	4.47	4.45	4.36	4.46	4.30	4.50	4.35	4.47	4.53	5.55
Ho	0.83	0.82	0.81	0.82	0.78	0.82	0.81	0.81	0.84	1.02
Er	2.12	2.10	2.12	2.19	2.07	2.16	2.13	2.15	2.19	2.63
Tm	0.29	0.28	0.29	0.29	0.28	0.29	0.28	0.29	0.30	0.34
Yb	1.82	1.80	1.83	1.86	1.74	1.87	1.84	1.81	1.84	2.18
Lu	0.25	0.25	0.25	0.26	0.24	0.25	0.25	0.25	0.26	0.30
∑ REE	249	245	243	252	237	250	247	249	253	356
Sr-Nd isotopic ratios										
$^{87}Sr/^{86}Sr$			0.703595			0.703669	0.703859		0.703776	
$^{143}Nd/^{144}Nd$			0.512846			0.512839	0.512844		0.512848	

Table 7: Continued

Sample	ST-6	ST-7	ST-8	ST-9	ST-11	ST-12	ST-13	ST-14	ST-2CO6
Major elements (wt.%)									
SiO_2	46.6	46.7	46.9	46.7	44.7	44.5	44.7	45.1	44.8
TiO_2	2.24	2.23	2.26	2.23	2.16	2.12	2.11	2.11	2.10
Al_2O_3	16.0	16.0	16.2	16.1	15.2	15.0	14.9	15.8	14.8
FeO_{tot}	9.28	9.25	9.15	9.23	10.1	10.2	10.2	10.2	10.2
MnO	0.16	0.16	0.15	0.16	0.20	0.20	0.20	0.21	0.20
MgO	8.15	7.85	8.05	7.81	8.35	8.70	8.87	6.59	9.13
CaO	10.5	10.3	10.1	10.1	11.0	10.6	10.7	11.0	10.8
Na_2O	4.80	5.20	4.80	5.24	5.57	5.61	5.49	5.65	5.30
K_2O	2.41	2.45	2.44	2.48	2.41	2.54	2.48	2.73	2.38
P_2O_5	0.85	0.86	0.81	0.85	1.08	1.06	1.05	1.18	1.04
Total	101.00	101.07	100.87	101.00	100.75	100.53	100.64	100.51	100.81
LOI	0.25	0.01	0.24	0.00	0.23	0.00	0.06	0.65	0.37
Mg#	61.0	60.2	61.1	60.1	59.5	60.4	60.9	53.6	61.6
SI	-27.7	-30.3	-26.4	-30.3	-38.9	-39.9	-38.5	-39.0	-36.6
Trace elements (ppm)									
Sc	14.8	14.3	16.4	16.8	13.6	14.5	13.8	10.7	13.4
Zn	79.8	81.8	81.4	84.2	97.1	94.3	95.6	101	91.9
Ga	28.1	28.3	28.0	29.7	34.6	33.5	33.7	38.6	32.7
Rb	64.0	54.8	55.3	51.7	62.2	53.6	52.6	55.9	51.7
Sr	1026	1032	961	1031	1203	1181	1164	1360	1144
Y	28.5	29.4	28.6	29.6	34.3	32.1	32.4	36.5	32.1
Zr	377	402	435	418	556	427	430	455	427
Nb	97.2	96.3	94.0	97.6	111	108	107	127	107
Cs	0.99	1.30	1.03	1.23	1.73	1.44	1.64	1.97	1.72
Ba	557	557	547	582	713	679	680	788	649
Cu	45.4	45.4	46.8	45.5	31.9	34.5	34.4	31.5	33.9
Ni	76.5	71.1	76.0	73.1	123	139	144	62.5	161
Co	36.7	31.9	34.1	32.0	36.0	39.6	38.1	31.3	40.3
Cr	167	147	156	159	121	120	127	97.2	140
V	201	186	199	186	206	198	200	189	198
Hf	6.07	6.49	6.97	6.63	8.82	6.70	6.67	6.99	6.72
Ta	5.94	6.96	6.60	5.45	6.82	5.72	6.48	5.85	5.75
Th	9.86	9.96	9.44	10.2	12.6	11.7	12.0	14.6	11.7
U	2.46	2.54	2.47	2.59	3.03	2.88	2.91	3.41	2.82
Rare earth elements (ppm)									
La	55.6	56.7	53.0	57.1	75.4	71.8	72.2	84.5	70.5
Ce	102	114	97.0	104	135	129	129	150	136
Pr	11.1	11.3	10.6	11.4	14.5	13.9	13.9	16.1	13.6
Nd	45.1	48.1	43.4	46.1	59.0	56.2	56.1	65.3	57.2
Sm	7.13	7.20	6.96	7.24	8.97	8.39	8.43	9.56	8.31
Eu	2.19	2.20	2.13	2.23	2.71	2.56	2.59	2.91	2.51
Gd	6.51	6.79	6.38	6.61	8.09	7.68	7.76	8.78	7.65
Tb	0.86	0.86	0.84	0.86	1.02	0.98	0.98	1.10	0.97
Dy	4.32	4.51	4.33	4.41	5.15	4.91	4.89	5.46	4.86
Ho	0.79	0.82	0.80	0.82	0.94	0.89	0.89	1.00	0.88
Er	2.03	2.12	2.07	2.09	2.43	2.31	2.30	2.59	2.27
Tm	0.27	0.29	0.28	0.28	0.32	0.30	0.30	0.34	0.31
Yb	1.69	1.83	1.74	1.77	2.04	1.91	1.91	2.16	1.96
Lu	0.24	0.25	0.24	0.24	0.28	0.26	0.26	0.30	0.27
∑ REE	239	257	230	245	316	301	301	350	307
Sr-Nd isotopic ratios									
$^{87}Sr/^{86}Sr$		0.703701	0.703730		0.703557				
$^{143}Nd/^{144}Nd$		0.512834	0.512832		0.512858				

The silica-saturation index (S.I.; Fitton et al., 1991) of the studied lavas ranges from -26 to -59: the highest in basanites/nepheline-basanites and the lowest in nephelinites. They are sodic in character, with low K_2O/Na_2O ratios ranging from 0.37 to 0.54 typical for *anorogenic* magmatic rocks (Wilson and Downes, 2006) and overlap the range of values determined for other alkaline basaltic rocks of the Pannonian Basin (0.32-0.79; Embey-Isztin et al., 1993).They have CaO/Al_2O_3 ratios (0.63-0.96) higher than the Little Hungarian Plain alkaline basalts values (0.51-0.64; Harangi et al., 1995).

Figure 4 shows the relationship between selected major and trace element and MgO contents compared to the available previous published data of the Pannonian Basin basaltic rocks. In terms of Al_2O_3, CaO, FeO and MgO, the Styrian lavas are identical to other Pannonian alkaline basaltic rocks (Fig. 4) (Ali and Ntaflos, 2011; Dobosi et al., 1995; Downes et al., 1995; Embey-Isztin et al., 1993; Harangi et al., 1995; Seghedi et al., 2004b).
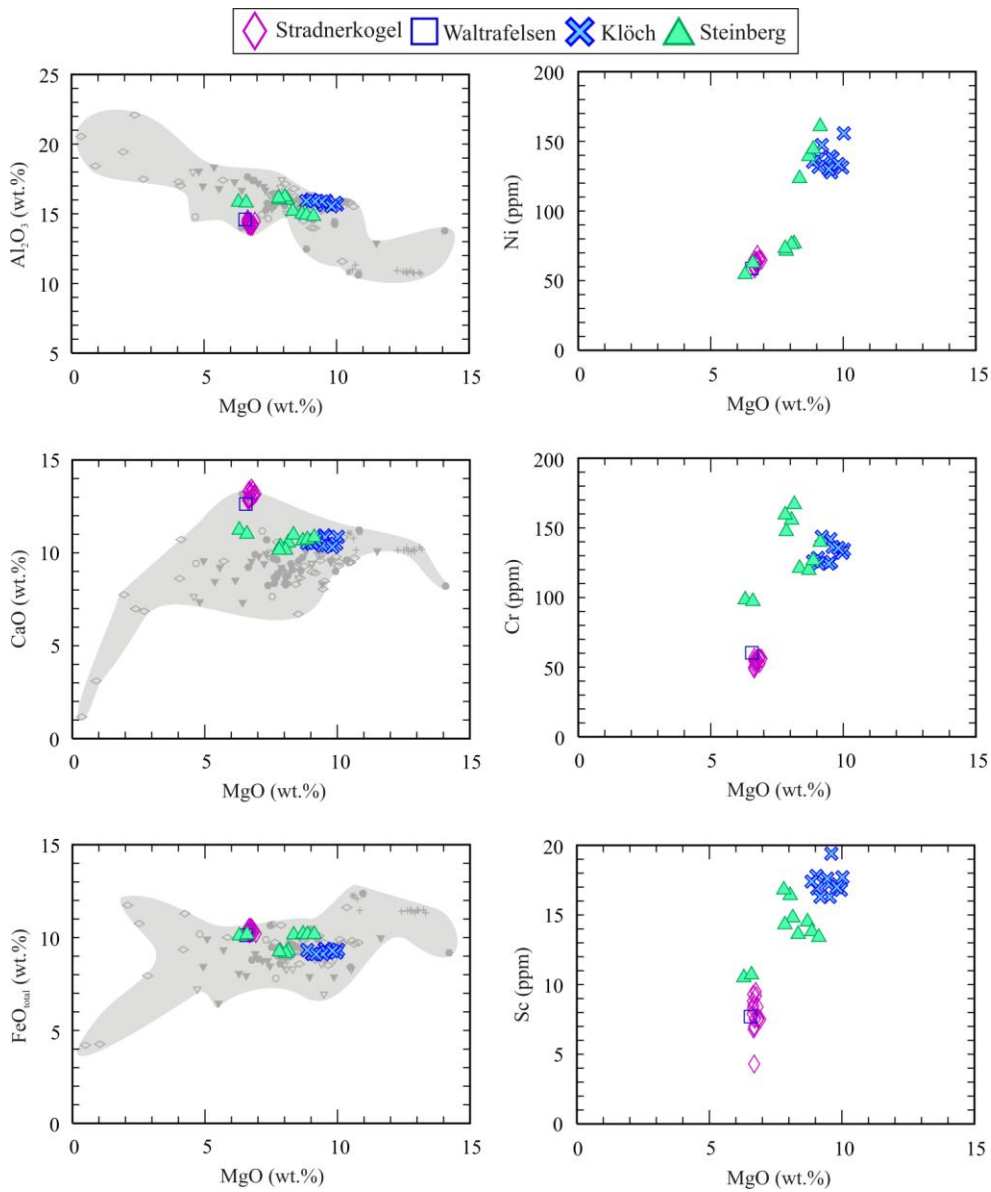

Fig. 4. Variation of selected major (wt.%) and trace element (ppm) vs. MgO (wt.%) in the Styrian lavas. The field of the Pannonian Basin alkaline basalts is also shown (data references as in Fig. 3).

The nephelinites (Stradnerkogel and Waltrafelsen) have the lowest Al_2O_3 and highest CaO of all the studied samples. The basanites/nepheline-basanites (Klöch and Steinberg) have higher Al_2O_3 and lower FeO contents than the Pauliberg basanites whereas CaO is somewhat similar in both (Ali and Ntaflos, 2011). The compatible trace element (Ni, Cr and Sc) are higher in the basanite/nepheline-basanites (Klöch and Steinberg) than in the nephelinites (Stradnerkogel and Waltrafelsen) (Fig. 4).

The lavas exhibit a relatively wide compositional range of trace elements (Table 7): Cr, 48.6-167 ppm; Ni, 54.4-161 ppm; V, 143-225 ppm; Sr, 913-1950 ppm; Ba, 545-1080 ppm and Rb, 50-100 ppm. They are generally enriched in the high field strength elements (HFSE): Zr, 336-556 ppm; Nb, 94-153 ppm; and Y, 27.65-46.5 ppm (Table 7). In addition, they display elemental ratios (average), such as Zr/Nb= 3.67, La/Nb=0.71 and Ba/Th=58.5, similar to HIMU-OIB (Zr/Nb=3.2-5, La/Nb=0.66-0.77 and Ba/Th=49-77; Weaver, 1991).

The primitive mantle (PM)-normalized multi-element patterns of the studied lavas are shown in Fig. 5a. They resemble ocean island basalts (OIB) in terms of enrichment in Nb (Nb/La=1.4, Nb/U=37) (Fig. 5a). Nephelinites display pronounced negative K and Ti anomalies compared to the neighbor elements (Fig. 5a).
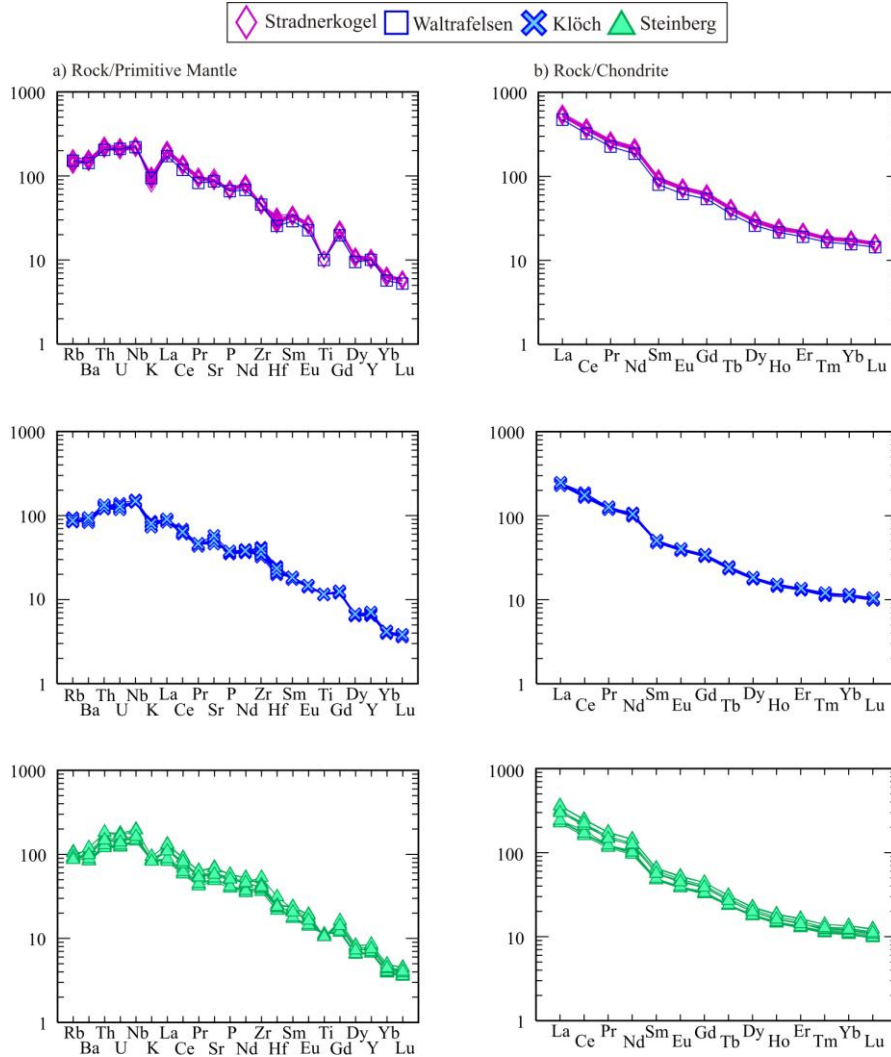
Fig. 5. a) PM-normalized multi-element diagrams. b) Chondrite-normalized REE patterns. Normalization values are from McDonough and Sun (1995).

On a PM-normalized multi-element diagrams, the patterns of the basanites/nepheline-basanites resemble those of the nephelinites, but with less pronounced K and Ti anomalies. The similarity of the trace element distribution patterns of the Klöch and Steinberg basanites/nepheline-basanites is remarkable (Fig. 5a). The studied basanites/nepheline-basanites and nephelinites have superchondritic Zr/Hf ratios (60-65 and 51-67 respectively) compared with those of chondrites/primitive mantle (Zr/Hf =38; Anders and Grevesse, 1989).

In a chondrite-normalized rare earth element (REE) diagram (Fig. 5b), these strongly alkaline lavas show a pattern of strong light REE (LREE) enrichment (La_N/Yb_N=20-31) without any Eu anomaly. Generally, the degree of LREE enrichment correlates positively with the degree of slica-undersaturation. Accordingly, the highly undersaturated nephelinites are the highest LREE enrichment in the Styrian Basin (Ali and Ntaflos, 2009, 2010).

The Styrian Basin lavas have Ce/Pb (>20; Embey-Isztin et al., 1993) and Nb/U ratios (37; on average) similar to OIB (Ce/Pb≈ 25±5; Nb/U≈ 47±10), higher than those of the primitive mantle (Ce/Pb≈ 9 and Nb/U≈30) and continental crust (Ce/Pb≈ 4 and Nb/U≈ 10) (Hofmann et al., 1986).

4.4. Isotope geochemistry

As shown in Table 7, the $^{87}Sr/^{86}Sr$ isotopic compositions of the investigated lavas range from 0.70350 to 0.70386 and $^{143}Nd/^{144}Nd$ from 0.512832 to 0.512858. Since they have low $^{87}Sr/^{86}Sr$ isotopic ratios and high $^{143}Nd/^{144}Nd$ ratios, they plot in the "depleted field" relative to the bulk Earth (Fig. 6), being similar to most of Neogene-Quaternary alkaline mafic lavas in Western and Central Europe (Wilson and Downes, 1991; Wilson and Patterson, 2001). The Sr-Nd isotopic compositions of the Styrian lavas are strongly enriched compared to MORB and fall within the range of OIB values (Fig. 6).
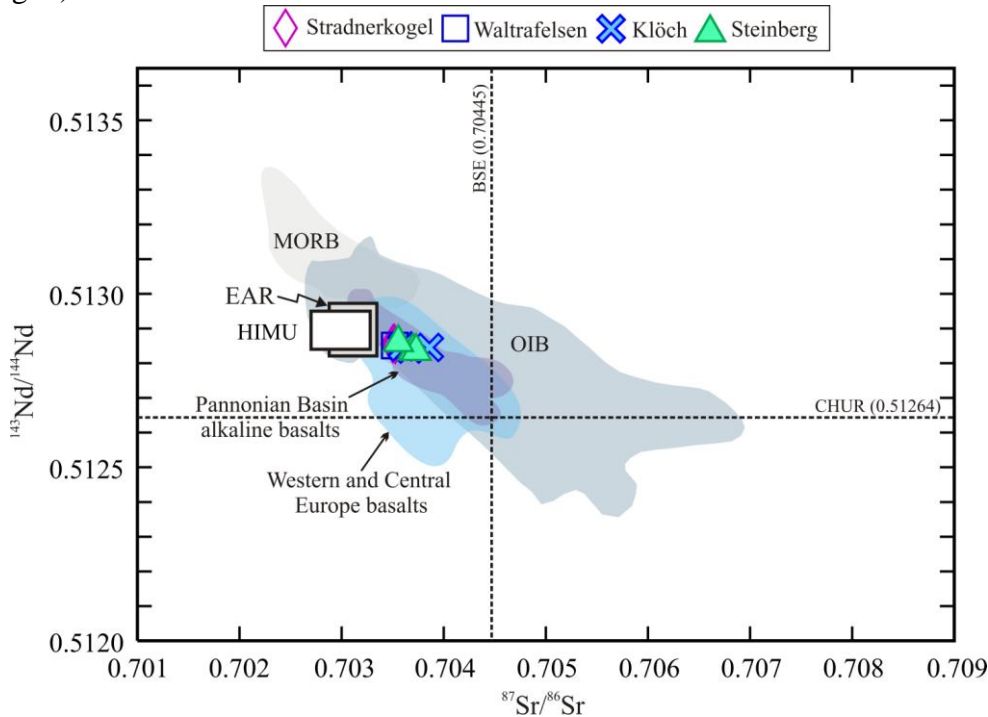
Fig. 6. Sr and Nd isotope variations of the Styrian lavas compared with fields of alkaline basalts from the Pannonian Basin (data after Ali and Ntaflos, 2011; Dobosi et al., 1995; Downes et al., 1995b; Embey-Isztin et al., 1993b; Harangi et al., 1995a; Salters et al., 1988; Seghedi et al., 2004b) and from Western and Central Europe (Wilson and Patterson, 2001). MORB and OIB fields are from Zindler and Hart (1986); EAR isotope compositions are from Lustrino and Wilson (2007).

The Sr and Nd isotopic ratios plot (Fig. 6) very close to EAR (European Asthenospheric Reservoir)-HIMU (high μ refers to high $^{238}U/^{204}Pb$). Moreover, they overlap the entire range of values for the Pannonian Basin alkaline basaltic rocks (Ali and Ntaflos, 2011; Dobosi et al., 1995; Downes et al., 1995; Embey-Isztin et al., 1993; Harangi et al., 1995; Salters et al., 1988; Seghedi et al., 2004b) and also those of Western and Central Europe basalts (Wilson and Patterson, 2001) (Fig. 6). The isotopic signatures of both the Stradnerkogel and Waltrafelsen nephelinites are similar (Fig. 6; Table 7). Compared with the other Neogene alkaline basalts in the western Pannonian Basin, the Styrian nephelinites are amongst the most depleted in the radiogenic Sr and Nd isotopic ratios ($^{87}Sr/^{86}Sr$, 0.703505 – 0.703529; $^{143}Nd/^{144}Nd$, 0.512851 – 0.512858) (Ali and Ntaflos, 2011; Embey-Isztin et al., 1993). In addition, the Stradnerkogel nephelinites have relatively high $^{206}Pb/^{204}Pb$ ratios of around 19.2 and are similar to those of the Nógrád basalts (Embey-Isztin et al., 1993; Salters et al., 1988).

5. Discussion

5.1. Constraints on the crystallization conditions

Rhönite is uncommon accessory mineral present in the groundmass of the Klöch basanites/nepheline-basanites and can be used to estimate the conditions of crystallization. Its occurrence point to crystallization in the presence of a fluid phase at pressures < 0.06 GPa (corresponding to depths of < 1.8 km) and over temperatures range of 840 and 1200 °C (Kunzmann, 1989).

Clinopyroxene phenocrysts cores in the Klöch and Steinberg basanites/nepheline-basanites have Ti/Al ratios vary between ~0.125 and ~0.25 suggesting moderate to high pressure crystallization whereas those of Stradnerkogel nephelinites extend to < 0.125 implying that they crystallized under slightly higher pressure than those of the Klöch and Steinberg basanites/nepheline-basanites (Dobosi et al., 1991) and ref. therein (Fig. 7). The clinopyroxene phenocryst rims and groundmass in the Stradnerkogel nephelinite have Ti/Al ratios close to 0.5 (low pressures of crystallization) whereas those of basanites/nepheline-basanites (Klöch and Steinberg) are around 0.25 (moderate pressures of crystallization) similar to what obtained by Dobosi et al. (1991) (Fig. 7). The clinopyroxene Al^{VI}/Al^{IV} ratios of all studied samples vary between 0 and 0.72. Some of the clinopyroxene cores in Stradnerkogel nephelinites and Steinberg basanites/nepheline-basanites have high Al^{VI}/Al^{IV} (0.63–0.72) suggesting high pressure crystallization (Wass, 1979). Compared to the other Styrian basalts, the clinopyroxene compositions from the studied nephelinites suggest higher pressure crystallization (Dobosi et al., 1991).
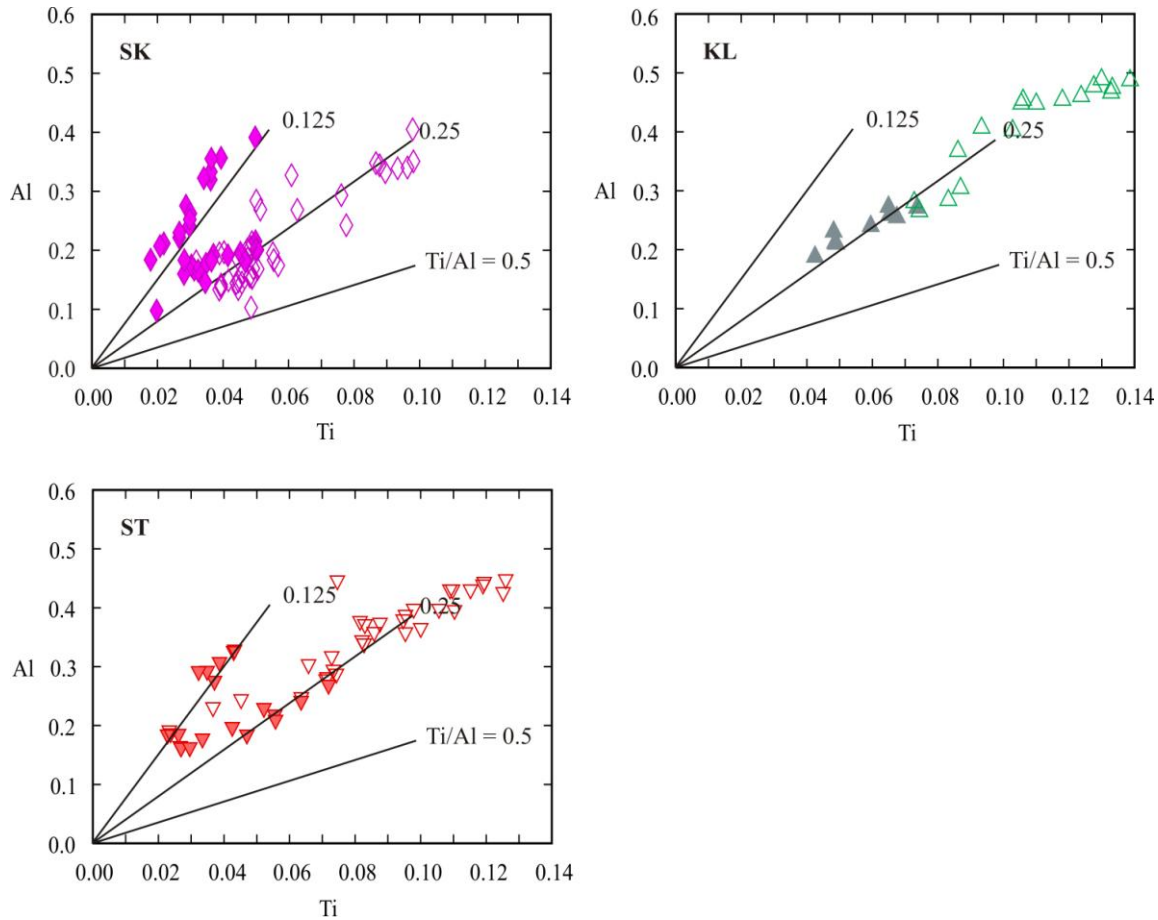
Fig. 7. Variation of Ti and Al (cations per formula unit based on 6 O) in clinopyroxenes of the Styrian lavas. Closed symbols represent phenocryst core whereas open one represent phenocryst rim and groundmass. Abbreviations, SK= Stradnerkogel; KL = Klöch; ST= Steinberg.

5.2. Role of crustal contamination

The degree of crustal contamination can be assessed using certain chemical parameters. Basaltic magmas affected by crustal contamination have La/Nb ratios>1.5, La/Ta>22, and K/P>7 (e.g. Hart et al. 1989). The Styrian lavas have low values of such elemental ratios (La/Nb=0.71; La/Ta=13.2; K/P=4.6, on average), along with their Sr–Nd isotopic composition all suggest that the magma was subjected to minimal or no crustal contamination. Moreover, they are generated from an OIB-like (Nb-rich) undersaturated magma which doesn't support the crustal contamination and/or interaction with lithospheric mantle (Smith et al., 1999; Zeng et al., 2010 and ref. therein). Furthermore, the Ba (544–1080 ppm) and Sr (913–1950 ppm) contents of these lavas are much higher than those of average continental crust (Ba=390 ppm; Sr=325 ppm; Rudnick and Gao, 2003). The occurrence of mantle xenoliths in most of these lavas (Embey-Isztin et al., 1993) indicates that the alkaline magma ascent may have been rapid enough from the site of partial melting to the surface to escape contamination. Moreover, the Pannonian Basin $\delta^{18}O$ values of alkalic mafic rocks (Embey-Isztin et al., 1993) suggest that the magmas were not significantly contaminated with crustal material during ascent. Significant crustal assimilation and/or interaction with lithospheric mantle can be ruled out because of their high (OIB-like) Ce/Pb and Nb/U ratios. Accordingly, the geochemical compositional variation can be used to provide constraints on the nature of their mantle source and melting condition.

5.3. Petrogenetic considerations: role of fractional crystallization and partial melting

The relatively low Mg# (53–54.7), Ni (58.4–68.9 ppm) and Cr (48.6–60.3) contents (Table 7) of nephelinites may indicate fractional crystallization of olivine and pyroxene. However in these lavas Ni, Cr and Sc do not display a clear trend with MgO (Fig. 4) and the FeO_{total}/MgO ratio (1.48–1.58) are generally constant, suggesting negligible fractional crystallization of olivine and pyroxene. Also, the Klöch and Steinberg basanites/nepheline-basanites do not show appreciable correlation between Ni, Cr and Sc and MgO (Fig. 4) indicating minimal olivine and clinopyroxene fractionation. Absence of plagioclase phenocrysts and the lack of a negative Eu anomaly in the basanites/nepheline-basanites suggest insignificant fractional crystallization of plagioclase (Fig. 5b).

Since the studied lavas are silica-undersaturated (S.I. range from -26 to -59) and have high MgO (6.30–10.0 wt.%), and there is no obvious correlation between MgO and other oxides (Fig. 4) and most of them contain mantle xenoliths (Embey-Isztin et al., 1993) major fractional crystallization can be ruled out from their origin.

The increase in both, total alkalis and CaO contents with decrease SiO_2 contents (Figs. 3 and 8) from basanites/nepheline-basanites to nephelintes, provides additional evidence against crystal fractionation processes. This trend of increasing total alkalis and CaO contents with decreasing SiO_2 contents has been observed in several OIB lavas (e.g. Polynesia, Samoa and Hawaii) (Keshav et al., 2004).
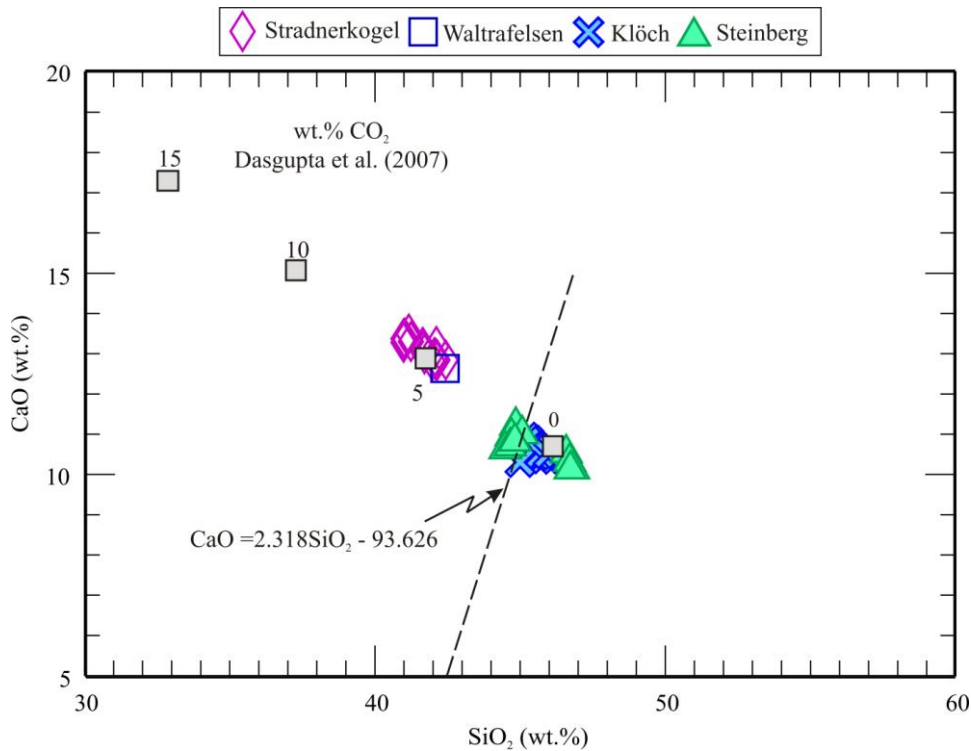
Fig. 8. SiO_2 and CaO contents of the Styrian lavas compared with partial melts of carbonated peridotite (Dasgupta et al., 2007). The dot line is an approximate filter that separates CO_2-enriched and deficient lavas (after Herzberg and Asimow, 2008).

The highly/moderately incompatible element ratios (e.g. Ba/Y and P_2O_5/TiO_2), the LREE/HREE and the CaO/Al_2O_3 ratios can provide constraints on both the depth (discussed below) and degree of partial melting (Wilson and Downes, 2006). Generally, they decrease with increase degrees of partial melting (Wilson and Downes, 2006). The positive correlation between the incompatible element ratios and the concentrations of highly incompatible element (Fig. 9a-c) and the negative correlation between CaO/Al_2O_3 and SiO_2 (Fig. 9d) suggest that partial melting processes have played a significant role in producing the range of magma compositions observed. A systematic increase in La/Yb_N (20–31) and CaO/Al_2O_3 (0.63–0.96) ratios display from basanite/nepheline-basanite to nephelinite consistent with decreasing degrees of partial melting. Moreover, the Styrian nephelinites have the lowest contents of compatible element (Ni and Cr) consistent with low degrees of partial melting which were also confirmed by their lowest S.I. (highly undersaturated) and strong LREE enrichment. Since the Ce/Yb and Sm/Yb ratios are not fundamentally affected by fractional crystallization processes they are useful indicator for the degree of partial melting. The high Ce/Yb (83-56) and Sm/Yb (4.97-3.83) ratios in the Styrian lavas clearly indicate low degrees of partial melting. All the studied samples are enriched in highly incompatible elements, LREE and LREE/HREE suggesting low degrees of melting of depleted mantle source (Wilson and Downes, 2006).
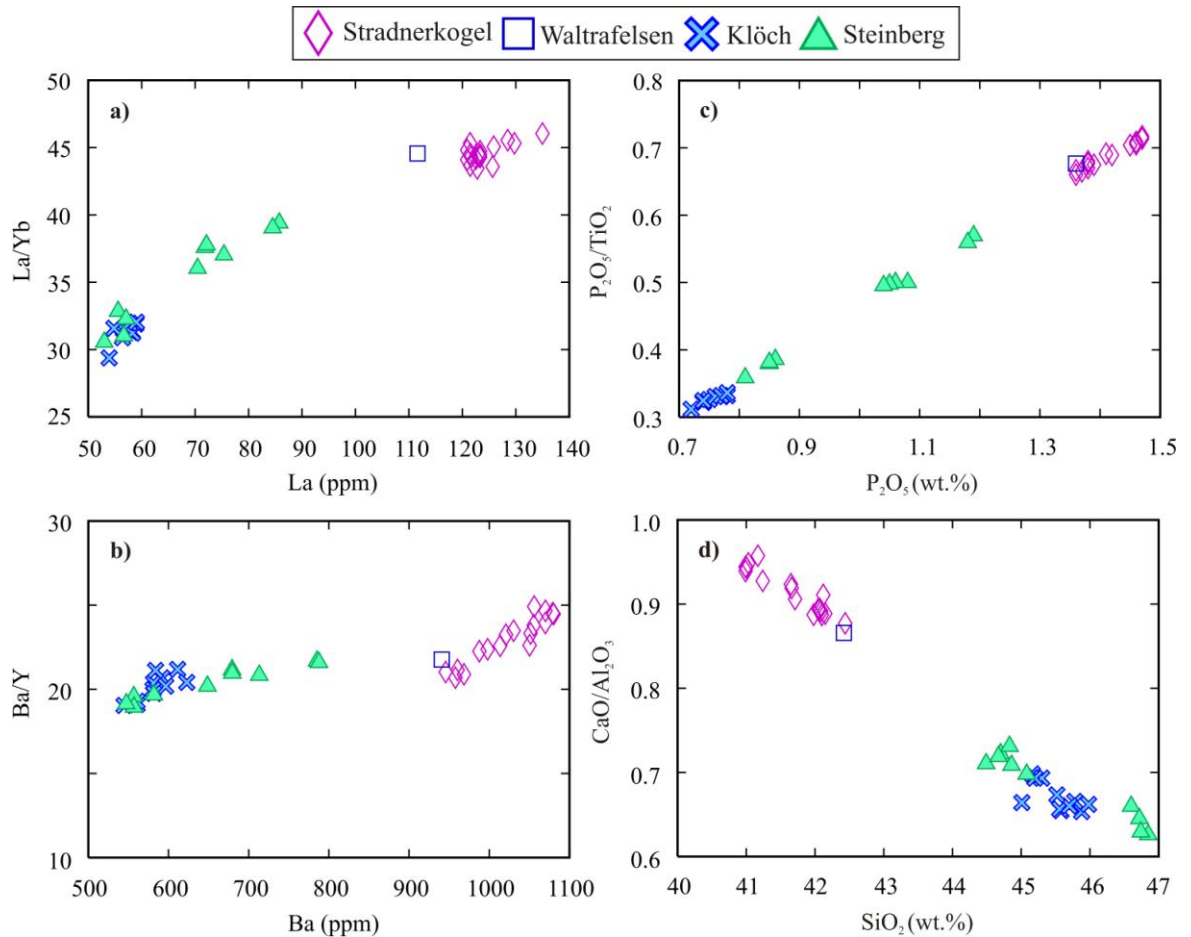
Fig. 9. (a-c) Plots showing highly/moderately incompatible element ratios vs. highly incompatible element concentrations for the Styrian lavas. (d) CaO/Al_2O_3 vs. SiO_2.

The relationship between Zr/Nb and Nb/Y compared to model melting curves for 0.5-4 % partial melting of spinel- and garnet-peridotite facies mantle from Harangi (2001b) are displayed in Fig. 10. This evidently shows that the mafic volcanic rocks of the Styrian Basin were derived from a garnet-lherzolite source at a greater depth (>80 km). The degrees of partial melting are around 1% and are lower than those of Pauliberg basalts (2 %, Ali and Ntaflos, 2011) and are in agreement with the degrees of partial melting estimated by Harangi (2001) for the CPR basalts.
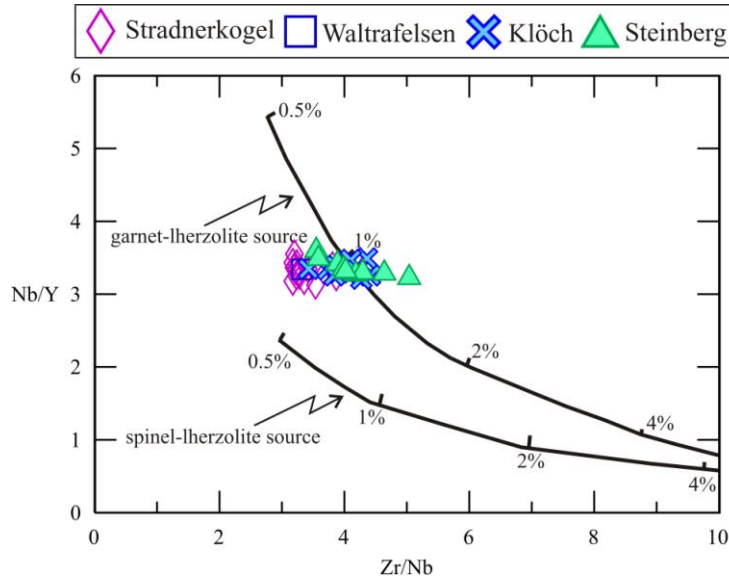
Fig. 10. Variation of Zr/Nb vs. Nb/Y for the most primitive mafic Styrian lavas. Curves are model melting curves from Harangi (2001) for 0.5-4% partial melting of spinel- and garnet-peridotite facies mantle. Model Parameters (from Harangi, 2001): source composition: Zr=11.3ppm, Nb=0.72ppm, Y=2.7ppm; source mineralogy (%): spinel-lherzolite is ol58- opx30-cpx10-sp2; garnet-lherzolite is ol59.9-opx25.5-cpx8.8-gt5.8; melting modes (%): ol1.2-opx8.1-cpx76.4-sp14.3 and ol1.2-opx8.1-cpx36.4-gt54.3.

In addition the S.I. (-26 to -59) of the studied lavas suggests low but variable degrees of partial melting as well. Low degree (undersaturated) melts either will erupt in a relatively primitive condition or they will be stored and solidified at shallow levels and the eruption of such melts will be enhanced by its higher volatile contents (Fitton et al., 1991). The increasing degree of silica-undersaturation from basanite/nepheline-basanite to nephelinite results mainly from decreasing degrees of partial melting at increasing depths in the mantle (e.g. Wilson, 1989).

5.4. Constraints on the depths and temperatures of melting

The depth of magma generation can be estimated using the major oxides of the primitive lavas. An artificial data-set has been produced by normalizing all major element compositions to 15% MgO (using olivine fractionation equation of Pearce 1978) by fractional addition of olivine to exclude any effect of fractionation. These data-set are comparable to the partial melt compositions of anhydrous lherzolite given by Hirose and Kushiro (1993). The change in SiO_2 contents correlates inversely with pressure, whereas FeO, CaO and Al_2O_3 are controlled mainly by degree of partial melting and composition of the source (Hirose and Kushiro, 1993). The most conspicuous feature of the data-set is a strong negative correlation between SiO_2 and FeO, as seen in many ocean island basalts (OIB) (not shown) (Dasgupta et al., 2010).

The SiO_2 content of the recalculated Styrian data-set varies from 40.8 wt.% to 45.8 wt.%, implying that the Styrian mafic magmas segregated at different pressures, i.e. at different depths. Scarrow and Cox (1995) provide linear regression equation [P (kbar) = 213.6 - 4.05 SiO_2] of the experimental data given by Hirose and Kushiro (1993) for the variation of pressure with SiO_2. This leads to estimates of apparent pressure of magma segregation of ~ 2.8 GPa to ~ 4.8 GPa, corresponding to a depth range of about 90 to 150 km. According to the estimations the basanite/nepheline-basanite magma could have been generated at about 90 to 115 km whereas the nephelinitic magma could have been generated at deeper level (~ 135 to 150 km). The calculated depth of magma segregation from the Styrian basanites/nepheline-basanites (~90 to 115 km) is comparable to those of Kissomlyó, Hercseg, Sitke and Klöch (95–110 km; Harangi, 2001) and those of Pauliberg basanites (106–110 km; Ali and Ntaflos, 2011). These estimates indicate that melting was commenced in the garnet stability field being in accordance with the trace element data (Fig. 5), and segregation is estimated to have occurred over the pressure range of 2.8–4.8 GPa (most of the erupted magmas have segregation depths >100 km). The present thickness of the lithosphere underneath the Styrian Basin is about 100 km (Horváth et al., 2006); consequently, the source region of the Styrian mafic magmas has an asthenospheric mantle origin.

Lee et al. (2009) introduced new thermobarometers depend on SiO_2 and MgO contents of mafic magma to constrain the pressures and temperatures of basaltic magma generation. They presented a Visual Basic Excel Macro for fractionation correction and P-T calculation. Using the most primitive lavas (MgO> 8.5 wt. %) and applying the method of Lee et al. (2009) for P-T estimations, the mafic magmas of the Klöch volcano could have been generated at 3–3.6 GPa (100–115 km depth) whereas the Steinberg could have been generated at 4–4.3 GPa (125–135 km depth). The estimated pressure of magma generation from the Styrian basanites/nepheline-basanites is mostly greater than 3 GPa (depth>100 km) which is also in accordance with Scarrow and Cox (1995) barometer. On the other hand, Albarède (1992) barometer gives pressures of 2.3–3 GPa which is significantly underestimated by up to 1 GPa at pressure greater than 3 GPa (Lee et al., 2009). The calculated temperatures of melting of the Styrian basanites/nepheline-basanites according to Lee et al. (2009), range from ~1430 $^{\circ}$C to ~1500 $^{\circ}$C and according to Putirka (2005), range from 1400–1430 $^{\circ}$C.

The Lee et al. (2009) thermobarometer cannot be applied to nephelinites because it is not calibrated for the effects of CO_2 on silica activity. However, using the Scarrow and Cox (1995) barometer, the inferred pressure for nephelinites is >4.3 GPa and, certainly, higher than this of the basanites/nepheline-basanites. The Styrian mafic magmas originated at greeter depths (garnet stability field) and are enriched in incompatible elements, consistent with generally low but variable degrees of melting. Indeed, the estimated depths of magma generation are further confirming that the magma must have been generated in the asthenosphere.

5.5. Mantle potential temperature (Tp) calculations for the Styrian source mantle

The occurrence of primitive lavas in the Styrian Basin is of great importance as can be used to calculate the Tp of their mantle source. PRIMELT2 software (Herzberg and Asimow, 2008) can calculate the Tp of the mantle source from the erupted primitive lava composition. The sample KL-2 is the most primitive lava (high Mg#, MgO, Ni and Cr) in the Styrian Basin having the characteristics of the primary magma suggesting minor crystal fractionation. The PRIMELT2 software indicates minor clinopyroxene fractionation, which leads to overestimation of the Tp.

Despite the evidence for clinopyroxene fractionation the calculated Tp for the Styrian Basin basanites/nepheline-basanites is ~1466 ^{o}C and corresponds ambient mantle temperatures (~1300–1454 ^{o}C) of upper mantle sources beneath MORB (Herzberg et al., 2007; Putirka et al., 2007), implying that the Styrian magmas arose from ambient mantle i.e. no thermal anomaly is indicated. In addition, the small degrees of melting and hence small volumes of the basaltic lavas erupted and low eruption rates suggest that the asthenospheric mantle Tp was low and consistent with ambient mantle temperatures. The Tp calculation from the Styrian Basin along with the arguments (e.g. missing of regional uplift, sporadic occurrence of the alkaline volcanism and the high-velocity body beneath CPR) provided by Harangi and Lenkey (2007) and Ali and Ntaflos (2011) and the study of Tschegg et al. (2010) all indicate that most of the Pannonian Basin basalts are melted from the mantle at ambient temperature and confirming that there is no plume activity beneath the Pannonian Basin.

5.6. Nature of the lavas and their source characteristics

The major and trace element and Sr-Nd isotope compositions of the primitive mafic magmatic rocks from the Styrian Basin can provide important constraints on the nature of the lavas and their mantle source characteristics and the conditions of partial melting.

The Nb/U and Ce/Pb ratios are important tracers to reveal distinct mantle sources (Hofmann, 1997). The Styrian Basin lavas have Ce/Pb (>20; Embey-Isztin et al., 1993) and Nb/U ratios (37; on average) similar to OIB, higher than those of the primitive mantle and continental crust (Hofmann et al., 1986). Moreover, the Ba/Ce (4.18-5.82) ratios are identical to those of OIB basalts globally (Halliday et al., 1995).

The mantle source of the basaltic magmas can also be identified using HFSE/LREE ratios particularly Nb/La one (Smith et al., 1999): low ratios (<1) would suggest a lithospheric origin whereas high ratios indicate an asthenospheric mantle source. The Styrian lavas have high Nb/La ratios (1.4; on average) consistent with an OIB-like asthenospheric mantle source and are similar to average OIB (Fitton et al., 1991).

HIMU-OIB signature of the studied lavas can be inferred from the elemental ratios (Zr/Nb= 3.67, La/Nb=0.71 and Ba/Th =58.5), (Weaver, 1991). The relative depletion of Rb and Ba that can be observed in the multi-element diagram (Fig. 5a) is a further typical feature of rocks with HIMU-OIB signature (Hofmann, 1997). The HIMU basalt, like the studied lava, has the lowest $^{87}Sr/^{86}Sr$ of any other OIBs, and their source has low Rb/Sr ratios as those of the more depleted MORBs (Hofmann, 2004). The Sr-Nd isotopic ratios are also similar to that of HIMU-OIB (e.g. Hofmann, 1997) and are comparable to EAR (Fig. 6). In addition, the Stradnerkogel nephelinites have relatively high $^{206}Pb/^{204}Pb$ ratios of around 19.2 being similar to HIMU-OIB (Embey-Isztin et al., 1993). Consequently, trace element and isotopic compositions suggest that the Styrian Basin lavas have geochemical characteristics similar to HIMU and EAR, originated from an asthenospheric mantle source.

The characteristic features of the studied nephelinites, including high $(La/Yb)_N$=29–31, superchondritic Zr/Hf =51–67 and negative K and Ti anomalies, are similar to those of carbonatites which may suggest that their peridotite mantle source had undergone enrichment with carbonatitic liquids (e.g., Chen et al., 2009; Zeng et al., 2010) infiltrated from great depths producing carbonated silicate melts (Dasgupta et al., 2007). This is further confirmed by the involvement of ~5% CO_2 in their genesis (Dasgupta et al., 2007) (Fig. 8). Accordingly the negative K anomaly seems to be a source character (Chauvel et al., 1992; Hofmann, 2004; Lustrino and Wilson, 2007).

In general, both nephelinites and basanites/nepheline-basanites have superchondritic Zr/Hf ratios (51–67) which cannot be explained by simply melting of dry peridotite source and requires involvement of volatiles (Zeng et al., 2010 and ref. therein). The major element composition of the HIMU lavas, like the studied nephelinites and basanites/nepheline-basanites, could be a consequence of "CO_2-fluxing" (Collerson et al., 2010) which was confirmed by the elevated Zr/Hf ratios.

The studied nephelinites are low in SiO_2 and high in CaO, consistent with low degrees of melting of carbonated peridotite (Fig. 8) and are similar to those of Canary Islands lavas (Dasgupta et al., 2007; Herzberg and Asimow, 2008; Hirose, 1997). For low degrees of partial melting of anhydrous peridotites that have experienced addition of CO_2 the melts have significantly lower SiO_2 and higher CaO if compared with low melts derived under the same conditions without CO_2 (Dasgupta et a., 2007 and Hirose, 1997). The Styrian nephelinites and basanites/nepheline-basanites differ in their SiO_2 and CaO contents (Fig. 8). Their differences could be attributed to the generation of the basanite/nepheline-basanite melt at lower pressures as the SiO_2 content of the partial melt of carbonated peridotite increases with decreasing pressure whereas CaO decreases (Dasgupta et al., 2007; Hirose, 1997). Moreover, the nephelinites plot in the CO_2 array and are consistent with peridotite partial melting in the presence of ~5% CO_2 (Dasgupta et al., 2007) (Fig. 8). The most likely CO_2-source is an undegassed reservoir containing primordial carbon and not related to subducted biogenic carbonate (Collerson et al., 2010 and ref. therein). The Klöch and Steinberg basanites/nepheline-basanites have high SiO_2 and low CaO compared to nephelinites, suggesting slightly high degrees of melting (Fig. 8). They plot to the right of the dashed line (Fig. 8), implying insignificant role of CO_2 during melting as a consequence of increasing degrees of melting and are similar to those of Galapagos Islands (Dasgupta et al., 2007; Herzberg and Asimow, 2008; Hirose, 1997).

The similarity of the trace element distribution patterns and Sr-Nd isotopic ratios of the Klöch and Steinberg basanites/nepheline-basanites is remarkable. Both nephelinites and basanites/nepheline-basanites have similar Sr-Nd isotopic ratios that vary within a very narrow range (Fig. 6) suggesting similar asthenospheric mantle source.

6. Conclusions

The Styrian alkaline mafic rocks range in composition from highly undersaturated nephelinites (Stradnerkogel and Waltrafelsen) to predominant basanites/nepheline-basanites (Klöch and Steinberg).

Rhönite occurrence point to crystallization in the presence of a fluid phase at pressures < 0.06 GPa (corresponding to depths of < 1.8 km) and temperatures range of 840 and 1200 $^{\circ}$C (Kunzmann, 1989).

High (OIB-like) Ce/Pb, Nb/U and Nb/La ratios of the Styrian mafic rocks exclude any significant crustal assimilation and/or interaction with lithospheric mantle and reflect asthenospheric mantle source characteristics. They are silica-undersaturated (S.I. range from -26 to -59) and have high MgO content (> 6 wt.%), and there is no evident correlation between MgO and other oxides (Fig. 4) suggesting minor role of fractional crystallization processes. The high Mg# (63–66) and high compatible element contents (Ni=128–156 ppm and Cr=124–144 ppm) of the Klöch basanites/nepheline-basanites indicate they are close to be a primary magma.

The increase of highly/moderately incompatible element ratios (e.g. Ba/Y and P_2O_5/TiO_2) with increasing the concentrations of the highly incompatible elements along with the negative correlation between CaO/Al_2O_3 and SiO_2 suggest that partial melting was the main process implicated in the generation of the Styrian magmas. The increasing of silica-undersaturation, alkalis, CaO/Al_2O_3, LREE from basanite/nepheline-basanite to nephelinite principally results from decreasing degrees of partial melting at increasing depths in the mantle. The depths of magma generation from basanites/nepheline-basanites are mostly >100 km to about 135 km (Lee et al., 2009; Scarrow and Cox, 1995) whereas, the nephelinitc magmas could be generated at depths of about 135-150 km (Scarrow and Cox, 1995). These magmas originated at greeter depths (garnet stability field) are enriched in incompatible elements, consistent with generally low, but variable, degrees of melting. Indeed, the estimated depths of magma generation are further confirming that the magma must have been generated in the asthenosphere. The temperatures of melting of the basanites/nepheline-basanites range from ~1400 ^{o}C to ~1500 ^{o}C (Lee et al., 2009; Putirka, 2005).

The most primitive Styrian sample, the basanite KL-2, suggests considerable olivine fractionation but minor clinopyroxene fractionation of its primary magma. Even if considered carefully, the calculated Tp (1466 ^{o}C) suggests that the Styrian magmas generated from mantle at ambient temperature and confirming that there is no plume activity beneath the study area.

The Styrian nephelinites exhibit negative K and Ti anomalies on the PM-normalized multi-element diagrams and have superchodritic Zr/Hf ratios (51-67). These geochemical signatures of the studied nephelinites, resemble those of carbonatites, may suggest that their mantle source has been metasomatized by carbonatitic liquids which is further indicated by presence of about 5% CO_2 in their genesis. The low SiO_2 and high CaO contents of the nephelinites are consistent with low degrees of partial melting of carbonated peridotite source. Compared to nephelinites, the basanites/nepheline-basanites display minor contribution of CO_2 and higher SiO_2 and lower CaO contents as a consequence of increasing degrees of melting of the carbonated peridotite mantle source.

The overall similarity of the trace element distribution patterns and the very narrow range of the Sr-Nd isotopic ratios of the studied nephelinites and basanites/nepheline-basanites suggest a similar asthenospheric mantle source, volatile-enriched, with EAR-type affinity.

Acknowledgements

References

Albarède, F., 1992. How deep do common basaltic magmas form and differentiate? Journal of Geophysical Research 97, 10997–11009.

Ali, Sh., Ntaflos, Th., 2009. Petrogenesis of Pliocene Alkaline Volcanic Rocks from Southeastern Styrian Basin, Austria. Geophysical Research Abstracts, Vol. 11 - EGU - General Assembly 2009, Vienna, Austria.

Ali, Sh., Ntaflos, Th., 2010. Comparative petrological studies of some alkaline basalts, western Pannonian Basin, Austria. Geophysical Research Abstracts, Vol. 12 - EGU - General Assembly 2010, Vienna, Austria.

Ali, Sh., Ntaflos, Th., 2011. Alkali basalts from Burgenland, Austria: Petrological constraints on the origin of the westernmost magmatism in the Carpathian–Pannonian Region. Lithos 121, 176–188.

Anders, E., Grevesse, N., 1989. Abundances of the elements: meteoritic and solar. Geochimica et Cosmochimica Acta 53, 197–214.

Balogh, K., Ebner, F., Ravasz, Cs., 1994. K/Ar alter tertiärer Vulcanite de südöstlischen Steiermark und des südlischen Burgenlands, in: Császár, G., Daurer, A. (Eds.), Jubiläumsschrift 20 Jahre Geologischen Zusammenarbeit Österreich-Ungarn Lobitzer, 55– 72.

Chauvel, C., Hofmann, A.W. Vidal, P., 1992. HIMU-EM: The French Polynesian connection. Earth and Planetary Science Letters 110, 99–119.

Chen, L.-H., Zeng, G., Jiang, S.-Y., Hofmann, A.W., Xu, X.-S., 2009. Sources of Anfengshan basalts: subducted lower crust in the Sulu UHP belt, China. Earth and Planetary Science Letters 286, 426–435.

Collerson, K.D., Williams, Q., Ewart, A.E., Murphy, D.T., 2010. Origin of HIMU and EM-1 domains sampled by ocean island basalts, kimberlites and carbonatites: The role of CO_2-fluxed lower mantle melting in thermochemical upwellings. Physics of the Earth and Planetary Interiors 181, 112–131.

Dasgupta, R., Hirschmann, M.M., Smith, N.D., 2007. Partial melting experiments of peridotitie+CO_2 at 3 GPa and genesis of alkalic ocean island basalts. Journal of Petrology 48, 2093–2124.

Dasgupta, R., Jackson, M.G., Lee, C.-T., 2010. Major element chemistry of ocean island basalts-conditions of mantle melting and heterogeneity of mantle source. Earth and Planetary Science Letters 289, 377–392.

Dobosi, G., Fodor, R.V., Goldberg, S.A., 1995. Late-Cenozoic alkalic basalt magmatism in northern Hungary and Slovakia: petrology, source compositions and relationship to tectonics. Acta Vulcanologica 7, 199–207.

Dobosi, G., Schultz-Güttler, R., Kurat, G., Kracher, A., 1991. Pyroxene chemistry and evolution of alkali basaltic rocks from Burgenland and Styria, Austria. Mineralogy and Petrology 43, 275–292.

Dombrádi, E., Sokoutis, D., Bada, G., Cloetingh, S., Horváth, F., 2010. Modelling recent deformation of the Pannonian lithosphere: Lithospheric folding and tectonic topography. Tectonophysics 484, 103–118.

Downes, H., Seghedi, I., Szakacs, A., Dobosi, G., Vaselli, O., James, D.E., Rigby, I.J., Thirlwall, M.F., Rex, D., Pécskay, Z., 1995. Petrology and geochemistry of late Tertiary/Quaternary mafic alkaline volcanism in Romania. Lithos 35, 65–81.

Ebner, F., Sachsenhofer, R.F., 1995. Palaeogeography, subsidence and thermal history of the Neogene Styrian Basin (Pannonian basin system, Austria). Tectonophysics 242, 133–150.

Embey-Isztin, A. Dobosi, G., 1995. Mantle source characteristics for Miocene–Pleistocene alkali basalts, Carpathian–Pannonian Region: a review of trace elements and isotopic composition, in: Downes, H., Vaselli, O. (Eds.), Neogene and related magmatism in the Carpatho-Pannonian Region. Acta Vulcanologica 7(2), 155–166.

Embey-Isztin, A., Downes, H., James, D.E., Upton, B.G.J., Dobosi, G., Ingram, G.A., Harmon, R.S., Scharbert, H.G., 1993. The petrogenesis of Pliocene alkaline volcanic rocks from the Pannonian Basin, Eastern Central Europe. Journal of Petrology 34, 317–343.

Fitton, J.G., James, D., Leeman, W.P., 1991. Basic magmatism associated with Late Cenozoic extension in the Western United States: compositional variations in space and time. Journal of Geophysical Research 96, 13693–13711

Halliday, A.N., Lee, D-C., Tommasini, S., Davies, G.R., Paslick, C.R., Fitton, J.D., James, D.E., 1995. Incompatible trace elements in OIB and MORB and source enrichment in the sub-oceanic mantle. Earth and Planetary Science Letters 133, 379–395.

Harangi, S., 2001. Neogene magmatism in the Alpine–Pannonian Transition Zone– a model for melt generation in a complex geodynamic setting. Acta Vulcanologica 13, 25–39.

Harangi, S., Downes, H., Seghedi, I., 2006. Tertiary-Quaternary subduction processes and related magmatism in the Alpine-Mediterranean region, in: Gee, D.G., Stephenson, R.A. (Eds.), European Lithosphere Dynamics. Geological Society of London Memoir 32, 167–190.

Harangi, S., Lenkey, L., 2007. Genesis of the Neogene to Quaternary volcanism in the Carpathian–Pannonian region: Role of subduction, extension, and mantle plume, in: Beccaluva, L., Bianchini, G., Wilson, M. (Eds.), Cenozoic Volcanism in the Mediterranean Area. Geological Society of America Special Paper 418, 67–92.

Harangi, S., VaseIli, O., Tonarini, S., Szabó, Cs., Harangi, R., Coradossi, N., 1995. Petrogenesis of Neogene extension-related alkaline volcanic rocks of the Little Hungarian Plain volcanic field (Western Hungary), in: Downes, H., VaseIli, O. (Eds.), Neogene and related magmatism in the Carpatho-Pannonian Region. Acta Vulcanologica 7(2), 173–187.

Hart, W.K.,Wolde, G.C.,Walter, R.C., Mertzman, S.A., 1989. Basaltic volcanism in Ethiopia: constraints on continental rifting and mantle interactions. Journal of Geophysical Research 94, 7731–48.

Herzberg, C., Asimow, P.D., 2008. Petrology of some oceanic island basalts: PRIMELT2.XLS software for primary magma calculation. Geochemistry, Geophysics, Geosystems 9. doi:10.1029/2008GC002057.

Herzberg, C., Asimow, P.D., Arndt, N., Niu, Y., Lesher, C.M., Fitton, J.G., Cheadle, M.J., Saunders, A.D., 2007. Temperatures in ambient mantle and plumes: Constraints from basalts, picrites, and komatiites. Geochemistry, Geophysics, Geosystems 8. doi:10.1029/2006GC001390.

Hirose, K., 1997. Partial melt compositions of carbonated peridotite at 3 GPa and role of CO_2 in alkali–basalt magma generation. Geophysical Research Letters 24, 2837–2840.

Hirose, K., Kushiro, I., 1993. Partial melting of dry peridotites at high pressures: determination of composition of melts segregated from peridotite using aggregate of diamonds. Earth and Planetary Science Letters 114, 477–489.

Hofmann, A.W., 1997. Mantle geochemistry: the message from oceanic volcanism. Nature 385, 219–229.

Hofmann, A.W., 2004. Sampling Mantle Heterogeneity through Oceanic Basalts: Isotopes and Trace Elements, in: Carlson, R.W. (Ed.), The Mantle and Core, Treatise in Geochemistry. Amstredam: Elsevier, pp. 61–103.

Hofmann, A.W., Jochum, K.P., Seufert, M., White, W.M., 1986. Nb and Pb in oceanic basalts, new constraints on mantle evolution. Earth and Planetary Science Letters 79, 33–45.

Horváth, F., Bada, G., Szafián, P., Tari, G., Ádám, A., Cloetingh, S.A.P.L., 2006. Formation and deformation of the Pannonian basin: Constraints from observational data, in: Gee, D.G., Stephenson, R.A. (Eds.), European Lithosphere Dynamics. Geological Society, London, Memoirs 32, 191–206.

Huismans, R.S., Podladchikov, Y.Y., Cloetingh, S.A.P.L., 2002. The Pannonian basin: Dynamic modelling of the transition from passive to active rifting. European Geosciences Union Stephan Mueller Special Publication Series 3, 41–63.

Keshav, S., Gudfinnsson, G. H., Sen, G., Fei, Y.-W., 2004: High-pressure melting experiments on garnet clinopyroxenite and the alkalic to tholeiitic transition in ocean-island basalts. Earth and Planetary Science Letters 223, 365–379.

Kunzmann, T., 1989. Rhönit: Mineralchemie, Paragenese und Stabilität in alkalibasaltischen Vulkaniten (Ein beitrag zur Mineralogenese der Rhönit-Änigmatit-Mischkristallgruppe). Doctoral dissertation. Ludwig-Maximillians-Universität, München, Germany, 152pp.

Le Bas, M.J., Le Maitre, R.W., Streckeisen, A., Zanettin, B., 1986. A chemical classification of volcanic rocks based on the total alkali-silica diagram. Journal of Petrology 27, 745–750.

Lee, C.-T., Luffi, P., Plank, T., Dalton, H., Leeman, W.P., 2009. Constraints on the depths and temperatures of basaltic magma generation on Earth and other terrestrial planets using new thermobarometers for mafic magmas. Earth and Planetary Science Letters 279, 20–33.

Le Maitre (Ed.), R.W., 2002. Igneous Rocks: A Classification and Glossary of Terms, 2nd Edition. Recommendations of the International Union of Geological Sciences Subcommission on the Systematics of Igneous Rocks. Cambridge University Press, 219 p.

Lustrino, M., Wilson, M., 2007. The circum-Mediterranean anorogenic Cenozoic igneous province. Earth Science Reviews 81, 1–65.

McDonough, W.F., Sun, S.S., 1995. The composition of the Earth. Chemical Geology 120, 223–253.

Morimoto, N., Fabries, J., Ferguson, A.K., Ginzburg, I.V., Ross, M., Seifert, F.A., Zussman, J., Aoki, K., Gottardi, G., 1988. Nomenclature of pyroxenes. Mineralogical Magazine 52, 535–550.

Pearce, T.H., 1978. Olivine fractionation equation for basaltic and ultrabasic liquids. Nature 276, 771–774.

Pécskay, Z., Lexa, J., Szakacs, A., Balogh, K., Shegedi, I., Konecy, V., Kovacs, M., Marton, E., Kaliciak, M., Szeki-Fux, V., Poka, T., Gyarmati, P., Edelstein, O., Rosu, E., Zec, B., 1995. Space and time distribution of Neogene–Quaternary volcanism in the Carpatho-Pannonian region, in: Downes, H., Vaselli, O. (Eds.), Neogene and related volcanism in the Carpatho-Pannonian Region. Acta Volcanologica Special Issue 7, 15–28.

Pécskay, Z., Lexa, J., Szakács, A., Seghedi, I., Balogh, K., Konečný, V., Zelenka, T., Kovacs, M., Póka, T., Fülöp, A., Márton, E., Panaiotu, C., Cvetković, V., 2006. Geochronology of Neogene magmatism in the Carpathian arc and Intra-Carpathian area: a review. Geologica Carpathica 57, 511–530.

Putirka, K.D., 2005. Mantle potential temperatures at Hawaii, Iceland, and the mid- ocean ridge system, as inferred from olivine phenocrysts: evidence for thermally driven mantle plumes. Geochemistry, Geophysics, Geosystems 6. doi:10.1029/2005GC000915.

Putirka, K.D., Perfit, M., Ryerson, F.J., Jackson, M.G. 2007. Ambient and excess mantle temperatures, olivine thermometry, and active vs. passive upwelling. Chemical Geology 241, 177–206.

Royden, L.H., 1993. Evolution of retreating subduction boundaries formed during continental collision. Tectonics 12, 629–638.

Rudnick, R.L., Gao, S., 2003. Composition of the continental crust, in: Rudnick, R.L. (Ed.), The Crust, in: Holland, H.D., Turekian, K.K. (Eds), Treatise on Geochemistry, vol. 3, Elsevier-Pergamon, Oxford, pp. 1–64.

Sachsenhofer, R.F., Lankreijer, A., Cloetingh, S.A.P.L., Ebner, F., 1997. Subsidence analysis and quantitative basin modeling in the Styrian Basin (Pannonian Basin system, Austria). Tectonophysics 272, 175–196.

Salters, V.J.M., Hart, S.R., Panto, G., 1988. Origin of late Cenozoic volcanic rocks of the Carpathian Arc, Hungary, in: Royden, L.H., Horvath, F. (Eds.), The Pannonian Basin; a study in Basin Evolution. American Association of Petroleum Geologists Memoir 45, 279–292.

Scarrow, J.H., Cox, K.G., 1995. Basalts generated by decompressive adiabatic melting of a mantle plume: a case study from the Isle of Skye, NW Scotland. Journal of Petrology 36 (1), 3–22.

Schmid, S.M., Bernoulli, D., Fügenschuh, B., Matenco, L., Schefer, S., Schuster, R., Tischler, M., Ustaszewski, K., 2008. The Alpine–Carpathian–Dinaridic orogenic system: correlation and evolution of tectonic units. Swiss Journal of Geosciences 101 (1), 139–183.

Seghedi, I., Downes, H., Szakacs, A., Mason, P.R.D., Thirlwall, M.F., Rosu, E., Pecskay, Z., Marton, E., Panaiotu, C., 2004a. Neogene–Quaternary magmatism and geodynamics in the Carpathian–Pannonian region: A synthesis. Lithos 72, 117–146.

Seghedi, I., Downes, H., Vaselli, O., Szakács, A., Balogh, K. and Pécskay, Z., 2004b. Post-collisional Tertiary–Quaternary mafic alkalic magmatism in the Carpathian–Pannonian region: a review. Tectonophysics 393, 43–62.

Seghedi, I., Maţenco, L., Downes, H., Mason, P.R.D., Szakács, A., Pécskay, Z., 2010. Tectonic significance of changes in post-subduction Pliocene–Quaternary magmatism in the south east part of the Carpathian–Pannonian Region. Tectonophysics. doi:10.1016/j.tecto.2009.12.003.

Smith, E.I., Sánchez, A., Walker, J.D., Wang, K., 1999. Geochemistry of mafic magmas in the Hurricane Volcanic Field, Utah: implications for small- and large scale chemical variability of the lithospheric mantle. Journal of Geology 107, 433–48.

Thöni, M., Miller, C., Blichert-Toft, J., Whitehouse, M.J., Konzett, J., Zanetti, A., 2008. Timing of high-pressure metamorphism and exhumation of the eclogite type-locality (Kupplerbrunn–Prickler Halt, Saualpe, south-eastern Austria): constraints from correlations of the Sm–Nd, Lu–Hf, U–Pb and Rb–Sr isotopic systems. Journal of metamorphic geology 26, 561–581.

Tschegg, C., Ntaflos, Th., Hein, I., 2009. Thermally triggered two-stage reaction of carbonates and clay during ceramic firing– a case study on Bronze Age Cypriot ceramics. Applied Clay Science 43 (1), 69–78.

Tschegg, C., Ntaflos, Th., Seghedi, I., Harangi, S., Kosler, J., Coltorti, M., 2010. Paleogene alkaline magmatism in the South Carpathians (Poiana Ruscă, Romania): Asthenosperic melts with geodynamic and lithospheric information. Lithos 120, 393–406.

Wass, S.Y., 1979. Multiple origins of clinopyroxene in alkalic basaltic rock. Lithos12, 115–l32.

Weaver, B.L., 1991. Trace element evidence for the origin of ocean–island basalts. Geology 19, 123–6.

Wilson, M., 1989. Igneous Petrogenesis. Kluwer, Netherlands, 450 pp.

Wilson, M., Downes, H., 1991. Tertiary-Quaternary extension-related alkaline magmatism in Western and Central Europe. Journal of Petrology 32, 811–849.

Wilson, M., Downes, H., 2006. Tertiary-Quaternary intra-plate magmatism in Europe and its relation to mantle dynamics, in: Gee, D.G., Stephenson, R.A. (Eds.), European Lithosphere Dynamics. Geological Society of London, Memoirs 32, 147–166.

Wilson, M., Patterson, R., 2001. Intra–plate magmatism related to short wavelength convective instabilities in the upper mantle: Evidence from the Tertiary–Quaternary volcanic province of western and central Europe, in: Ernst, R.E., Buchan, K.L. (Eds.), Mantle Plumes: Their Identification through Time. Geological Society of America Special Paper 352, 37–58.

Zeng, G., Chen, L.-H., Xu, X.-S., Jiang, S.-Y., Hofmann, A.W., 2010. Carbonated mantle sources for Cenozoic intra-plate alkaline basalts in Shandong, North China. Chemical Geology 273, 35–45.

Zindler, A., Hart, S., 1986. Chemical geodynamics. Annual Review of Earth and Planetary Sciences 14, 493–571.

APPENDIX

Supplementary Tables (A & B)

Table A: Average values for international geo–standards GSR-3 and BHVO-1 obtained by XRF and ICP-MS respectively relative to recommended data.

Sample	GSR-3	GSR-3	%RSD (n=6)
wt%	recommended	XRF	
SiO$_2$	45.71	45.18	0.24
TiO$_2$	2.42	2.41	0.46
Al$_2$O$_3$	14.16	14.23	0.20
Fe$_2$O$_3$	13.72	13.57	0.50
MnO	0.17	0.18	0.00
MgO	7.96	8.05	1.33
CaO	9.02	9.01	0.53
Na$_2$O	3.46	3.44	0.52
K$_2$O	2.38	2.31	0.44
P$_2$O$_5$	0.97	0.91	0.36
Total	99.98	99.29	
ppm			
Ba	526	596.38	2.51
Co	46.5	41.97	5.36
Cr	134	132.75	4.03
Cu	48.6	77.36	8.53
Ga	24.8	19.69	2.17
Ni	140	136.03	4.14
Rb	37	43.84	1.03
Sc	15.2	22.71	4.33
Sr	1100	1160.71	0.23
V	167	160.48	2.42
Zn	150	153.31	0.98
Zr	277	272.98	0.44
	BHVO-1	BHVO-1	%RSTD (n=4)
ppm	recommended	ICP-MS	
Y	26	26.27	1.22
Nb	19	19.40	2.62
La	15	15.07	1.40
Ce	39	38.55	0.20
Pr	5.7	5.44	4.96
Nd	25.2	24.38	0.91
Eu	2.06	1.95	1.91
Sm	6.2	5.83	1.10
Eu	2.06	1.89	0.94
Gd	6.4	5.81	1.28
Tb	0.96	0.88	0.70
Dy	5.2	4.95	1.41
Ho	0.99	0.94	1.14
Tm	0.33	0.31	2.59
Yb	2.02	2.00	1.03
Lu	0.291	0.27	0.71
Hf	4.38	4.09	3.34
Ta	1.23	1.15	2.98
Th	1.08	1.17	7.41
U	0.42	0.39	1.98

* GSR-3 and BHVO-1 geostandards (Gonvindaraju, 1989)

* %RSD - relative standard deviation

* Gonvindaraju, K., 1989. Compilation of working values and sample description for 272 geostandards. Geostandards Newslett Spec Issue 13, 1-113.

Table B1: Representative electron microprobe analyses and chemical formulae of olivines (cations based on 4 O) in Burgenland basalts.

Sample No.	PLB1-9c	PLB1-10r	PLB1-19	PLB7-4c	PLB7-5r	PLB7-15c	PLB7-16r	PLB7-61c	PLB7-62r	PLB8-8	OB1-15c	OB1-16r	OB1-20c	OB1-21r	OB1-47
SiO_2	39.1	36.7	39.1	41.2	38.6	39.4	38.7	40.6	39.0	38.3	40.3	39.1	39.2	38.4	40.0
TiO_2	0.05	0.10	0.04	<0.02	0.05	<0.02	0.02	0.02	<0.02	0.11	<0.02	0.02	<0.02	0.08	<0.02
Al_2O_3	0.03	<0.02	<0.02	<0.02	<0.02	0.02	<0.02	<0.02	<0.02	0.02	0.03	0.04	0.03	0.02	0.04
FeO_{total}	17.7	28.4	16.1	8.2	20.7	19.4	21.4	12.5	19.5	21.1	13.9	18.9	16.0	20.2	14.3
MnO	0.28	0.59	0.27	0.12	0.42	0.34	0.40	0.17	0.37	0.46	0.23	0.22	0.22	0.26	0.14
NiO	0.15	0.04	0.18	0.38	0.19	0.21	0.14	0.32	0.22	0.12	0.34	0.19	0.23	0.14	0.29
MgO	42.2	31.1	43.3	50.2	39.7	41.3	39.6	46.8	40.8	38.8	45.4	41.1	43.3	39.9	45.2
CaO	0.25	0.51	0.26	0.05	0.22	0.08	0.23	0.03	0.19	0.22	0.22	0.31	0.23	0.28	0.22
Total	99.79	97.47	99.29	100.12	99.90	100.69	100.44	100.35	100.15	99.10	100.37	99.79	99.23	99.38	100.19
Si	0.998	1.015	0.997	1.003	0.999	1.003	0.999	1.003	1.001	1.002	1.004	1.002	0.998	0.997	1.000
Al	0.001	0.000	0.001	0.000	0.000	0.001	0.000	0.000	0.000	0.000	0.001	0.001	0.001	0.001	0.001
Ti	0.001	0.002	0.001	0.000	0.001	0.000	0.000	0.000	0.000	0.002	0.000	0.000	0.000	0.002	0.000
Fe_{total}	0.377	0.656	0.343	0.166	0.448	0.412	0.461	0.258	0.419	0.460	0.289	0.405	0.340	0.439	0.300
Mn	0.006	0.014	0.006	0.002	0.009	0.007	0.009	0.004	0.008	0.010	0.005	0.005	0.005	0.006	0.003
Mg	1.607	1.280	1.644	1.818	1.533	1.567	1.521	1.724	1.561	1.512	1.684	1.571	1.645	1.545	1.684
Ca	0.007	0.015	0.007	0.001	0.006	0.002	0.006	0.001	0.005	0.006	0.006	0.009	0.006	0.008	0.006
Ni	0.003	0.001	0.004	0.007	0.004	0.004	0.003	0.006	0.005	0.003	0.007	0.004	0.005	0.003	0.006
Mg#	0.81	0.66	0.83	0.92	0.77	0.79	0.77	0.87	0.79	0.77	0.85	0.80	0.83	0.78	0.85

c = core; r = rim; g = groundmass

Mg#= $Mg/(Mg+Fe_{total})$

Table B2: Representative electron microprobe analyses and chemical formulae of clinopyroxenes (cations based on 6 O) in Burgenland basalts.

Sample No.	PLB5-101c	PLB5-102r	PLB5 -108g	PLB7-37g	PLB7-53g	PLB7-54c	PLB7-55r	PLB10-49c	PLB10-50r	OB1-2c	OB1-3r	OB1-10c	OB1-11r	OB1-12c	OB1-13r
SiO_2	52.7	49.7	48.2	48.9	50.0	50.1	46.2	49.4	44.2	52.2	50.2	52.6	50.4	52.4	48.0
TiO_2	0.84	2.34	3.0	2.6	2.15	1.49	3.8	2.42	4.6	0.62	1.57	0.60	1.61	0.80	2.7
Al_2O_3	2.01	3.2	4.6	3.6	3.0	4.0	6.0	3.4	7.1	2.6	2.48	2.23	2.9	2.36	4.3
Cr_2O_3	0.80	0.13	0.03	<0.02	0.09	1.39	0.35	<0.02	<0.02	0.80	0.11	0.64	0.13	0.33	<0.02
Fe_2O_3	1.67	2.7	5.8	3.8	1.65	2.34	3.8	3.5	4.8	1.07	1.83	1.17	1.87	1.64	2.7
FeO	3.8	4.5	1.93	3.5	5.3	3.4	3.6	3.8	3.6	4.2	5.7	4.4	5.5	4.0	6.6
MnO	0.14	0.13	0.16	0.11	0.13	0.12	0.13	0.12	0.12	0.12	0.14	0.12	0.18	0.14	0.18
MgO	17.1	15.0	13.5	14.0	15.0	15.5	12.8	14.5	11.9	17.6	15.3	18.1	15.2	17.1	13.2
CaO	20.9	22.1	22.1	22.5	21.9	21.1	22.1	22.7	22.2	19.3	21.1	19.0	21.5	20.8	21.1
Na_2O	0.54	0.38	1.22	0.70	0.32	0.68	0.80	0.51	0.78	0.52	0.27	0.50	0.28	0.44	0.51
Total	100.52	100.16	100.54	99.73	99.55	100.07	99.58	100.29	99.20	99.07	98.70	99.36	99.60	100.10	99.38
Si	1.926	1.851	1.804	1.837	1.869	1.854	1.747	1.844	1.693	1.923	1.892	1.933	1.882	1.923	1.819
Al^{IV}	0.074	0.139	0.196	0.161	0.131	0.146	0.253	0.149	0.307	0.077	0.108	0.067	0.118	0.077	0.181
Al^{VI}	0.012	0.000	0.006	0.000	0.000	0.028	0.013	0.000	0.012	0.037	0.002	0.030	0.010	0.025	0.012
Fe(iii)	0.046	0.076	0.161	0.106	0.046	0.065	0.107	0.097	0.135	0.030	0.052	0.032	0.052	0.045	0.078
Cr	0.023	0.004	0.001	0.000	0.003	0.041	0.010	0.000	0.000	0.023	0.003	0.019	0.004	0.010	0.000
Ti	0.023	0.066	0.086	0.073	0.060	0.042	0.108	0.068	0.131	0.017	0.045	0.017	0.045	0.022	0.077
Fe(ii)	0.117	0.140	0.060	0.110	0.165	0.104	0.112	0.116	0.112	0.128	0.178	0.134	0.170	0.123	0.209
Mn	0.004	0.004	0.005	0.004	0.004	0.004	0.004	0.004	0.004	0.004	0.005	0.004	0.006	0.004	0.006
Mg	0.934	0.832	0.754	0.784	0.838	0.852	0.724	0.806	0.679	0.970	0.861	0.989	0.849	0.936	0.746
Ca	0.818	0.885	0.888	0.907	0.876	0.837	0.897	0.908	0.911	0.764	0.850	0.749	0.860	0.819	0.858
Na	0.038	0.027	0.089	0.051	0.023	0.049	0.058	0.037	0.058	0.037	0.020	0.036	0.020	0.031	0.038
Total	4.015	4.024	4.051	4.034	4.015	4.021	4.034	4.031	4.043	4.010	4.016	4.010	4.017	4.014	4.024
Wo	41.8	45.0	45.4	46.2	44.9	43.8	47.1	46.1	47.9	39.5	43.3	38.5	44.0	41.8	44.3
En	47.7	42.4	38.5	40.0	42.9	44.6	38.0	41.0	35.8	50.2	43.8	50.9	43.3	47.8	38.6
Fs	8.51	11.2	11.5	11.2	11.0	9.03	11.8	11.0	13.3	8.36	11.9	8.76	11.7	8.79	15.1
Ac	1.94	1.38	4.54	2.61	1.17	2.57	3.07	1.89	3.04	1.91	1.00	1.85	1.04	1.59	1.94
$Al_{(total)}$	0.087	0.139	0.202	0.161	0.131	0.174	0.266	0.149	0.319	0.113	0.110	0.097	0.128	0.102	0.193
Al^{VI}/Al^{IV}	0.168	0.000	0.032	0.000	0.000	0.191	0.049	0.000	0.038	0.477	0.015	0.451	0.083	0.319	0.066
Ti/Al	0.265	0.471	0.423	0.453	0.461	0.239	0.408	0.455	0.412	0.151	0.405	0.171	0.352	0.216	0.401
Mg#	0.85	0.79	0.77	0.78	0.80	0.83	0.77	0.79	0.73	0.86	0.79	0.86	0.79	0.85	0.72

Table B3: Representative electron microprobe analyses and chemical formulae of phlogopites in Burgenland basalts.

Sample No.	PLB1-1	PLB7-40	PLB7-44	PLB8-6	PLB8-7	PLB8-9	PLB8-15	PLB10-11	PLB10-21	PLB10-54
SiO_2	40.1	38.5	38.7	37.2	37.7	38.1	38.1	38.2	37.4	37.9
TiO_2	5.0	8.5	8.0	9.1	9.3	9.2	9.1	8.9	9.8	9.9
Al_2O_3	11.1	12.5	12.7	13.7	13.0	13.0	13.1	13.0	13.1	13.1
FeO_{total}	9.7	9.4	8.5	9.5	9.3	9.5	9.0	10.6	11.2	11.0
MnO	0.09	0.06	0.07	0.07	0.08	0.06	0.07	0.08	0.08	0.07
MgO	18.5	17.1	17.9	16.6	16.4	16.7	16.9	16.1	15.1	15.4
CaO	0.21	0.02	0.13	0.10	0.09	0.08	0.14	0.11	0.21	0.04
Na_2O	0.48	0.75	0.61	0.69	0.69	0.64	0.58	0.48	0.48	0.55
K_2O	9.0	9.1	9.5	9.0	9.0	9.0	8.5	9.5	9.1	9.2
Total	94.16	95.92	96.11	95.86	95.58	96.10	95.46	96.88	96.47	97.17
Cations based on 22 O										
Si	5.361	5.068	5.075	4.909	4.989	5.008	5.018	5.014	4.951	4.972
Al	1.752	1.938	1.963	2.124	2.022	2.005	2.024	2.006	2.046	2.020
Ti	0.500	0.846	0.792	0.903	0.926	0.906	0.905	0.882	0.973	0.975
Fe_{total}	1.087	1.038	0.929	1.052	1.032	1.039	0.986	1.168	1.237	1.205
Mn	0.010	0.007	0.008	0.008	0.009	0.007	0.008	0.009	0.009	0.008
Mg	3.686	3.350	3.495	3.262	3.229	3.274	3.316	3.150	2.971	3.013
Ca	0.030	0.003	0.018	0.014	0.013	0.011	0.020	0.015	0.030	0.006
Na	0.125	0.192	0.155	0.177	0.177	0.163	0.148	0.122	0.123	0.140
K	1.541	1.537	1.582	1.524	1.522	1.501	1.424	1.588	1.541	1.546
Mg#	0.77	0.76	0.79	0.76	0.76	0.76	0.77	0.73	0.71	0.71

Table B4: Representative electron microprobe analyses and chemical formulae of plagioclase feldspars (cations based on 32 O) in Burgenland basalts.

Sample No.	PLB5-103c	PLB5-104r	PLB5-105c	PLB5-106r	PLB8-9c	PLB8-10r	PLB8-13	OB1-14	OB1-20c	OB1-21r	OB1-22	OB1-24c	OB1-25r
SiO_2	55.3	61.2	54.2	60.1	54.9	54.7	62.9	54.2	54.4	60.1	51.9	57.5	58.2
TiO_2	0.31	0.27	0.29	0.25	0.26	0.25	0.20	0.22	0.17	0.09	0.16	0.21	0.16
Al_2O_3	27.2	23.5	28.0	24.1	27.9	28.5	22.5	28.4	28.5	23.4	29.5	26.3	25.6
FeO_{total}	0.72	0.61	0.83	0.79	0.61	0.49	0.50	0.98	0.88	1.39	0.71	0.71	0.59
CaO	10.2	5.4	11.2	6.2	10.0	10.3	3.5	11.0	11.1	5.1	12.3	8.2	7.5
Na_2O	5.6	7.8	5.1	7.4	5.6	5.4	8.4	4.9	5.0	6.9	4.3	6.3	6.7
K_2O	0.30	1.09	0.30	0.89	0.31	0.32	1.82	0.34	0.33	1.66	0.32	0.68	0.81
Total	99.54	99.85	99.95	99.69	99.58	99.93	99.88	100.06	100.34	98.63	99.15	99.93	99.55
Si	10.039	10.949	9.842	10.794	9.954	9.887	11.218	9.822	9.823	10.871	9.524	10.348	10.489
Al	5.810	4.941	5.988	5.095	5.968	6.059	4.731	6.052	6.058	4.995	6.367	5.571	5.442
Ti	0.042	0.036	0.040	0.034	0.035	0.034	0.027	0.030	0.023	0.012	0.022	0.028	0.022
Fe_{total}	0.109	0.091	0.126	0.119	0.093	0.074	0.075	0.149	0.133	0.210	0.109	0.107	0.089
Ca	1.983	1.041	2.184	1.187	1.938	2.001	0.676	2.143	2.146	0.983	2.413	1.575	1.442
Na	1.969	2.695	1.785	2.562	1.973	1.889	2.894	1.729	1.755	2.421	1.518	2.208	2.334
K	0.070	0.249	0.069	0.204	0.072	0.074	0.414	0.079	0.076	0.383	0.075	0.156	0.186
Ab%	49.0	67.6	44.2	64.8	49.5	47.7	72.6	43.8	44.1	63.9	37.9	56.0	58.9
An%	49.3	26.1	54.1	30.0	48.7	50.5	17.0	54.2	54.0	26.0	60.2	40.0	36.4
Or%	1.70	6.20	1.70	5.20	1.80	1.90	10.4	2.00	1.90	10.1	1.90	4.00	4.70

Table B5: Representative electron microprobe analyses and chemical formulae of alkali feldspars in Burgenland basalts.

Sample No.	PLB1-50	PLB7-19	PLB10-25	OB1-27	OB1-29	OB1-34
SiO_2	63.6	64.0	62.2	64.8	64.3	62.9
TiO_2	0.27	0.37	0.12	0.20	0.16	0.21
Al_2O_3	22.0	20.1	19.2	20.2	20.8	19.2
FeO_{total}	0.28	0.54	0.29	0.48	0.47	0.54
CaO	2.44	1.25	0.88	1.24	1.76	2.01
Na_2O	8.5	5.3	3.0	6.4	6.8	5.7
K_2O	2.31	7.9	11.4	6.4	5.3	7.7
Total	99.32	99.39	97.01	99.72	99.60	98.28
Cations based on 32 O						
Si	11.366	11.635	11.714	11.677	11.572	11.620
Al	4.631	4.298	4.250	4.278	4.396	4.185
Ti	0.036	0.051	0.017	0.027	0.022	0.029
Fe_{total}	0.042	0.082	0.046	0.072	0.071	0.083
Ca	0.468	0.244	0.178	0.239	0.339	0.398
Na	2.937	1.851	1.099	2.242	2.379	2.041
K	0.527	1.840	2.730	1.466	1.219	1.805
Ab%	74.7	47.0	27.4	56.8	60.4	48.1
An%	11.9	6.2	4.4	6.10	8.60	9.40
Or%	13.4	46.8	68.1	37.1	31.0	42.5

Table B6: Representative electron microprobe analyses and chemical formulae of feldspathoids in Burgenland basalts.

Mineral	Nepheline						Leucite		
Sample No.	PLB1-40	PLB1-42	PLB8-1	PLB10-13	PLB10-14	PLB10-27	PLB7-21	PLB7-82	PLB8-16
SiO_2	47.4	47.3	48.3	49.4	49.2	50.6	55.0	55.3	55.5
TiO_2	0.02	0.02	0.07	0.07	0.09	0.12	0.10	0.09	0.14
Al_2O_3	32.0	31.5	32.3	29.8	32.3	31.5	23.2	23.1	23.7
FeO_{total}	0.94	1.36	0.73	1.25	0.66	0.58	0.43	0.67	0.54
MgO	0.16	0.21	0.03	0.19	0.03	<0.02	0.02	<0.02	<0.02
CaO	0.03	0.07	0.71	1.75	0.96	1.33	0.16	0.07	0.04
Na_2O	17.0	17.0	15.3	14.1	15.8	15.7	0.14	0.12	0.11
K_2O	3.3	3.4	2.9	2.09	2.8	2.09	20.5	20.8	20.5
Total	100.85	100.85	100.30	98.67	101.92	101.88	99.59	100.09	100.53
	Cations based on 32 O						Cations based on 6 O		
Si	8.873	8.883	8.991	9.307	9.027	9.230	2.000	2.003	1.997
Al	7.044	6.956	7.075	6.611	6.982	6.759	0.995	0.986	1.004
Ti	0.003	0.003	0.010	0.010	0.012	0.016	0.003	0.002	0.004
Mg	0.045	0.059	0.008	0.053	0.008	0.000	0.001	0.000	0.000
Fe_{total}	0.147	0.213	0.114	0.197	0.101	0.088	0.013	0.020	0.016
Na	6.158	6.176	5.529	5.167	5.611	5.532	0.010	0.008	0.008
Ca	0.006	0.014	0.142	0.353	0.189	0.260	0.006	0.003	0.002
K	0.787	0.819	0.691	0.502	0.664	0.486	0.949	0.960	0.939

Table B7: Representative electron microprobe analyses and chemical formulae of titanomagnetites and spinels in Burgenland basalts.

Mineral	Titanomagnetite						Spinel		
Sample No.	PLB1- 3	PLB7-83	PLB8-64	PLB10-5	OB1-31	OB1-32	PLB7-32	PLB7-66	PLB15-84
SiO_2	0.07	0.07	0.04	0.06	0.11	0.08	0.04	0.08	0.06
TiO_2	30.0	13.6	15.7	6.3	25.4	19.4	6.9	12.1	1.48
Al_2O_3	0.31	3.4	2.8	2.24	1.11	1.16	6.4	4.5	4.3
Cr_2O_3	1.27	4.0	2.7	0.09	0.03	<0.02	24.1	11.6	9.0
Fe_2O_3	6.5	34.5	33.6	52.4	13.9	27.2	25.0	29.1	50.1
FeO	53.0	36.5	38.1	34.0	50.9	45.7	27.6	33.1	23.4
MnO	0.92	0.47	0.45	0.32	1.79	0.90	0.33	0.46	1.16
MgO	1.96	4.1	4.5	1.19	0.03	0.70	6.2	5.5	4.4
CaO	0.29	0.02	0.03	0.18	0.18	0.16	0.48	0.23	0.12
Total	94.31	96.64	97.85	96.86	93.38	95.33	97.04	96.66	94.11
Cations based on 32 O									
Si	0.021	0.020	0.012	0.017	0.034	0.024	0.012	0.023	0.018
Ti	7.007	3.044	3.478	1.471	6.090	4.556	1.478	2.669	0.342
Al	0.112	1.191	0.957	0.816	0.418	0.426	2.160	1.536	1.563
Cr	0.312	0.946	0.624	0.022	0.008	0.000	5.465	2.679	2.169
Fe(iii)	1.520	7.737	7.441	12.185	3.327	6.414	5.395	6.401	11.548
Fe(ii)	13.777	9.102	9.383	8.796	13.565	11.959	6.604	8.107	6.003
Mn	0.243	0.118	0.111	0.082	0.483	0.239	0.080	0.115	0.301
Mg	0.910	1.836	1.986	0.549	0.014	0.327	2.660	2.398	2.018
Ca	0.098	0.007	0.009	0.061	0.063	0.055	0.146	0.072	0.038

Table B8: Representative electron microprobe analyses and chemical formulae of ilmenites in Burgenland basalts.

Mineral	Ilmenite				
Sample No.	PLB10-1	PLB15-85	PLB15-93	OB1-15	OB1-16
SiO_2	0.02	0.04	0.02	0.02	0.07
TiO_2	51.7	45.0	53.3	50.9	51.3
Al_2O_3	0.09	1.29	0.97	0.07	0.05
Cr_2O_3	<0.02	1.35	0.078	<0.02	<0.02
FeO_{total}	37.5	40.0	32.2	44.7	43.4
MnO	1.34	0.16	0.12	0.67	0.69
MgO	7.6	4.5	7.0	1.98	2.47
CaO	0.17	0.17	0.24	0.17	0.18
Total	98.51	92.46	93.97	98.57	98.23
Cations based on 6 O					
Si	0.001	0.002	0.001	0.001	0.003
Ti	1.914	1.814	2.010	1.950	1.963
Al	0.005	0.082	0.058	0.004	0.003
Cr	0.000	0.057	0.003	0.000	0.000
Fe_{total}	1.544	1.791	1.349	1.904	1.844
Mn	0.056	0.007	0.005	0.029	0.030
Mg	0.556	0.356	0.522	0.150	0.187
Ca	0.009	0.010	0.013	0.009	0.010

CURRICULUM VITAE

Shehata Ali Shehata Ali

Personal data

First Name:	Shehata
Family Name:	Ali
Date of Birth:	08. 01. 1974
Place of Birth:	El-Minia, Egypt
Nationality:	Egyptian
Marital status:	Married + 3 children
Language Spoken:	English, Arabic (native)
E-mail:	*Shehata.ali@univie.ac.at;*
	Shehata_aly@yahoo.com
Website:	*http://public.univie.ac.at/index.php?id=30639;*
	http://www.minia.edu.eg/

Education

1992   Finished High School (El-Minia, Egypt)

1996   B.Sc. in Geology at the Faculty of Science, Minia University, Egypt

2004   M.Sc. in Geology at the Faculty of Science, Minia University, Egypt

2011   PhD in Earth Sciences at the Department of Lithospheric Research, University of Vienna

Position held

1999   Student Researcher at the Geology Department, Faculty of Science, Minia University, Egypt

2003   Demonstrator at the Geology Department, Faculty of Science, Minia University, Egypt

2004   Assistant Lecturer at the Geology Department, Faculty of Science, Minia University, Egypt

2007   Scholarship from the Ministry of Education, Youth and Sports in Czech Republic

2007   Scholarship from the Ministry of Higher Education, Missions Sector, in Egypt

Teaching Experience

Since 1999, I have been teaching a number of courses to the undergraduate student in Igneous and Metamorphic Rocks, General Geology, Economic Geology, Crystallography and Mineralogy, at the Geology Department, Faculty of Science, Minia University, Egypt

Scientific Membership

European Geosciences Union (EGU) - member since 2009
Carpathian-Balkan Geological Association (CBGA) – member since 2010

Scientific Publications

Ali, Sh. and Ntaflos, Th. (2011a): Alkali basalts from Burgenland, Austria: Petrological constraints on the origin of the westernmost magmatism in the Carpathian-Pannonian Basin. Lithos 121, 176-188.

Ali, Sh., Ntaflos, Th., Upton, B.G.J. and Cornelius, T. (2011b): Petrogenesis and mantle source characteristics of Quaternary alkaline mafic lavas in the western Carpathian–Pannonian Region, Styria, Austria (in submission stage).

Abdel Ghani, M. S., Mohamed, H. A., El-Mahallawi, M. M. and **Shehata, Sh. A.** (2004): Petrology and geochemistry of the granitoid rocks of Gebel Abu Hamr area, North Eastern Desert, Egypt. 6th Inter. Conf. on Geochemistry, Alex. Univ.,Egypt 15-16 Sept.,2004, 125-145.

Mohamed, H. A., Abdel Ghani, M. S., El-Mahallawi, M. M. and **Shehata, Sh. A.** (2003): Petrogenetic implications of mineral chemistry of Abu Hamr granitoid rocks, North Eastern Desert, Egypt. 3rd Inter. Conf. Geol. Africa, Assiut Univ., Egypt, 1, 281-300.

Conferences

Ali, Sh. and Ntaflos, Th. (2010a): Mantle source characteristics of Late Miocene-Pleistocene alkaline basalts, western Pannonian Basin, Austria. XIX Congerss of the Carpathian-Balkan Geological Association (CBGA), Thessaloniki, Greece 23-26 Sept., 2010.

Ali, Sh. and Ntaflos, Th. (2010b): Comparative petrological studies of some alkaline basalts, western Pannonian Basin, Austria. Geophysical Research Abstracts, Vol. 12 - EGU - General Assembly 2010, Vienna, Austria.

Ali, Sh. and Ntaflos, Th. (2009): Petrogenesis of Pliocene Alkaline Volcanic Rocks from Southeastern Styrian Basin, Austria. Geophysical Research Abstracts, Vol. 11 - EGU - General Assembly 2009, Vienna, Austria.

References

- **Ao. Univ. Prof. Dr. Theodoros Ntaflos**
  Dept. of Lithospheric Research, University of Vienna
  Althanstrasse 14, 1090 Vienna, Austria
  theodoros.ntaflos@univie.ac.at
  http://public.univie.ac.at/index.php?id=21269

  Tel.: +43-1-4277-53314
  Fax: +43-1-4277-9534

- **Prof. Szabolcs Harangi**
  Dept. of Petrology and Geochemistry, Eötvös Loránd University
  Pázmány sétány 1/C, H-1117 Budapest, Hungary
  szabolcs.harangi@geology.elte.hu
  szabolcsharangi@gmail.com
  http://petrology.geology.elte.hu/harangi_Eng.html

  Phone (Office): +36-13722500/ext 8355
  Phone (Mobile): +36-209340440

- **Associate Prof. Ioan Seghedi**
  Institute of Geodynamics, Romanian Academy of Sciences, Bucharest
  Str. Jean-Luis Calderon 19-21, Bucharest, Ro-020032
  seghedi@geodi.ro

  Tel: +40213172126
  Fax: +40213172129

- **Prof. Dr. M. M. El-Mahallawi**
  Geology Department, Faculty of Science, Minia University
  El Minia, Egypt
  mahallawi2001@yahoo.com